UNIVERSITY OF ŽILINA

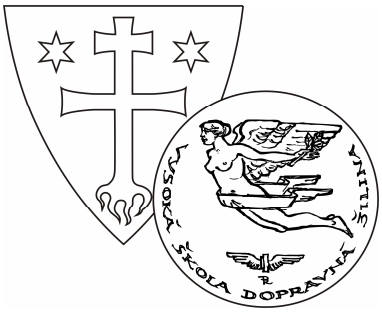

TRANSCOM 2009

8-th EUROPEAN CONFERENCE OF YOUNG RESEARCH AND SCIENTIFIC WORKERS

PROCEEDINGS

SECTION 7

CIVIL ENGINEERING

ŽILINA June 22 - 24, 2009
SLOVAK REPUBLIC

UNIVERSITY OF ŽILINA

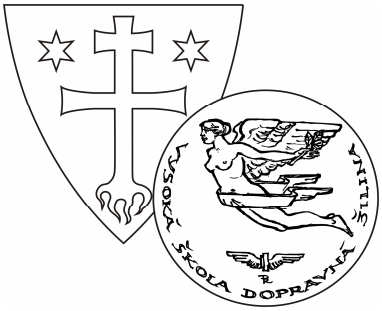

TRANSCOM 2009

8-th EUROPEAN CONFERENCE
OF YOUNG RESEARCH AND SCIENTIFIC WORKERS

under the auspices of

Prof. Ing. Ján Mikolaj, PhD.
Minister of Education, Slovak Republic

&

Prof. Ing. Ján Bujňák, PhD.
Rector of the University of Žilina

SECTION 7

CIVIL ENGINEERING

ŽILINA June 22 - 24, 2009
SLOVAK REPUBLIC

Edited by Ľuboš Remek, Iveta Pavelková and Peter Brída

ISBN:….

TRANSCOM 2009
8-th European conference of young research and scientific workers

TRANSCOM 2009, the 8th international conference of young European researchers, scientists and educators, aims to establish and expand international contacts and co-operation. The main purpose of the conference is to provide young scientists with an encouraging and stimulating environment in which they present results of their research to the scientific community. TRANSCOM has been organised regularly every other year since 1995. Between 160 and 400 young researchers and scientists participate regularly in the event. The conference is organised for postgraduate students and young research workers up to the age of 35 and their tutors. Young workers are expected to present the results they had achieved.

The conference is organised by the University of Žilina. It is the university with about 13 000 graduate and postgraduate students. The university offers Bachelor, Master and PhD programmes in the fields of transport, telecommunications, forensic engineering, management operations, information systems, in mechanical, civil, electrical, special engineering and in social sciences.

SECTIONS AND SCIENTIFIC COMMITTEE

1. TRANSPORT AND COMMUNICATIONS TECHNOLOGY

Scientific committee: Baumann S. (D), Cenek P. (SK), Droździel P. (PL), Janáček J. (SK), Jánošíková Ľ. (SK), Kremeňová I. (SK), Novák A. (SK), Palúch S. (SK), Rievaj V. (SK), Řezáč M. (CZ), Schnieder E. (D), Surovec P. (SK), Žarnay P. (SK)

2. ECONOMICS AND MANAGEMENT

Scientific committee: Bartošová V. (SK), Blašková M. (SK), Březinová O. (CZ), Duncan F.H. (USA), Hittmár Š. (SK), Kos B. (PL), Kucharčíková A. (SK), Lyakin A. (RUS), Rostášová M. (SK), Rybakov F. (RUS), Strenitzerová M. (SK), Strišš J. (SK), Tomová A. (SK)

3. INFORMATION AND COMMUNICATION TECHNOLOGIES

Scientific committee: Bärwald W. (D), Dado M. (SK), Drozdová M. (SK), Hanuliak I. (SK), Keil R. (D), Klimo M. (SK), Kolev P. (BG), Kotsopoulos S. (GR), Madleňák R. (SK), Matiaško K. (SK), Spalek J. (SK), Vaculík J. (SK), Vaculík M. (SK), Vrček N. (HR)

4. ELECTRIC POWER SYSTEMS. ELECTRICAL AND ELECTRONIC ENGINEERING

Scientific committee: Altus J. (SK), Blažek V. (D), Čápová K. (SK), Dobrucký B. (SK), Dodds S.J. (GB), Santarius P. (CZ), Vittek J. (SK)

5. MATERIAL ENGINEERING. MECHANICAL ENGINEERING TECHNOLOGIES

Scientific committee: Adamczak S. (PL), Bokůvka O. (SK), Borkowski S. (PL), Dzimko M. (SK), Guagliano M. (I), Kunz L. (CZ), Meško J. (SK), Nicoletto G. (I), Palček P. (SK), Skočovský P. (SK), Takács J. (H)

6. MACHINES AND EQUIPMENTS. APPLIED MECHANICS

Scientific committee: Dekýš V. (SK), Gerlici J. (SK), Kalinčák D. (SK), Malenovský E. (CZ), Medvecký Š. (SK), Merkisz J. (PL), Nemček M. (CZ), Pawelczyk M. (PL), Sága M. (SK), Zapoměl J. (CZ), Žmindák M. (SK)

7. CIVIL ENGINEERING

Scientific committee: Bouchair H. (F), Dmitrovskaja L. (RUS), Garbuz A. (UA), Ižvolt L. (SK), Melcer J. (SK), Ivanov J. (BG), Teleman E.C. (RO), Vičan J. (SK), Zolotov M. (UA)

8. SOCIAL SCIENCES

Scientific committee: Banáry B. (SK), Baštinec J. (CZ), Cabanová V. (SK), Gulová L. (CZ), Kráľová Z. (SK), Růžičková M. (SK), Šindelářová J. (CZ), Vikoren V. (N)

9. SECURITY ENGINEERING. FORENSIC ENGINEERING

Scientific committee: Danihelka P. (SK), Horák R. (CZ), Navrátil L. (CZ), Poledňák P. (SK), Reitšpís J. (SK), Seidl M. (SK), Šenovský M. (CZ), Šimák L. (SK), Vasiliev D. (BG), Zamiar Z. (PL)

ORGANIZING COMMITTEE

CHAIRPERSON Bokůvka Otakar

EXECUTIVE SECRETARY Vráblová Helena

MEMBERS Bábel J., Belan J., Braciník P., Brída P., Brumerčík F., Dobrotková M., Dubcová Z., Frajtová-Michalíková K., Harušinec J., Hnátová Z., Houšková L., Imrišková E., Jánošíková G., Kačiaková B., Kardoš M., Kormancová M., Krasňan M., Kuzmová M., Ladovský T., Ližbetinová L., Mihalov K., Močková M., Mráz M., Murín M., Neslušan M., Ondrejka R., Pachová S., Pavelková I., Pilát P., Potkan T., Remek Ľ., Smetana M., Sršníková D., Stránska S., Štofková K., Tulejová L., Valentíková E., Varmus M., Vaško A., Vaško M., Záborský M.

SECTION 7 CIVIL ENGINEERING

REVIEWERS:

Čelko Ján
Ďurčanská Daniela
Ďurica Pavol
Gavulová Andrea
Ižvolt Libor
Ižvoltová Jana
Komačka Jozef
Kotula Patrik
Kovařík Karel
Melcer Jozef
Moravčík Martin
Vičan Josef

Note:

Authors are responsible for language contents of their papers

CONTENTS

AXINTE, ELENA – TELEMAN, ELENA-CARMEN – ROŞCA, ELENA-VICTORIA, Iaşi, Romania: Studies regarding the wind action upon plane solar collectors placed on residential buildings 9

BARTOVIC, MARTIN, Žilina, Slovak Republic: Using of traffic detection device SR4 in transport survey (Survey on Obvodová Street) 15

BERGEROVÁ, ZUZANA – PAPAN, DANIEL, Žilina, Slovak Republic: Spectral analysis of the bridge structures 19

BEŽILLA, TOMÁŠ, Žilina, Slovak Republic: Influence of Binder Content on Permanent Deformation Resistance by Cyclic Triaxial Compression Test 23

BUJŇÁKOVÁ, PETRA, Žilina, Slovak Republic: Modelling of precast prestressed bridge girders under static load 27

BYSIEC, DOMINIKA, Kielce, Poland: Analysis of geometric parameters of chosen family two-layered spherical structures generated on the basis of regular octahedron 31

DACHOWSKI, RYSZARD – STĘPIEŃ, ANNA, Kielce, Poland: Examination of physical characteristics of the modified sand-lime products 35

DOLEŽEL, JIŘÍ – NOVÁK, DRAHOMÍR, Brno, Czech Republic: Experiment vs. probabilistic nonlinear analysis of shear failure of precast prestreseed hollow-core slab Elematic type 39

GOCÁLOVÁ, ZUZANA – ŠESTÁKOVÁ, JANA – MEČÁR, MARTIN, Žilina, Slovak Republic: Efficiency of the Ballast Material Recycling 45

HUBERTOVÁ, MICHALA, Brno, Czech Republic: Light-weight Fibre Reinforced Self Compacting Concrete 51

KATZER, JACEK – CARVALHO, MARCIO, Koszalin, Poland: A comparison of Portuguese and Polish thermal requirements and varied approach to construction of external wall 61

KANDERKOVÁ, MARTA, Žilina, Slovak Republic: Corridors of Transport Infrastructure (Heavy lines through the Europe) 65

KORTIŠ, JÁN, Žilina, Slovak Republic: The main steps of education process for numerical simulation 73

KUBOVČÍK, ONDREJ, Žilina, Slovak Republic: The Numerical Aalysis of the Airflow Modeling in the Closed System 77

KUCHARCZYKOVÁ, BARBARA – ŽÍTT, PETR – DANEK, PETR, Brno, Czech Republic: The Behaviour of Structural Members made from Lightweight and Ordinary Reinforced Concrete – Experiment, Analysis 81

MARTINICKÁ, IVANA, Žilina, Slovak Republic: Mutual Comparison of Plane Computing Models of Vehicles 85

MAZUREK, GRZEGORZ – IWAŃSKI, MAREK, Kielce, Poland: The impact of THE Low – Viscosity modIfier on the properties of asphalt concrete 89

POLÓNYI, PETER – VILLIM, ANDREJ – FIGULI, LUCIA – BAJTALA, MAREK, Žilina, Slovak Republic: The diagnostics of suspended construction of the footbridge 93

REMEK, ĽUBOŠ – VALUCH, MILAN, Žilina, Slovak Republic: RSV program and its use as a tool in the process of risk assessment and management 97

SÝKORA, MARIÁN – VIČAN, JOSEF, Žilina, Slovak Republic: Design of compression members for durability 101

SÝKOROVÁ, RENÁTA, Žilina, Slovak Republic: Bridge computational model for vehicle – bridge interaction 105

VILLIM, ANDREJ, Žilina, Slovak Republic: Estimation of variance components of 2D Geodetic Network 109

Transcom 2009, 22-24 June 2009
University of Žilina, Žilina, Slovak Republic

Studies Regarding the Wind Action Upon Plane Solar Collectors Placed on Residential Buildings

[*] Elena AXINTE, [**] Elena-CarmenTELEMAN, [***]Elena-Victoria ROŞCA
[*] Ph.D., academic professor, Technical University "Gh. Asachi' of Iaşi, Faculty of Civil Engineering and Building Services, 43, Prof. Dr. D. Mangeron, Iaşi, 700080, Romania, eaxinte@ce.tuiasi.ro
[**] Ph.D., lecturer, Technical University "Gh. Asachi' of Iaşi, Faculty of Civil Engineering and Building Services, 43, Prof. Dr. D. Mangeron, Iaşi, 700080, Romania, teleman@ce.tuiasi.ro
[***] Ph.D., lecturer, Technical University "Gh. Asachi' of Iaşi, Faculty of Civil Engineering and Building Services, 43, Prof. Dr. D. Mangeron, Iaşi, Romania, vrosca@yahoo.com

Abstract. As the countries meeting in Kyoto signed the agreements regarding the sustainability of the new projects of development, the idea of converting solar heat into thermal energy regains priority. An efficient solution is to place solar collectors on low rise buildings of 4…5m height avoiding the occupancy at the ground level.
Studies in atmospheric boundary layer wind tunnels, based on physical modelling of turbulent flow of the air around the building on which the solar collectors are placed may pay a tribute to the real understanding of the wind effects on the mechanical systems of sustaining and fixing the framework of these structures on flat roofs.
The flat surfaces of the IST 1x6 modules (types of collectors) are subjected to wind pressure and suction in the same time, the pressure coefficients obtained during the tests in the wind tunnel being the resultant of the normal coefficients on both opposite surfaces.
Wind action on the solar collectors mitigates the numerous effects caused by the obstacles between the incident flow and the structure of the collector itself; screening effect determined by the disposition of several collectors in the plane of the flat roof is an important supplementary effect.

Keywords: plane solar collector, wind action, atmospheric boundary layer wind tunnel, local wind pressures.

1. Introduction

All around the world, the sustainability concept means, in the terms of constructions, the process of designing and exploitation of structures with low energy consumption and regarding this concept, the un-conventional resources prevail upon the classic ones, as preferred solutions. The problem is very modern and world wide spread, as the Kyoto's report emphasizes and extended studies and programs have been directed in the last decades to this direction at the highest level inside European Union, some of the members like Greece, Portugal, Spain countries becoming already beneficiaries.

The methods used to capture and stock solar heat are various and some, rather old, like the simple green houses; others are much more sophisticated and modern too, like the systems placed in cosmic space. Still, the most popular form of use is the solar collectors placed near the ground level.

The technologies used for collecting and transformation the solar radiations have their own history dating from more than a century, but it is only the last decades that they draw the attention of the modern society, as a consequence of the substantial growth of the prices of

fossil resources of energy, namely the oil and natural gases. Important funds allocated for the research in this field by the great power producer companies had come up with alternative technologies, among them being those designed for collecting, stocking and converting solar radiation in thermal energy or in electric power.

Although the solar radiations as a reserve of energy are continuously studied, the scientists haven't yet found the best ways to use them in practice. One domain of research has been singled out of all, since the transformation here is produced with a sufficiently high efficiency and this is the solar radiation converted into heat. Solar collectors on the roofs of the residential buildings are a common sight in the southern countries of E.U. like Greece, Italy, France, Spain, Portugal and Bulgaria along with the countries from the former Yugoslavia and also Turkey. In the countries mentioned and not only in their case, the governmental authorities and the population understand that in this manner, an important economy of natural resources and money saving are possible and last but not least, the reduction of pollution.

After a long period of declining the importance of the concept of using the solar energy for heating in the domestic buildings, the attention is now focused once again on it.

In the present, the solar collectors are converting the radiations into heat for building services and they prove to be efficient, safe during the exploitation and reliable, with a minimum emission of pollutant gases; in the same time they are easy to install on almost every type of roof or on frameworks on the ground (fig.1).

a. b. c. d.

Fig. 1. Some possibilities of placing flat solar modulated cellular collectors: a. on the family houses, b. on the residential buildings, c. at ground level, d. on low rise buildings

Still, the best position of the plane collectors is on areas that are not designed for other necessities.

A common feature of all the solar collectors is the wind action no matter the exposure. From the engineer's point of view, the following problems may arrive:

- The collectors' design means to insure the capacity to produce energy for heating the necessary volume of water and to create the proper structural system for the collectors from the security in exploitation point of view; having in mind the dynamic wind speed profile which accelerates on roofs, a special attention must be paid to obtain minimum consumptions starting from the structural solutions adopted;
- After defining the structural shape, a study of the influence on the wind flow pattern upon the solar collectors is compulsory.

In both cases complex phenomena will appear having in view the following:

- The laminar flow combined with local turbulence pattern imposed by the specific of the surfaces or other obstacles opposing the wind, the shape and volume of the collectors and the local convective effects due to radiation, etc.;
- Complex thermal transfer in the field - convection associated with conduction and radiation;
- Mechanics of the steel structures (static and dynamic response).

The study of the mechanical interaction between the wind and the collectors that is presented further on had in view the prior hypotheses:

- There are different types of solar collectors;
- Design projects are elaborated for the use of the solar collectors, the structural solutions of sustaining the panels and the fixing and anchoring being included in these studies;
- The design of the structures for the sustaining and fixing of the solar collectors has in view mainly the wind action.

2. The aerodynamic field surrounding the solar collectors

There are several situations that characterize the wind action upon the solar collectors in fact the wind solar collectors' interaction, because the wind characteristic features (the wind attack angle, the local spatial turbulence, the dynamic frequency, the turbulence scale) are influenced by the collectors. We may put in evidence here:

- The position of the solar collectors placed on a volumetric compact building;
- The grouping of the solar collectors that may be alone or in several rows;
- The system adopted for the fixing the collectors that may be detached from the plane of roof.

In order to evaluate the altered shape of the distribution of the wind pressure on the roof of low rise buildings equipped with solar collectors an experimental research program was developed in the Atmospheric Boundary Layer Wind Tunnel of the Laboratory of Buildings Aerodynamics from the Faculty of Civil Engineering and Building Services in Iași.

The Romanian code for wind loading on structures based on EUROCODE 1 [1,2], regarding the evaluation of wind forces on structural elements is determined with the relationship:

$$F_w = q_{ref} c_e(z) c_f c_d A_{ref} \tag{1}$$

In the case of the flat (or plane) solar collectors, the coefficients of the force of wind pressure c_f may be determined as global coefficients, thus obtaining the resultant of maximum local wind force action for different directions of the wind directions. Also, these coefficients are evaluated locally, on smaller surfaces, the maximum wind pressure being put in evidence in this way.

The expression of the local coefficients acting on the plane of the collector will be an algebraic sum:

$$c_{LR} = \pm c_{ns} \pm c_{ni} \tag{2}$$

between the coefficients determined on the external surface of the collector, placed usually in wind, c_{ns} and the internal pressure coefficient, c_{ni}, determined on the surface placed usually in the wake of the wind action (fig. 2).

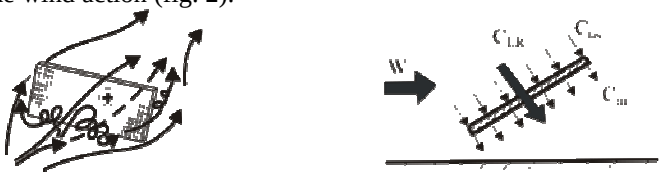

a. b.

Fig. 2. The wind flow around a plate inclined with an angle from the wind direction, (a) and the elements of determination of coefficient c_{LR}, (b)

The code gives information concerning the wind local pressure coefficients on a mono pitched roof, not having in view the particular situations of several parallel inclined surfaces very closely situated one to the other, as in the case of the rows of solar collectors. In the same time, the influence of the surroundings upon the distribution of wind pressure on the surface of the solar collectors is not considered explicitly. The studies in the atmospheric boundary layer

tunnels on physic models may enlarge the knowledge on the behaviour of these elements facing the real wind effects.

3. Experimental research in Atmospheric Boundary Layer Wind Tunnel

Studies in A.B.L. tunnels are based mainly on a thorough physical modelling at scale, both of the buildings or different structures and of the wind action in the boundary layer closely situated to the ground level. The model of a standard low rise building at a 1:50 scale was made, the category of roughness being the one specific for usual urban environment (fig.3a).

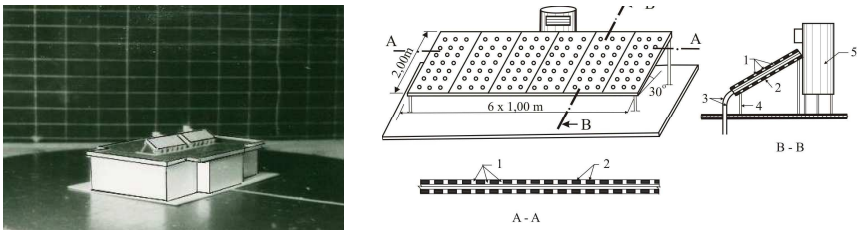

a b

Fig. 3. a.-The model of the building: B/H=0.70; H/L=0.20; b.- The model of the solar collector module IST 1x6: 1- pressure taps, 2- cellular spaces for averaging the wind pressure, 3- pressure tubes connecting the taps with the pressure transducer, 4- sustaining piles, 5- tank.

Being placed longitudinal to the axis of the tunnel, a 15º rotation of the building model, allowed the measurements of the wind pressure acting in skewed directions with respect to the building.

The solar collectors system IST 1x6 is made of 6 plane collectors placed with the short side horizontally and in parallel rows, very closely situated, the angle of inclining from vertical plane being 60°. The module has the dimensions of 6.00x2.00 m and a cylindrical tank centrally placed is fixed behind the row of collectors. The plates were modelled in such a way that the measurement of the resultant pressures will be attained (c_{ns} and c_{ni} in fig. 2b) on every surface of the plate (fig. 3b), without affecting the free space under the solar collectors.
The solar collector modules were placed in several versions: (a) a single module, (b) two modules placed close on to the other, (c) three modules placed one behind the other (d) four modules placed in pairs on two rows.

Once mounted on the roof, the solar collectors systems IST 1x6 will alter the distribution of the wind pressures. The deviation of the wind flow in the impact area with the building (roof or terrace edge) will increase the effect of suction upon the collectors. The graphs in figure 4 put in evidence the forces (integrating the local pressures on the whole surface of the planes in different versions studied).

The values of the coefficients are determined based on the values of the reference pressure considered at the terrace (roof) level of nearby buildings.

The wind flow in the pressure field in which the solar collectors are placed is complex and influence by the geometry and dimensions of the building and in the same time by the wind incident angle.

The presence of the vortices detached from the edges of the roof and at the corners, increase the turbulence around the building itself therefore, placing the collectors in this area being avoided.

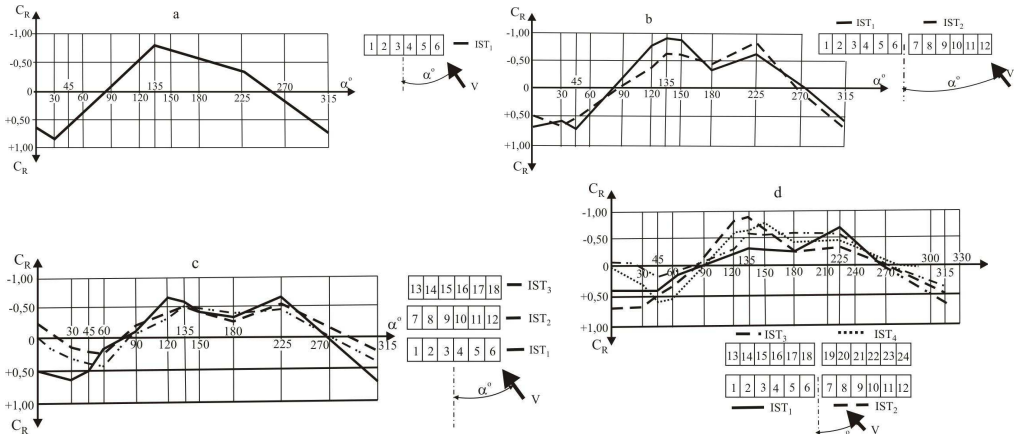

Fig. 4. Local pressure coefficients (C_{LR}) in the different studied versions (a....d)

4. Conclusions

The study of the wind action upon the solar collectors in A.B.L. wind tunnels is necessary due to the complexity of the theoretic model of the turbulent flows and also due to the mutual interaction between the air flow and the field in which the collectors are situated. Interaction between the wind and the solar collectors is influenced by the wind dynamic characteristics (wind direction, frequency of the fluctuations, turbulence scale), by the building itself and by the collectors (position, grouping, system of fixing adopted). Wind action upon the solar collectors summarizes numerous effects caused by the complex obstacles between the wind action and the collector itself. For example, in the case of the solar collectors placed in parallel rows a sheltering effect was put in evidence.

The interaction between the number of the solar collector placed on the building and their distribution and on the other hand, the shape and the dimensions of the building have a capital influence upon the distribution of the wind pressure upon the solar collectors themselves. All these elements are very important in the process of optimizing the design of the whole system of modular plane solar collectors IST 1x6.

References

[1] RADU, A., AXINTE, E., TEHOHARI, C., *Steady wind pressures on solar collectors on roofed buildings*, In Journal of Wind Engineering and Industrial Aerodynamics, 23 (1986), p. 249-258, Ed. ELSEVIER Amsterdam, ISSN 0167-6105.

[2] RADU, A., AXINTE, E., *Wind forces on structures supporting solar collectors*, In Journal of Wind Engineering and Industrial Aerodynamics, 32 (1989), p. 93-100, Ed. ELSEVIER Amsterdam, ISSN 0167-6105.

[3] AXINTE, E.: *Modelarea fizică a interacţiunii vânt-structură pentru proiectarea captatoarelor solare*, Teză de doctorat, I.P. Iaşi, 1988.

[4] AXINTE, E.- PESCARU, R.A: *Studiul acţiunii vântului în tunel aerodinamic*, Ed. tehnică, ştiinţifică şi didactică "Cermi" Iaşi, 2000, ISBN 973-8000-51-3

[5] WOOD, GS., DENOON, RO., KWOK, KCS.,: *Wind loads on industrial solar panel arrays and supporting roof structure* - all 2 versions - Wind and Structures, 2001 - csa.com

[6] WOOD, GS., DENOON, RO., KWOK, KCS, EDDY, BJ., WORRALL, SJ.: *Influence of Solar Panel Arrays on the Wind Loading of Industrial Roofs* - First International Symposium on Wind and Structures for the, 2000 (WAS2000) - Techno-Press

[7] ENV 1991-2-4/2000: *Eurocode 1: Bazele calculului şi acţiuni pe structuri – Partea 2-4: Actiuni asupra structurilor- Acţiunea vântului*

[8] NP-082-04: *Cod de proiectare. Bazele proiectării şi acţiuni asupra construcţiilor. Acţiunea vântului*

Transcom 2009, 22-24 June 2009
University of Žilina, Žilina, Slovak Republic

Using of Traffic Detection Device SR4 in Transport Survey (Transport Survey on Obvodová Street)

[*]Martin Bartovic
[*]University of Žilina, Faculty of Civil Engineering, Department of Highway Engineering, Univerzitná 1, 010 01 Žilina, Slovakia, martin.bartovic@fstav.uniza.sk

Abstract. The text briefly introduces the reader by the using of traffic detection device SR4 from Sierzega Elektronik GmbH in real survey and evaluation possibilities of data recorded by the device with using the supplied software.

Keywords: traffic flow, traffic detection device, speed, vehicles

1. Introduction

The traffic detection device SR4 can be used in the surveys, which is necessary to know the basic, respectively derived characteristics of the traffic flow. It can be used as a separate research facility or as complementary to the facilities pursuing noise, emissions and pollutants. The article presents possible types of evaluation on an actual survey example.

The article presents the partial evaluation of actual survey on the Obvodová Street., which is held from 9.3.2008 to 16.3.2008

The facility is owned by the Department of Highway Engineering, Faculty of Civil Engineering, University of Žilina.

2. The device parameters and measuring methodology

The device operates on the Doppler Effect principle.

Doppler Effect *is called the change in wavelength (and hence frequency) of electromagnetic or acoustic waves caused by the relative motion of source and observer*

So the device during his operation time sends radar waves in the traffic flow, whose wavelength varies due to the movement of passing vehicles. This change will evaluate the device and provide as an output (along with other characteristics) speed of vehicles.

The device is placed on a road sign column or on a freestanding tripod. So that the radar beam and the traffic lane form an angle of 30°.

Due to their size and when it is placed on an upright traffic sign is the device unobtrusive, which ensures that it hasn't a affect on the traffic flows. With this is the credibility of the obtained results ensured.

Fig. 1. Placing of the measuring device on an upright traffic sign.

The device works with the following technical parameters

Measuring range: **8** to **255 km/h**
Accuracy of measurement:
Speed: **3%**
Vehicle length: **20%**
Safety distance: **0,2 s**

Fig. 2. Device hull and his components

and is able to operate for a period of circa 72 hours (dependent on battery charge and weather conditions) at operating temperatures from -20 to 60°C. The device has a recording capacity of 430 000 vehicles, whereby the internal memory record the speed of each vehicle, his length, the time in which the vehicle was recorded and the time lag from the previous vehicle. With the software supplied to the device can be then these data statistically processed and evaluated.

3. Software processing of the recorded data

Data recorded by the device are transmitted to the computer through a Bluetooth signal. The basic software interface display, after downloading of the recorded data, the measured values, filter settings for the recorded data, basic statistical evaluations and his parameters and the graphical evaluation with his adjustments given by the software.

4. Data evaluation obtained from the survey by traffic detection device

The survey on Obvodová Street was held from 9.3.2009 to 16.3.2008. It was a continuous survey, which began on 9.3.2008 at 8:00 and ended 16.3.2008 at 8:00, what gave a uninterrupted record from 168 hours.

Due to the limited number of sites are below listed just the main types of graphical evaluations supported by the supplied software (Fig. 3-5).

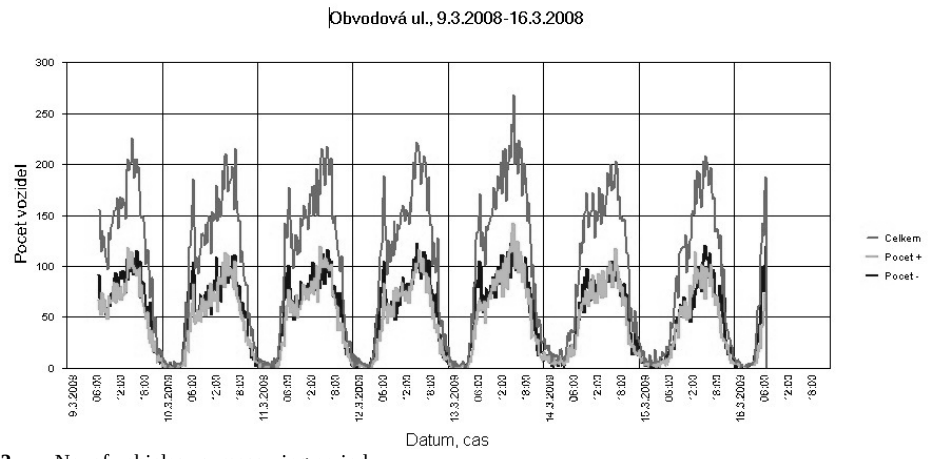

Fig. 3. No. of vehicles vs. measuring period

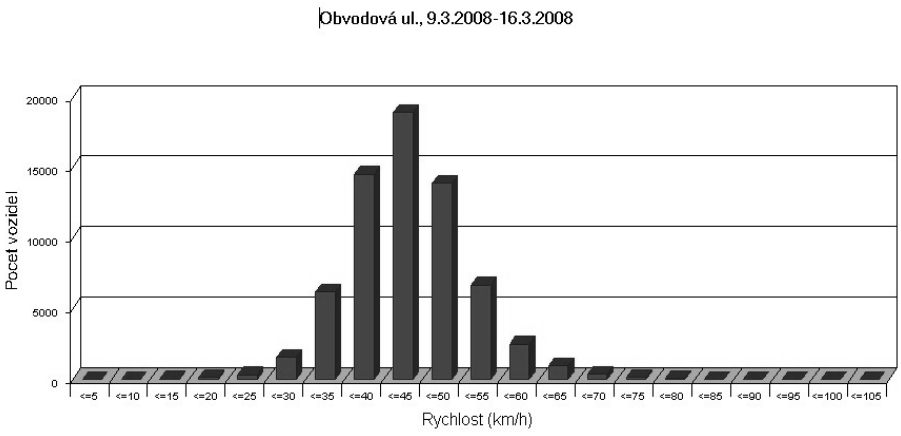

Fig. 4. No. of vehicles vs. speed

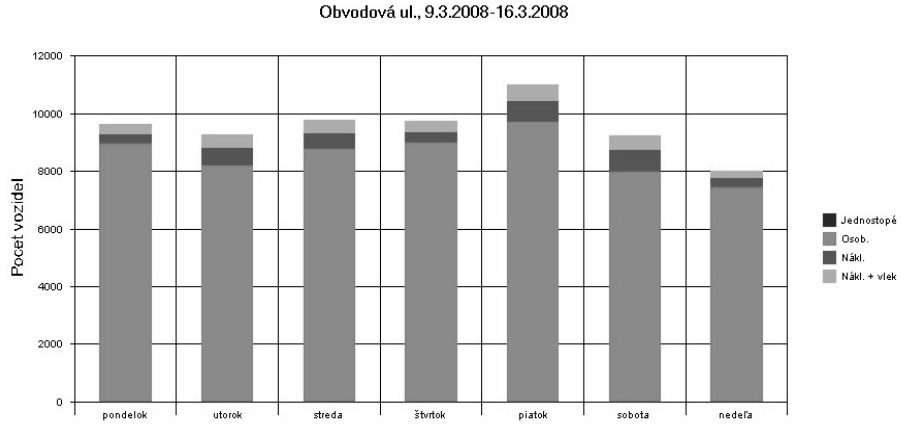

Fig. 5. No. of vehicles in category 1 to 4 vs. weekday

As is evident from fig.3 highest traffic intensity was reached on Friday, 13.3.2008 at 16:15 to 16:30. The device differs the vehicles in 4 categories according to their length, in the record can not be distinguished between the public transport vehicles and trucks.

By creating of graphical evaluation, can the user define the time and speed interval and so adjust the output to given specifications. By creating of graphical evaluation will be at the same time a table created which can be exported, as well as a basic range of recorded data, to a text file, respectively to a spreadsheet editor file. This can be used if the graphical evaluation given by the software is nonconforming with the requirements, or if the offered option does not contain the required evaluation style.

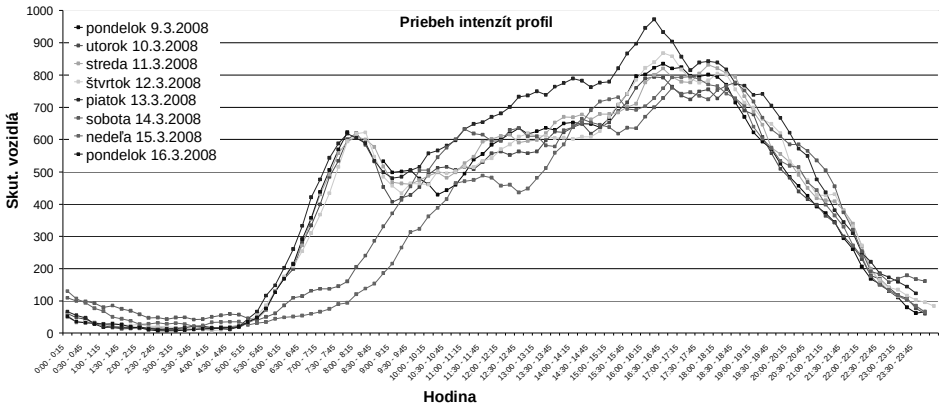

Fig. 6. Traffic intensity at the survey time (after exporting from the processed data into a spreadsheet editor)

Since the software does not support the evaluation of intensities used in the transport engineering was used, for his creating, the possibility to export data into a spreadsheet editor. The result of this process is the graph in fig.6. The peak hour of traffic intensity occurs at the time of 15:45-16:45, which includes the traffic intensity peak quarter-hour of the software offered graphic evaluation.

Fig. 3 and 6 also shows the difference between weekend traffic and traffic during the working week, which creates two separate peaks of intensity. The first occurs in the morning (8:00-8:30), when residents of adjacent settlement move to work and the second in afternoon peak, while the difference between these two peaks represents the volume of traffic attracting of the shopping centers. During the weekend it's this morning peak missing and the intensity reaches the peak around the 17:00. Course of intensities can be divided into three groups:

1.) Intensity in the days of Monday to Thursday, when the intensities have a very similar course,

2.) Friday - when in the afternoon hours occur the shopping peak

3.) Weekend traffic without morning peak

Fig.4 shows the speed distribution of traffic on the road. Most of the vehicles are moving in the speed range 35-50 km/h, but it is also visible a partial overrun of the maximum speed watt was at the survey time 50 km/h. This overrun constitutes 24% of the traffic volume and is only a few exceptions in the range of 10 km / h.

5. Conclusion

The device is a great benefit to traffic surveys. It fully replaces people as a census of traffic and works without a break in all weather conditions and in contrast to the manual traffic counting offers it as an output transport stream characteristics such as speed and time gap of separate vehicles, from which can be derive more traffic flow characteristics.

Transcom 2009, 22-24 June 2009
University of Žilina, Žilina, Slovak Republic

Spectral Analysis of the Bridge Structures

[*]Zuzana Bergerová, [*]Daniel Papán,
[*]University of Žilina, Faculty of Civil Engineering, Department of Structural Mechanics, Komenského 52, 01026 Žilina, Slovakia, zuzana.bergerova@fstav.uniza.sk
[**] University of Žilina, Faculty of Civil Engineering, Department of Structural Mechanics, Komenského 52, 01026 Žilina, Slovakia, dano@fstav.uniza.sk

Abstract. The paper deals with spectral analysis of selected two roadway bridges excited by road and railway traffic. The frequency parameters were also obtained from analytic model via *FEM* software. For both bridge structures the comparisons between theoretical and experimental spectral parameters were performed.

Keywords: spectral analysis, analytic model, random vibration, frequency transfer, natural frequencies and modes.

1. Introduction

The increasing of the traffic intensity seems to be actual problem. Many buildings and bridges are situated near roads, railways and they are affected by paraseismic load due to traffic means. During the structure lifetime a moving load causes structure fatigue and cracks and the service and additional dynamic loads may decrease serviceability of the bridge in future. One of the most useful methods of the bridge structure assessment are theoretical and experimental evaluation of the spectral characteristics of all subsystems (traffic mean, soil, structure, ect.).

2. Theoretical spectral analysis functions

The parasiesmic vibration of the structures can be analysed by random vibration approach mainly in evaluation areas as follows [1]:

- **The time domain (signal in time),**
  effective value (mean value, max value, min value, ect.)

$$\sigma_x = RMS = x_{ef} = \sqrt{\frac{1}{T}\int_0^T x(t)^2\,dt}\,. \tag{1}$$

- **correlation (correlation between two random processes),**
  autocorrelation function (cross correlation function, ect.)

$$R_{xx}(\tau) = \lim_{T\to\infty}\frac{1}{T}\int_0^T x(t)x(t+\tau)dt\,. \tag{2}$$

- **the frequency domain (harmonic analysis),**

- **spectral evaluation (transformation time processes to frequency domain),**

  power spectral density

$$G_{xx}(f) = 2\int_{-\infty}^{\infty} R_{xx}(\tau) e^{-i2\pi f\tau} dt \cdot \tag{3}$$

  coherency function

$$\gamma_{xy}(f)^2 = \frac{\left|G_{xy}(f)\right|^2}{G_{xx}(f) G_{yy}(f)} \leq 1. \tag{4}$$

  gain factor, transfer function

$$H(if) = \frac{G_{xy}(f)}{G_{xx}(f)}. \tag{5}$$

- **probabilistic area (statistic parameters),**
- **informatics (effective – determined signal in noise).**

3. The traffic means and bridge structures spectral characteristics

For the base frequency parameters of the traffic means (vehicle, train) a very simplified analytic models were created. The stiffness constants method was used for calculation on two variants of analytic model:

- quarter planar model (one axle of vehicle)
- space model (according most characteristic masses)

The parameters for computing model creation were considered as a standard average values from literature [2] for full and empty traffic mean.

The bridge structures base dynamic parameters are obtained from software – system *IDA NEXIS* using FEM approach. This system enables to crate space and plane dynamic model respecting geometry, mass distribution and border condition of the bridge structures[3].

4. Spectral analysis – case studies

The dynamic response of the existing bridge structures were received via relevant measurement equipment. All presented off-line experimental measurements were performed by Laboratory of the Department of Structural Mechanics, Faculty of Civil Engineering, University of Žilina instrumentation. Fig.1 shows the scheme of the measure equipment setup.

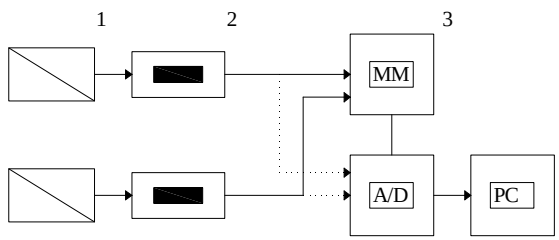

1 – accelerometers
(B&K 8306,Robotron KB12-RFT)
2 – integration amplyfiers
(B&K 2635, Robotron 00042)
3 – recording source (B&K 7005)
laptop or PC with software (DAS 16, DISYS,NI LabView) with
A/D converter

Fig. 1. Experimental equipment.

Case studies on the selected bridge constructions and selected locations:

Spectral characteristics – Bridge over the road to Kysuce – Žilina.

The bridge structure measurement and evaluation of vibration due to traffic means from roadway Kysuca – Žilina were performed. The *FE* model and numerical results were also calculated and compared with experiment (Fig. 2).

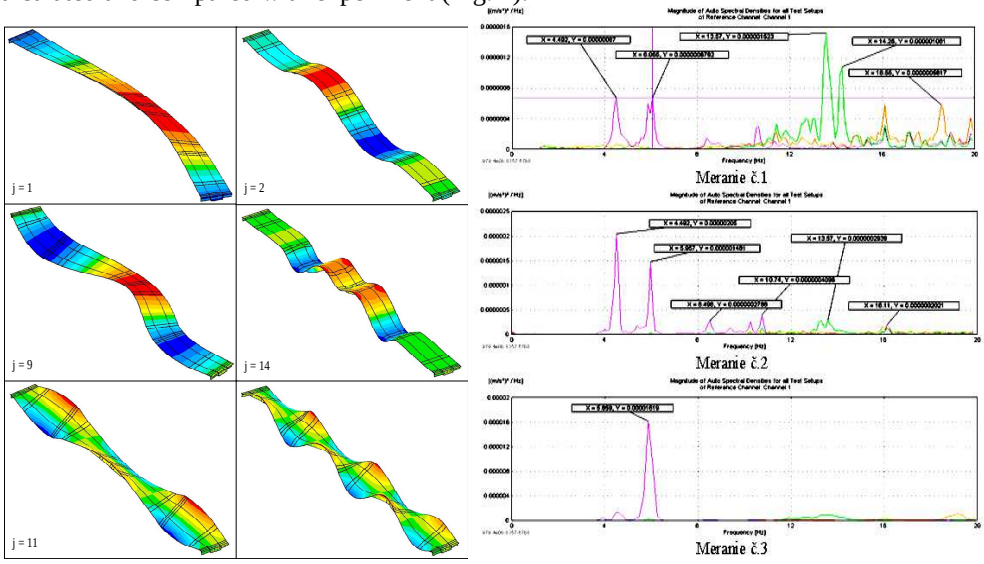

Fig. 2. Bridge over the road to Kysuca – Žilina case study spectral characteristics examples.

Spectral characteristics – Bridge Near TESCO hypermarket – Road CI / 11 Žilina – scaffold bridge

The bridge structure measurement and evaluation of vibration due to traffic means from railway Žilina – Košice were performed. The *FE* model and numerical results were also calculated and compared with experiment (Fig. 2).

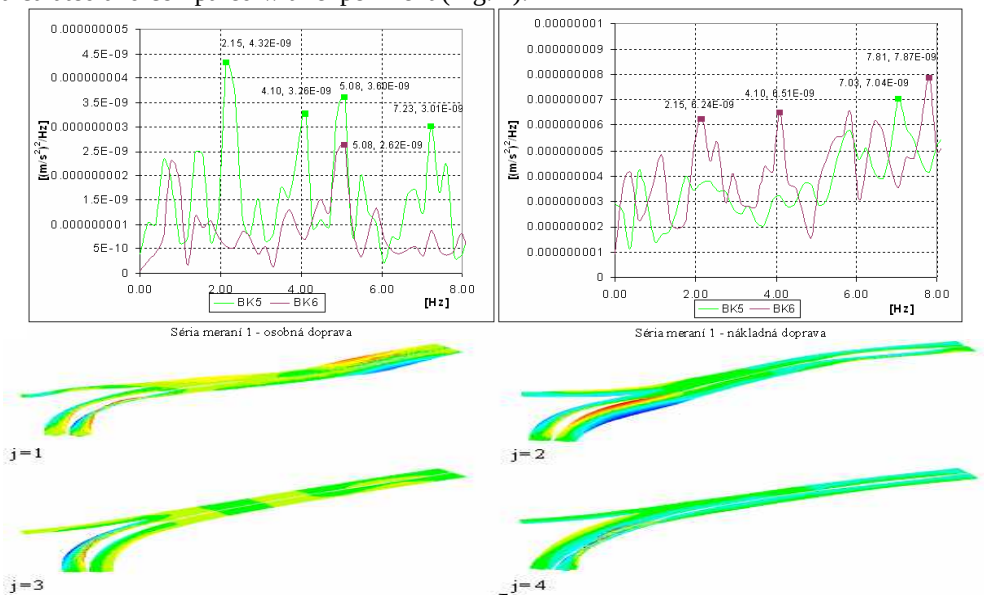

Fig. 3. Near TESCO hypermarket – Road CI/11 Žilina – scaffold bridge case study spectral characteristics examples.

Vibration of the soil due to traffic means

Near the inspected bridge structures the measurement of the vibration due to traffic means were performed. The ground vibration intensity decreasing in dependence on the distance from the vibration source was proceed. The gain factor functions and the other spectral functions were also analyzed in two locations: Near the MŠK Žilina football stadium (roadway traffic) and near Teplička nad Váhom (railway traffic). The results examples are on Fig. 4 and Fig. 5.

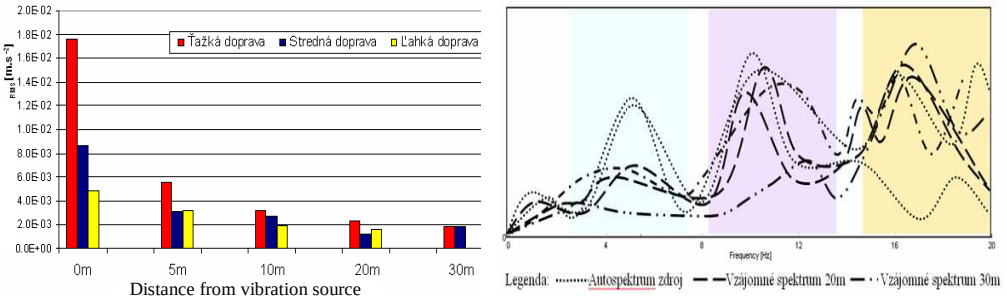

Fig. 4. MŠK Žilina football stadium locality results examples.

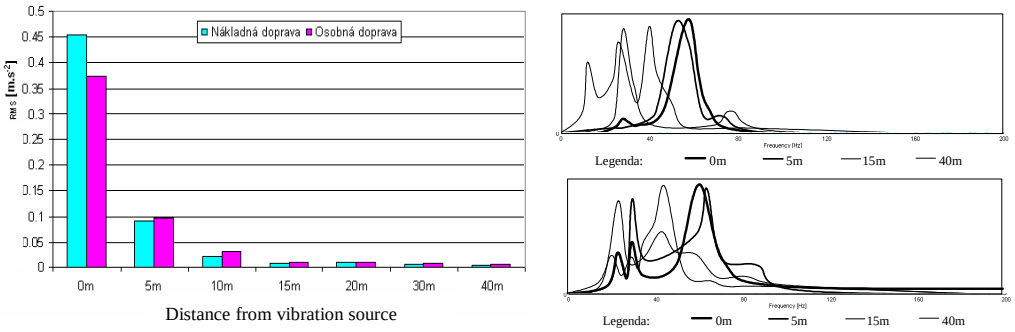

Fig. 5. Teplička nad Váhom results examples.

5. Conclusions

The main aim of the analysis was to identify the spectral characteristics of selected bridge structures and response due to microtremor effect involved by roadway and railway traffic. For both bridges the dominant frequency bands were identified which correspond to natural frequency peaks in numerical model. For all these case studies of the selected bridges the frequency transfer functions (via spectral characteristics) were obtained. The vibration level which decreases depending on the distance from the vibration source was observed. These case studies showed some dominant frequency bands of bridges dynamic response for railway and for roadways.

References

[1] BENČAT, J. , BERGEROVÁ, Z. *Prenos vibrácií a odozva konštrukcia v procese interakcie základová pôda - budova*., Stretnutie katedier stavebnej mechaniky, Gabčíkovo, 2008.

[2] MELCER, J. *Dynamické výpočty mostov na pozemných komunikáciách*, EDIS ŽU, Žilina, 1997.

[3] PAPÁN, D. *Spektrálne charakteristiky zaťaženia a odozvy mostných konštrukcií vo vzťahu k technickej seizmicite – dizertačná práca*, Žilina, 2008.

Transcom 2009, 22-24 June 2009
University of Žilina, Žilina, Slovak Republic

Influence of Binder Content on Permanent Deformation Resistance by Cyclic Triaxial Compression Test

[*]Tomáš Bežilla
[*]University of Žilina, Faculty of Civil Engineering, Department of Highway engineering, Komenského 52, 01026 Žilina, Slovakia, tomas.bezilla@fstav.uniza.sk

Abstract. Wheel tracking tests are mainly used to verify a permanent deformation resistance of asphalts. A triaxial test can eliminate disadvantages of these tests, particularly the different stress distribution in a test sample in comparison with a pavement. Some research results and conclusions signifying a possibility to use the triaxial test to determine the influence of binder content to permanent deformation resistance are presented in the paper.

Keywords: asphalt, triaxial test, creep curve

1. Introduction

One of the properties required in asphalt mixes design is their resistance to permanent deformation. In the case of specifications of asphalt concrete, the permanent deformation resistance is verified on the base of results of wheel tracking test or cyclic triaxial compression test. Cyclic triaxial compression test better simulate a process of asphalt mixes stress in real pavement. The results acquired from triaxial test depend on composition of asphalt mix (the type and amount of material) and test conditions. Research task has been to determine influence of binder content on creep speed by triaxial test under test conditions defined for wearing courses and binder courses.

2. Testing and results

The research of influence of binder content was realized with one type of asphalt mixture AC 11 with gradation corresponding to asphalt mixture ABS aggregate limits gradation [3]. Tests were made on mixtures with different content of binder. Specifically with optimal content of binder 4,6 % estimated on the based of specific aggregate surface, under optimal content 4,2 % and over optimal content 5,2 %. The asphalt mixture contains polymer modified asphalt.

There were made test samples (Marshall sample) from asphalt mixture. They were compacted for wearing courses conditions (2x75 numbers of blows of Marshall compactor) and binder courses (2x50 numbers of blows of Marshall compactor). Samples were tested in the triaxial chamber according to test conditions presented in Tab.l. From the record of axial deformation dependence on amount of the repeated loading (Fig.1 and Fig.2) there is evaluated the mixture resistance to permanent deformation. The results acquired from tests of mix designed for wearing courses cannot be compared with results acquired from tests of mix designed for binder courses. It's due to differences of test conditions for wearing courses and binder courses.

Tab.1 The test conditions for wearing course and binder course [1]

Layer	Tempering temperature	Test temperature	Side compression	Axial load	Frequency	Impulse form
wearing course	15 °C	50 °C	150 kPa	300 kPa	3 Hz 1s/1s	sinusoid blocks
binder course		40 °C	50 kPa	200 kPa	3 Hz 1s/1s	sinusoid blocks

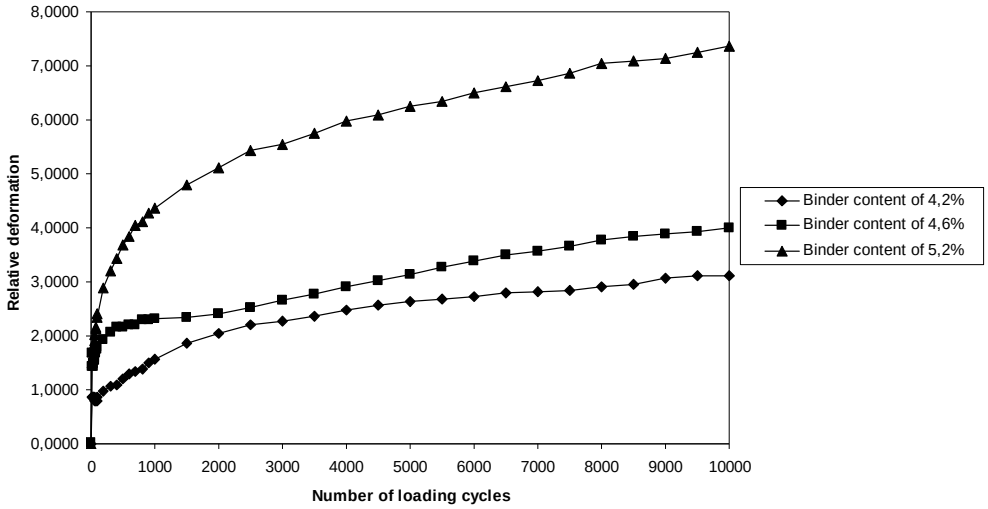

Fig. 1. The creep curve of AC11 for wearing course

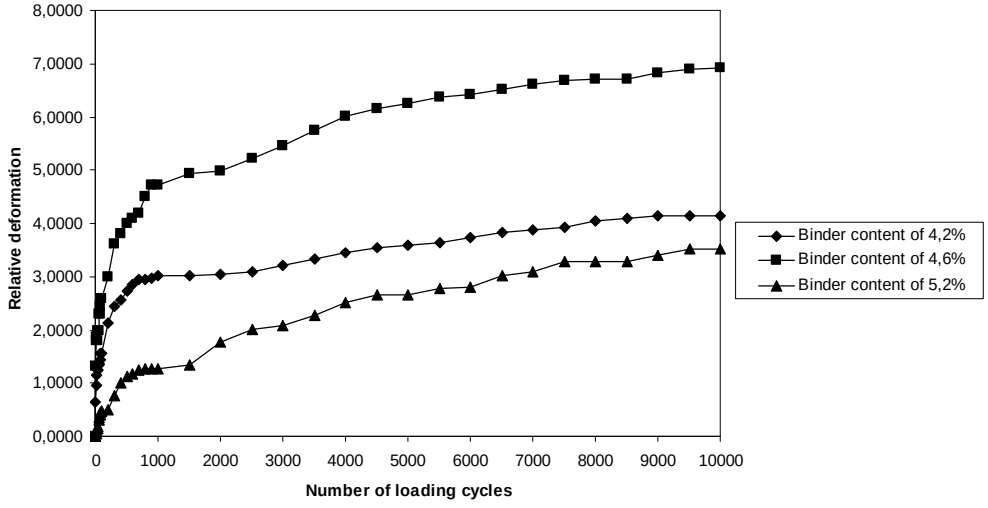

Fig.2. The creep curves of AC11 for binder course

The results displayed in Fig.1 and Fig.2 can be explicated so that, the steeper is creep curve in linear part the more susceptible is the asphalt mixture to permanent deformation. Current research showed that the cyclic triaxial compression test allows differentiate asphalt mixtures with different content of binder on the base of the creep curve slope. Interesting result is observation that the final slopes of the linear phase of the curve are approximately similar for mixtures not exceeding optimal content of binder. If binder content exceeds the optimal quantity of binder, slope of the linear phase of the curve will be steeper and increase of deformation is faster. A mixture with excessive binder content will be more susceptible to deformation.

3. Evaluation of Experimental Measurements

Then following ~~of~~ the creep curve evaluation, the asphalt mixture resistance to permanent deformation is reviewed on the base of the creep rate *f*c for particular mixes according to [2]. It has been supposed that there will be visible differences between particular values of creep rate *f*c after evaluation on the based of different creep curve slopes for particular binder content in the mixture.

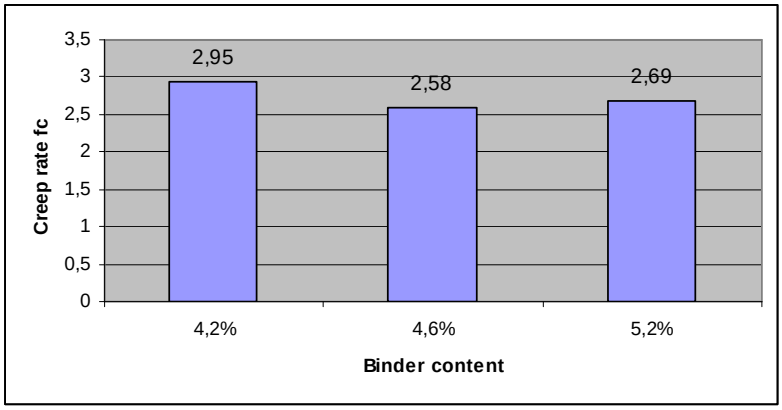

Fig.3 Parameter *f*c values of AC11 for wearing course

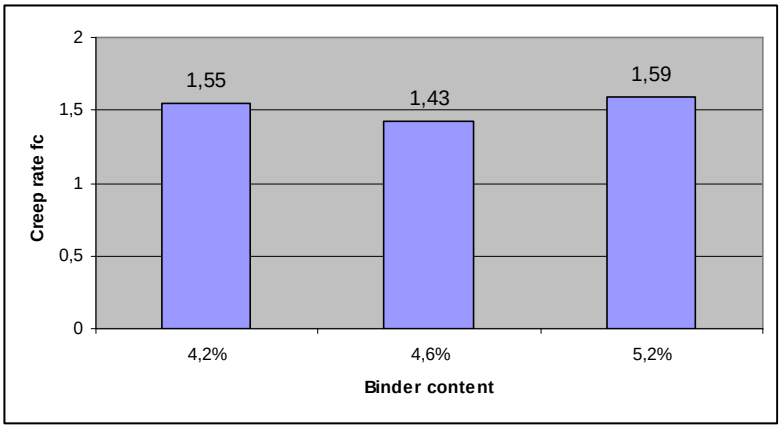

Fig.4 Parameter *f*c values of AC11 for binder course

As can be seen on Fig.3 and Fig.4, all 3 values of parameter *f*c are in the same category. Therefore quality range of asphalt mix with different content of binder cannot be identified - tab.2. All 3 mixtures of AC11 for wearing courses are in the category f_{cmax4} and all 3 mixtures of AC11 for binder courses are in the category $f_{cmax1,6.}$ These differences in categories of the mixture with same content of binder are due to different test conditions, in which the mixture is designed.

Tab.2 Category of creep speed [4]

Creep rate f_c µm/m/n	**Category f_{cmax}**
0,2	$f_{cmax0,2}$
0,4	$f_{cmax0,4}$
0,6	$f_{cmax0,6}$
0,8	$f_{cmax0,8}$
1,0	f_{cmax1}
1,2	$f_{cmax1,2}$
1,4	$f_{cmax1,4}$
1,6	$f_{cmax1,6}$
2	f_{cmax2}
4	f_{cmax4}
6	f_{cmax6}
8	f_{cmax8}
10	f_{cmax10}
12	f_{cmax12}
14	f_{cmax14}
16	f_{cmax16}
without requirements	f_{cmaxNR}

4. Conclusion

From present results it has not been proved influence of binder content. But it has been proved influence of test conditions on parameter *f*c. These are the first test results of the asphalt mixtures resistance to permanent deformation by triaxial cyclic compression test. The measurements next continue with more mixtures with a view to find relation between permanent deformation and the particular factors that influence it.

References

[1] STN EN 13108-20 (73 6163) Bituminous mixtures. Material specifications. Part 20: Type testing

[2] STN EN 12697-25 Bituminous mixtures. Test methods for hot mix asphalt. Cyclic compression test

[3] STN 73 6121 Road building. Asphalt pavement courses, 1996

[4] STN EN 13108-1 (73 6163) Bituminous mixtures. Material specifications. Part 1: Asphalt Concrete

Transcom 2009, 22-24 June 2009
University of Žilina, Žilina, Slovak Republic

Modelling of Precast Prestressed Bridge Girders Under Static Load

[*]Petra Bujňáková, [*]Martin Moravčík
[*]University of Zilina, Faculty of Civil Engineering, Department of Structures and Bridges, Komenského 52, 01026 Žilina, Slovakia, {petra.bujnakova, martin.moravcik}@fstav.uniza.sk

Abstract. Recent possibilities of the numerical modelling of precast prestressed bridge girders based on material models are discussed in this paper. The numerical model of prestressed girder made of different strength of concrete was analysed using finite element method in computing nonlinear system ATENA. Three reduced models of high performance concrete (HPC) prestressed girders and one model of normal strength (NSC) prestressed girder have been constructed, tested and compared to numerical models of flexural resistance under static loading conditions.

Keywords: high performance concrete, numerical model, prestressed girder, flexural loading,

1. Introduction

High performance concrete (HPC) is becoming more widely utilized in bridge structures. The primary reasons for selecting HPC are to produce more economical product, provide a feasible technical solution, or a combination of both. The increasing interest of high performance concrete in the precast, prestressed girders has lead to simulation their behavior under service load. The effective method used to control and often replaced the valid load test is numerical modelling.

The objective of this research is to investigate the experimental and numerical behavior of prestressed girders and provides some recommendations of modelling of HPC and NSC prestressed girder. The load intensity, displacement, crack resistance, stress and strain distribution were monitoring during analysis.

2. Material properties

The performance of concrete had been improved using of chemical and mineral admixtures. These admixtures have to influence of compressive strength, workability and durability of concrete. The high performance concrete differs from normal strength concrete in greater strength from 50 to 120 MPa and less ductile deformation behavior under load. The low water cement ratio w/c of high performance concrete (0,2-0,35) affects the lower total shrinkage and creep than NSC [1].

The performance benefits of HPC are following: long term mechanical properties, early high strength, volume stability, higher modulus of elasticity, longer life in severe environments. The other benefits from utilization of HPC in bridge structures are fewer girders per cross section, longer span length, slender sections, less material, reduced maintenance and extended life cycle.

The autogenous shrinkage of young high performance concrete is significantly higher than NSC, while drying shrinkage is more strongly in NSC. This has practical importance in constraint stresses and must be considered by design.

2.1. Design of prestressed girders

The design of concrete compressive strength for HPC girders was 85 MPa and for reference NSC girder was 55 MPa. The concrete strength of all deck was in range 37 MPa. The concrete deck was cast after 15 days since the girders were fabricated.

The model of the prestressed girders came out from standardized bridge cross section. The shape of the girder was modified for the experimental testing. The length and depth of NSC and HPC girders had an identical length 5,0 m and the depth 550mm, see Fig.1.

The HPC girder designed from concrete class C 70/85, is 430 mm high and the thickness of composite deck is 120 mm. The depth of NSC girder designed from concrete class C 45/55, is 450 mm and the composite deck is 100 mm in thicknesses. The design class of concrete deck was C 30/37. The girders are fully prestressed with low relaxation strands ϕ L_s 15,5/1800 MPa. The HPC girders are prestressed with 6 ϕ L_s 15,5/1800 and NSC girder is prestressed with 4 ϕ L_s 15,5/1800. The spacing between prestressing strands is 50 mm in each girder.

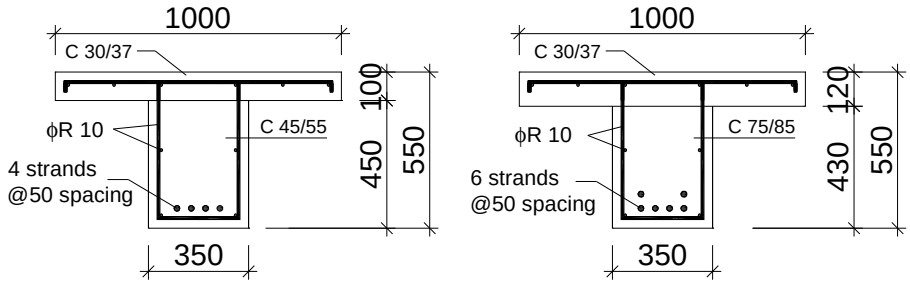

Fig. 1. Girder details - the cross section

During the fabrication process, the HPC and NSC samples were tested in the laboratory at ages 1,2,7,28 and 56 days for its mechanical properties such as, compressive strength, density of concrete and modulus of elasticity. The mechanical properties of concrete gained from laboratory testing at an age 56 days were used in numerical analysis.

3. Numerical analysis

The numerical model was created in computing program ATENA, which is determined for nonlinear finite element analysis of prestressed structures, based on fracture mechanics. It is designed specially for computer simulation of concrete structural behavior under a static load [4].

3.1. Material parameters

Numerical model is based on material model SBETA with experimental values of HPC and NSC compressive strength and modulus of elasticity, see Tab.1. This material model includes the effect of real concrete behavior:

- non-linear behavior in compression including hardening and softening

- reduction of compressive strength after cracking
- tension stiffening effect
- crack models -fixed and rotated crack direction

Material properties			NSC girder	HPC girder	NSC deck
Mean compressive strength	$f_{cm,cube}$	(MPa)	71.40	101.05	52.30
Compressive strength	f_c	(MPa)	60.01	85	43.78
Tensile strength	f_t	(MPa)	4.41	4.9	3.5
Modulus of elasticity	Ec	(GPa)	29.67	40.66	25.30
Poisson´s ratio	μ	(-)	0.2	0.2	0.2

Tab. 1. Material properties of NSC and HPC

The compressive strength f_c has been automatically generated by computing system from measured cube compressive strength $f_{cm,cube.}$

It is much difficult to measure the tensile strength development with time therefore the concrete specimens were not tested on tensile strength. The tensile strength used in numerical analysis was determined by the formula in STN EN 1992-1-1 [3]. Development of the tensile strength of NSC and HPC with time may be estimated from:

$$f_{ctm}(t) = (\beta_{cc}(t))^{\alpha}.f_{ctm} \qquad (1)$$

where

$\beta_{cc}(t)$ is the function to describing the development of compressive strength with time concrete age

α=1 for time $t < 28$ days

α=2/3 for time $t \geq 28$ days

f_{ctm} is the mean tensile strength of concrete at an age 28 days

$$\beta_{cc}(t) = \exp\left\{s\left[1-\left(\frac{28}{t}\right)^{1/2}\right]\right\} \qquad (2)$$

s is the coefficient which depends on the strength class of the cement

The cables are modelled as discrete elements and the bilinear stress-strain law was used for cables and reinforcement. The distance of stirrups was modelled according to experimental model at 100 mm in both girders. The prestressing force in NSC and HPC girder was reduced to the calculated prestress losses at age 160 days, when all prestressed girders were tested.

Each girder was set on fixed abutments through elastic bearings. The geometrical properties and supports of the girders correspond to experimental models of HPC and NSC prestressed girders, shown in Fig. 2.

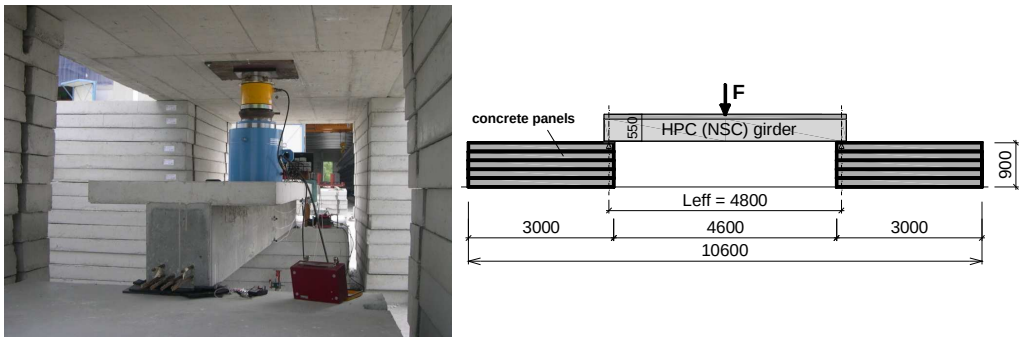

Fig. 2. Experimental model - Loading scheme

The numerical model with longitudinal and transversal reinforcement, prestressing cables, supports, mesh and monitoring points are presented in Fig.3. Load steps were realised incrementally with described displacement at the top of girder.

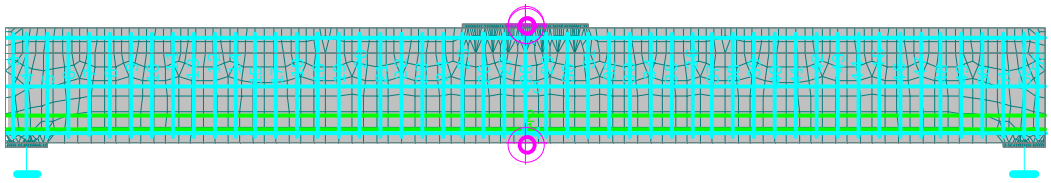

Fig.3. Numerical model of HPC prestressed girder

4. Conclusion

The theoretical value of bending moment of HPC (584.7 kNm) and bending moment of NSC girder (400.1 kNm) in ultimate limit state was exceed but the girders did not reached a failure in numerical and experimental analysis.

The first visible crack of HPC girder was detected at loading force F_{cr}= 400 kN (girder 1) and F_{cr}= 420 kN (girder 2). The first crack in numerical model of HPC was visible at load step F = 412,3 kN. The first theoretical and experimental visible crack of NSC girder was detected at loading force F_{cr}= 255 kN.

Vertical deflection and crack propagation of numerical models are similar to experimental results. The real measured strain of HPC and NSC are lower than theoretical and numerical values given by nonlinear analysis.

The material model SBETA with fixed crack model can be useful for numerical modelling of HPC and NSC prestressed bridge girders. It is possible to simulate a load test without significant problems.

References

[1] Constitutive modelling of high strength/high performance concrete, State-of-art report, fib Bulletin 42, January 2008

[2] STN EN 1992-1-2: Design of concrete structures, part 2: Concrete bridges, 2006

[3] STN EN 1992-1-1: Design of concrete structures, part 1:General rules and actions, 2005

[4] ATENA Program Documentation: User´s manual for ATENA 2D, Praha, March 2005

Transcom 2009, 22-24 June 2009
University of Žilina, Žilina, Slovak Republic

Analysis of Geometric Parameters of Chosen Family Two-Layered Spherical Structures Generated on the Basis of Regular Octahedron

*Dominika Bysiec
*Kielce University of Technology, Al. 1000-lecia Państwa Polskiego 7, 25-314 Kielce, POLAND

Abstract. The aim of the study is to present the chosen family of two-layered frame domes generated from the second method of triangular face subdivision of regular octahedron. It is assumed that the resulting vertices and edges constitute the nodes and members, respectively. Chosen spherical structures reflects the method of two polyhedra joint inscribed in sphere with different R1 and R2 radiuses.

Keywords: regular octahedron-based polyhedra, frame dome, two-layered spherical structures, joining bars, bars length

1. Introduction

To obtain regular octahedron-based polyhedra, with the bigger face's number, each face of the basic octahedron can be divided according to one of three methods.

I method II method III method

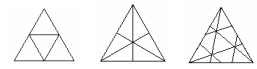

Fig.1. Three methods of face triangulation for a regular octahedron, t,k – consecutive natural numbers.

t \ k	1	2	3	4	5	6	7	8	…
1	8	**24**	56	104	168	248	344	456	
2	24	32	56	**96**	152	224	312	416	
3	56	56	72	104	152	**216**	296	392	
4	104	96	104	128	168	224	296	**384**	
5	168	152	152	168	200	248	312	392	
6	248	224	216	224	248	288	344	416	
7	344					344	392	486	
8								512	
…									…

Tab.1. Regular octahedron-based polyhedra obtained by applying three methods of transformation.

Using the formula $N=2\cdot(3\cdot n^2)$, we receive 24-hedron, 96-hedron, 216-hedron, etc. that is the consecutive polyhedra generated from the second triangular face division method, which are the subject of study.

24-hedron 96-hedron 216-hedron 384-hedron … etc.

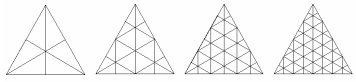

Fig.2. Consecutive face subdivisions using the second method of triangulation to generate regular octahedron-based polyhedra

2. Two-layered spherical structures

The construction of regular polyhedron-based geodesic domes was initiated by R.B.Fuller [2].

The chosen family of two-layered structures was obtained by the proper regular octahedron-based one-layered grids joining [3], [4].

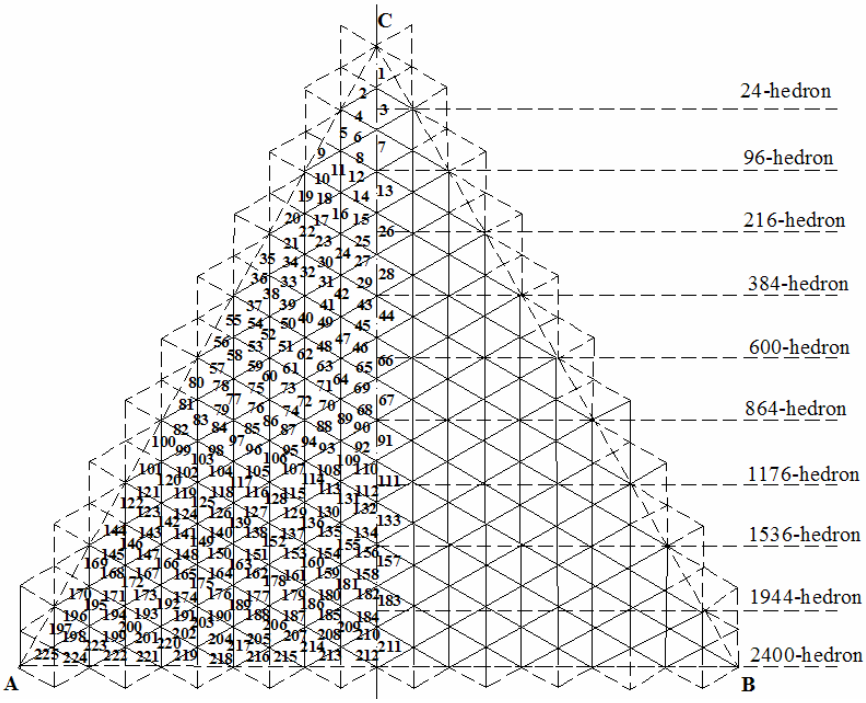

Fig.3. Topology of 1/8 grid of 2400-hedron with bars pointed out.

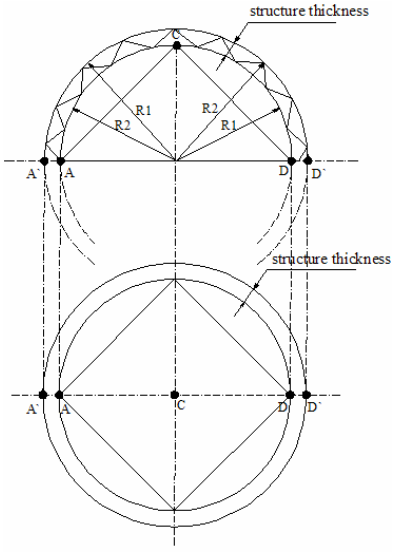

One-layered grids of domes lie on two independent spheres. The distance between them, that is the thickness of two-curvatured structure, is determined by the radiuses R1 and R2 relation of concentric spheres describing nodes of each grid. These nodes are lying on two independent spheres. The thickness change of two-layered structure is possible by the change of spherical radiuses' relation describing nodes of each layer.

The cubature of two-layered frame dome depends on the needs and can be different (smaller - the frame above equator, or bigger – the frame below equator).

Fig.4. Two-curvatured spherical structure created by means of two radiuses of spheres describing nodes of each layer.

On the basis of the second method of triangular face of octahedron division and proper joining method we generate the following two-layered frame domes: 8-hedron/24-hedron, 24-hedron/96-hedron, 96-hedron/384-hedron, 216-hedron/864-hedron, 384-hedron/1536-hedron, 600-hedron/2400-hedron, etc. The analysis, covering structures bars' lengths and joining bars' lengths was carried out for six mentioned examples. The 1/8 part of exampled grid of two-layered spherical structure was presented. The results of bars' lengths were shown in nomogram, assuming R1 = const and R2 = variable for the left part of graph, and R1 = variable and R2 = const for the right part of graph.

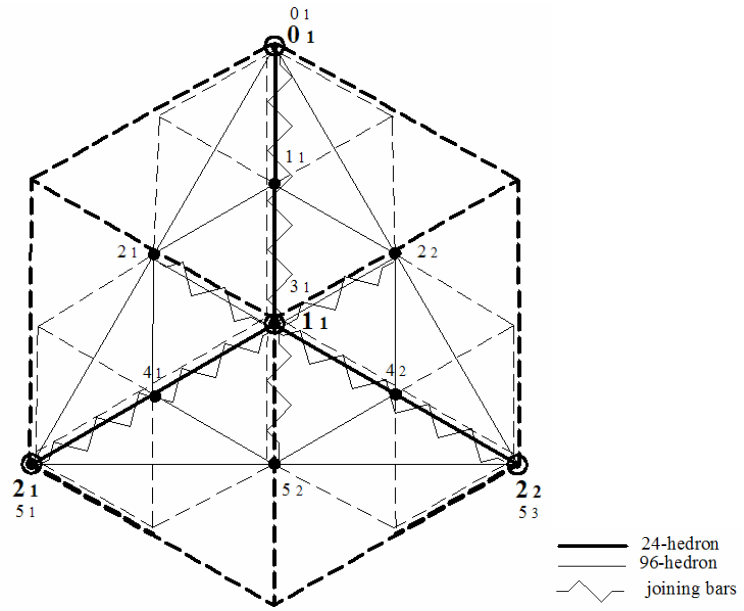

Fig.5. Chosen topology of two-layered bar structures (inscribed in one face of octahedron) generated from 24-hedron and 96-hedron.

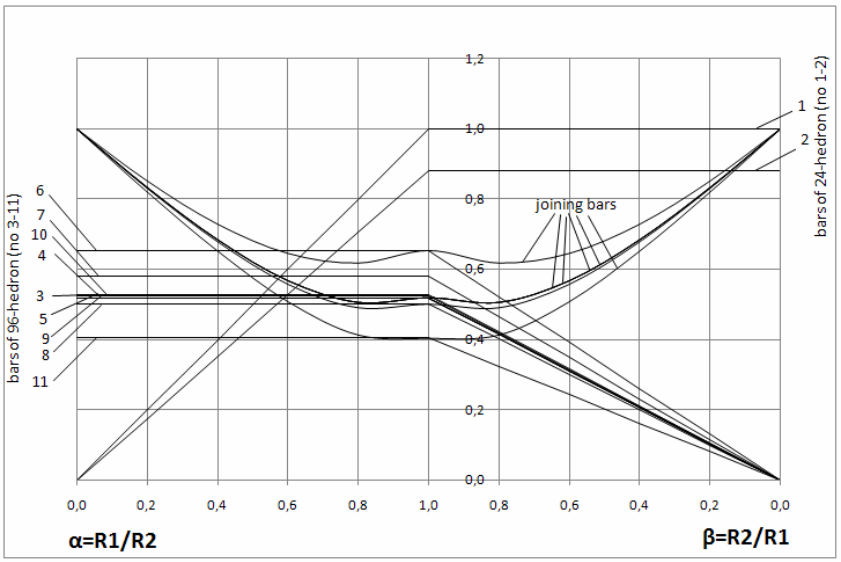

Fig.6. Nomogram of bars lengths exemplified by two-layered structure formed from 24-hedron and 96-hedron.

Taking into account chosen family of six two-layered frame domes, the table (Tab.2.) with numbers of bars and nodes of the whole spherical structures was prepared. The results were presented in the graph (Fig.7.).

consecutive two-layered structures	8/24	24/96	96/384	216/864	384/1536	600/2400
number of internal layer's bars	12	36	144	324	576	900
number of external layer's bars	36	144	576	1296	2304	3600
number of joining bars	16	48	168	360	624	960
total number of bars	**64**	**228**	**888**	**1980**	**3504**	**5460**
number of nodes	**20**	**64**	**244**	**544**	**964**	**1504**

Tab.2. Specification of number of bars and nodes of the whole two-layered structures.

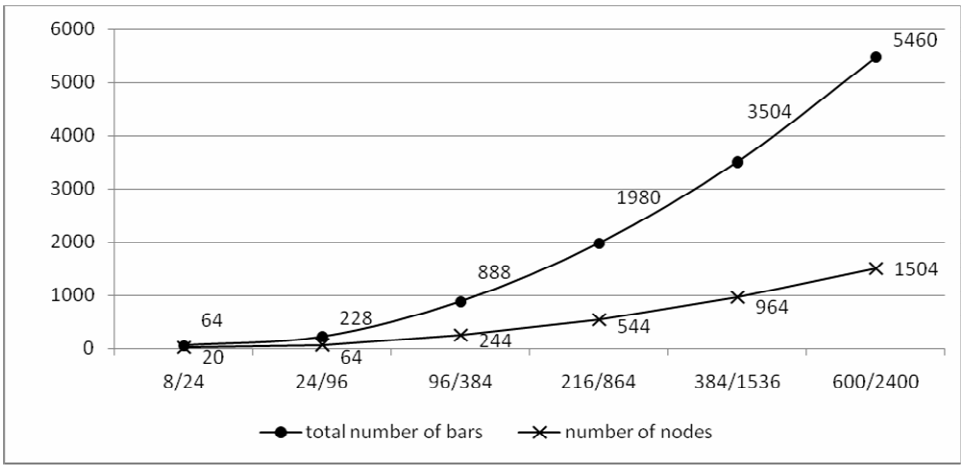

Fig.7. Results of bars and nodes numbers of the whole two-layered structures.

3. Conclusion

Two-layered frame dome, generated by joining bars joints of two one-layered structures is characterized by the lower stability. The thickness of two-layered structure can be different, depending on the change of spherical radiuses' relation describing nodes of each layer.

Two-layered frame domes can be used as structures with the more extensive range than one-layered frame domes. The choice of nodes as the support is free.

The topology and analysis of the chosen family of two-layered spherical structures can be the subject of appropriate structure choice for the designer.

References

[1] FULIŃSKI J.: *Geometria kratownic powierzchniowych.* PWTN. Seria B 178, 1973.

[2] FULLER B.R.: *Geodesic Tent.* United States Patent Office, patent 2, 914, 074, Nov. 24/1959.

[3] MIRSKI J.Z.: *Siatki powstałe z przekształceń 8-scianu foremnego*. ZN. AR we Wrocławiu. Melioracja XLI, nr 212/1992, s.27-39.

[4] BYSIEC D., MIRSKI J..Z.: *Determining the geometric parameters of frame octahedron-based geodesic domes.* XIV LSCE. Warsaw, 5 December, 2008; page 28-33.

Transcom 2009, 22-24 June 2009
University of Žilina, Žilina, Slovak Republic

Examination of Physical Characteristics of the Modified Sand-Lime Products

[*]Ryszard Dachowski, [*]Anna Stępień
[*]University of Technology, Department of civil and environmental engineering,
Al. 1000-lecia P.P.7, 25-317 Kielce, Poland, tobrd@tu.kielce.pl

Abstract. An Important feature of sand-lime products is their high weather resistance. Moreover, they are resistant to biological and chemical corrosion. Friendliness for inhabitants and environment is also one of their many advantages. Undoubtedly, considering its soundproof features, the large weight becomes the advantage in this case. According to factors mentioned above, the purpose of research is to estimate physical characteristics of the modified sand-lime bricks. Examination was focused on the modified products with increased volume weight and the standard products. It used products with the basaltic aggregate and products without any supplements for comparison. Following physical characteristics of the sand-lime bricks have been estimated: impregnability, absorptiveness and gross and net density. Corrected features allow further modification with respect to acoustic.

Keywords: sand-lime products, acoustic isolation, basaltic aggregate.

1. Theoretical foundations

Sand-lime products are an engineering material of a significant endurance. One of their important characteristics is high weather resistance. Sand-lime bricks are very popular in Scandinavia, Germany or Netherlands. They are very friendly for inhabitants and environment as well as resistant to biological and chemical corrosion. Moreover, considering its soundproof features, the large weight becomes the advantage in this case.

The penetration of the sound-absorbing energy through the dam is very dynamic and appears as a result of dam's vibration taken together. Subsequently, the whole structural and material configuration fulfils the part of acoustic insulation.

Dams of a large weight assure sound proofing (acoustic insulation) best. Nevertheless, what is very significant is what weight in count on $1m^2$ possesses the applied material. The best building materials are: concrete, a sand-lime brick and a full brick. In addition, the theory of weight is an important question in this matter [1, 2].

The purpose of examination is to estimate regulated physical characteristics of the material: impregnability, absorption, gross and net density. Later examination intends to prove a hypothesis that decrease of material's capacity would retain its previous features or even improve them. Sand-lime products show a very good soundproof quality.

2. Methodology of experimental examinations

For experimental half-industrial research, the bored sand-lime (solid) brick elements have been prepared with the following dimensions 180 x 150 x 220 mm of the 15th class. These elements have been produced in the Production Plant of Sand-lime bricks according to the latest technological requirements.

The preliminary analysis of various fillers to improve the acoustic insulation as well as physical properties has been executed. Following materials have been chosen for the proposed experimental examinations: barite, basalt, magnetite and hematite as well as silica and ash dust and calcareous meal. In addition, the thickness of particular material groups is an essential criterion.

The above examination intends to prove hypothesis that the decrease of the sizes of material (i.e. sand-lime product) through the usage of one of the above-mentioned fillers, will allow to obtain the identical or even better soundproof features. The choice of the filler was based on many criterions of the economical – technological analysis. The assignment set concerned the production of sand-lime products with a supplement in the form of the basaltic aggregate with granulation of 2 - 4 mm.

Proportional content of the aggregate has been established as 50%. Therefore, the amount of the aggregate has been laid out a priori. Following further examinations, the mathematical planning of experiment tool with the double-factored plan will be applied.

At the given stage, following characteristics have been estimated: impregnability, absorption, gross and net density.

The number of samples, for proportional content of the filler on which the examination will be conducted as well as for the standard product (comparable) (according to PN - EN 771-2:20 06, p. A. 2.4, Figure A.1) amounts to 6 units. Therefore, the examination of heterogeneous features was conducted on 12 samples.

3. Experimental research

3.1. Absorption

Research was conducted according to PN-EN 772-11.

After drying sand-lime products to constant mass in 105^{o}C, samples were left to cool down in the room temperature. Subsequently, they were measured, weighted, and immersed in water in 5 mm depth under the face surface for the specified time.

During the time of conducting the research, water subsidence was filled as a result of capillary rise of the products until the moment of realizing that the products are incapable of further absorption. After the research, water absorption modulus was calculated regarding sand-lime bricks with traditional structure and those modified caused by the capillary rise (mentioned above) for every sample.

3.2. Humidity and impregnability

Research was conducted according to PN-EN 722-10.

Samples were weighted in air-dry condition. Consequently, they were placed in a dryer with air circulation in 105^{o}C. After drying, the products were weighted on the scale with the 0,1% accuracy of measurement of their weight. Humidity of sand-lime bricks w_s was calculated in the ratio to the weight during and after the drying. Subsequently, the products were placed in a dish and immersed in water for next 48 hours. Afterwards, the samples were removed from water, dried, weighted and the results were compared.

3.3. Gross and net density by volume

Research was conducted according to PN-EN 772-13.

In order to determine gross density by volume, the samples (solid elements) were dried in a dryer with air circulation in 105^{o}C. After the sand-lime bricks reached the constant weight, the samples were weighted. Gross volume of the product was calculated by deducting the

volume of holes from length, height and width dimensions. Net density of each sample was fixed, by taking into account omitted holes.

4. Results of experimental research

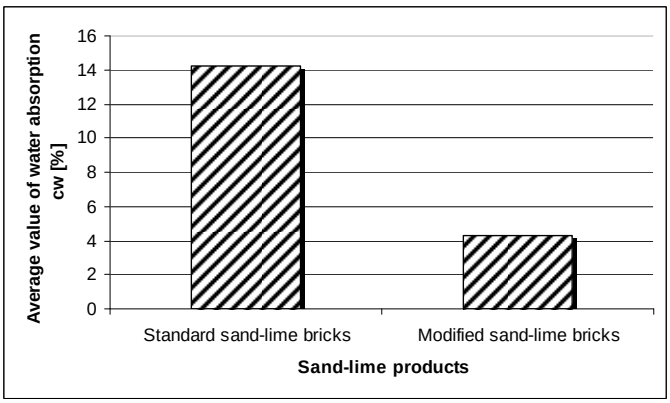

Fig. 1. Water absorption modulus of the standard and modified sand-lime bricks.

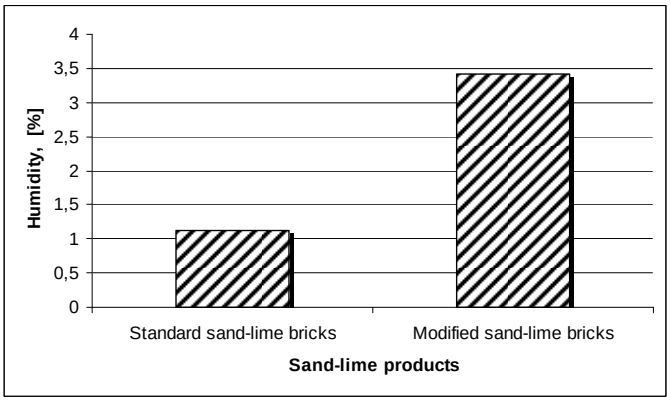

Fig. 2. Humidity value of the standard and modified sand-lime bricks.

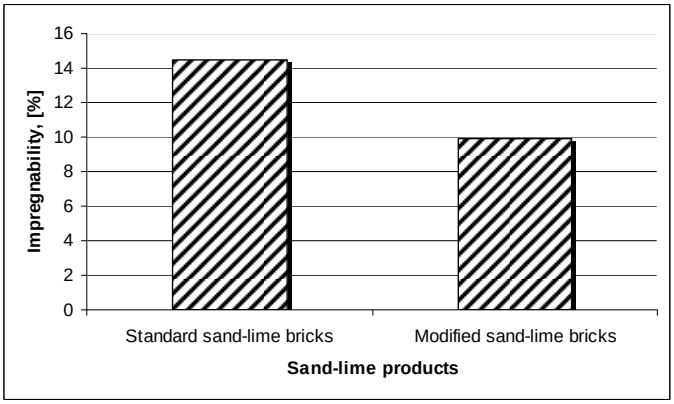

Fig. 3. Impregnability of the standard and modified sand-lime bricks.

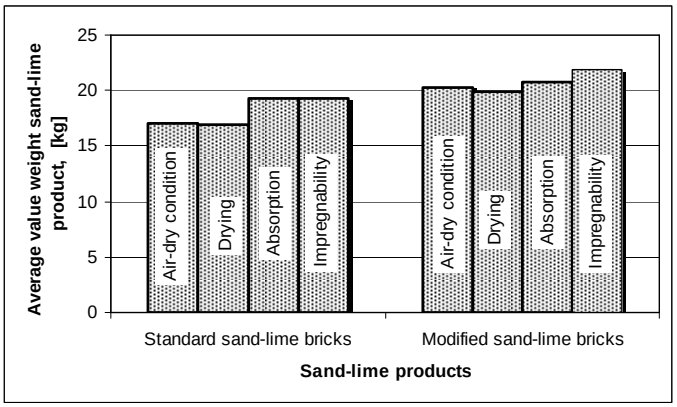

Fig. 4. Weight of the standard and modified sand-lime bricks.

Average value of water absorption in the standard sand-lime products lies in upper limit of admissible norms. It amounts to around 4% for the modified sand-lime products with the basaltic aggregate which is related to contents of the coarse-grained aggregate. Therefore, the capillary rise is definitely lower. Additionally, humidity of the standard products has been decomposed very unequally on the surface of the element, while, the modified products used to absorb humidity relatively equally.

Using normalised indicators during calculating the humidity of products it has been established that average value of humidity of the standard products should fit into 1%. However, in reference to the elements modified by the aggregate, the value is over three times higher.

The above examination entailed the test of impregnability of the sand-lime bricks.

The experiment demonstrated that the standard products with the characteristics of lower humidity and dead weight were capable of absorbing more water than modified sand-lime products.

In each examination the activities of the mass of sand-lime products was observed and documented each time.

5. Conclusions

Conducted research that demonstrated absorptiveness of sand-lime products declared that due to capillary rise the sand-lime bricks with traditional structure absorbed around three times more water than the modified sand-lime bricks.

Test of impregnability has demonstrated similar relationships. Standard products absorbed about 1.5 times more water than the modified products.

Conducted research, which investigated humidity of sand-lime bricks, declared that humidity of the standard products is three times less than the modified products.

References

[1] DACHOWSKI, R, LINCZOWSKI, C. *Porównanie najpopularniejszych ściennych materiałów budowlanych stosowanych w budownictwie jednorodzinnym.* Przemiana. Kielce, 1998.

[2] LINCZOWSKI, C., DACHOWSKI, R. *Silikaty.* Zakład Produkcji Silikatów LUDYNIA Sp. Z o.o, 2001.

Transcom 2009, 22-24 June 2009

University of Žilina, Žilina, Slovak Republic

Experiment vs. Probabilistic Nonlinear Analysis of Shear Failure of Precast Prestreseed Hollow-Core Slab Elematic Type

[*]Jiří Doležel, [*]Drahomír Novák

[*] Brno University of Technology, Faculty of Civil Engineering, Institute of Structural Mechanics, Veveri 331/95, 605 00 Brno, Czech Republic, dolezel.j@fce.vutbr.cz, novak.d@fce.vutbr.cz

Abstract. A hollow core slab is a precast, prestressed concrete member with continuous voids provided to reduce weight. Primarily used as floor or roof deck systems, hollow core slab also have application as wall panels. From statical point of view we take construction unit as simply supported beam with uniform continuous load. An assumed mechanical failure of unit occurs after exhaustion of load bearing capacity resp. shear capacity or its combination. This paper presents the comparison of probabilistic nonlinear analysis with real experiments to check the shear capacity (one line loading by ČSN EN 1168) of given unit type. Probabilistic analysis is based on numerical simulation of Monte Carlo type (Latin Hypercube Sampling) and FEM analysis. Parameters of nonlinear computational model are considered as random variables including statistical correlation.

Keywords: Precast prestressed hollow-core slab, nonlinear analysis, probabilistic analysis, random variables, experiment.

1. Introduction

The hollow core slab ELEMATIC type is precast prestressed mass produced element lightened in its length by six hollows. Seven prestressing strands with low relaxation, 1860 S-12.5, are placed at bottom edge. Concrete is toughed as class C50/60. Basic material and design statical characteristics of panel was given by calculation according to CSN EN 1992-1-1 and CSN 73 1201.

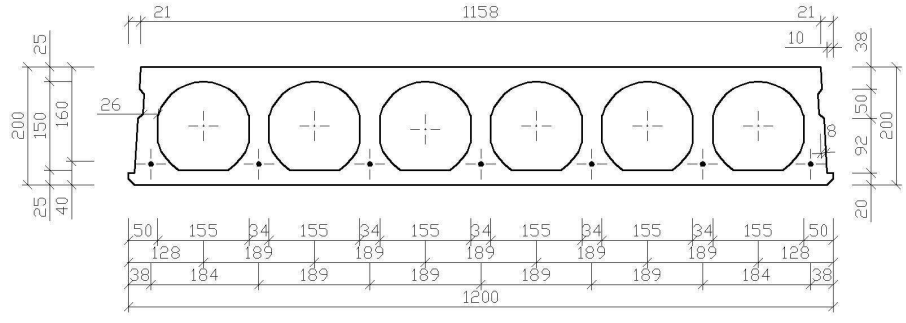

Fig. 1. Cross-section of ELEMATIC unit.

2. Nonlinear stochastic analysis

Non-linear numerical analysis of concrete structure is based on principles of nonlinear fracture mechanics and finite element method (FEM). In connection to stochastic calculation one of most modern methods to check the esistance and reliability of failure of structure and structural member of concrete is utilized.

The aim of nonlinear stochastic analysis of ELEMATIC unit is to determine probability distribution function (PDF) R of shear capacity. The shear capacity is given by value of concentrated load conformable with CSN EN 1168. Statical scheme of test is shown in Fig. 2.

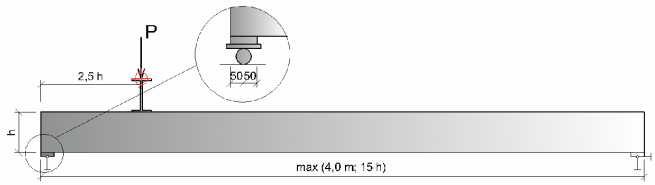

Fig. 2. Test configuration by code CSN EN 1168.

2.1. Numerical FEM model

The basis of deterministic nonlinear calculation is to create numerical FEM model in ATENA 2D software [1], [2], Fig. 3. As concrete material model, 3D Nonlinear Cementitious 2 was selected. Tensile strength, specific fracture energy and modulus of elasticity of concrete were obtained during experimental fracture-mechanical test [3] and following identification [4]. Prestressing of strands is modeled by bi - linear working diagram with hardening. Perfect bond between strand and concrete is assumed.

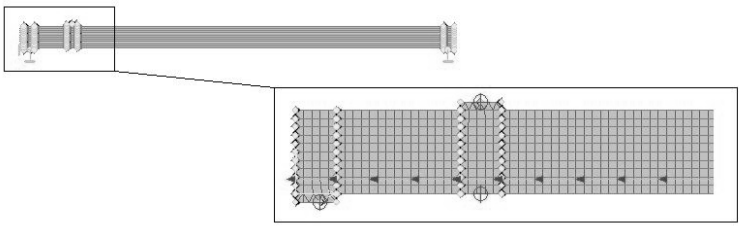

Fig. 3. Numerical FEM model (ATENA 2D)

2.2. Stochastic analysis

Material characteristics of concrete were considered as random variable for probabilistic analysis. The stochastic model is considered according to recommendation of organization JCSS [5] and also on the basis of numerical identification from experimental testing. Statistical correlations among some variables were considered in sampling scheme. Software package SARA and stochastic module FREeT was used for calculation.

Variables	Unit	Distribution type	Mean	CoV
Tensile strength f_c	MPa	LN (2 par.)	58,0	0,08
Compressive strength f_t	MPa	LN (2 par.)	4,7	0,21
Modulus of elasticity E_c	GPa	LN (2 par.)	26,5	0,13
Fracture energy G_f	Nm^{-1}	LN (2 par.)	129,3	0,17

Tab. 1. Probabilistic models of material parameters of concrete

Mean value, variation coefficient and optimal type of probability distribution of critical load of unit were estimated from statistical evaluation of 25 virtual simulations shear failure. Modeling uncertainties in computation is done using a of new random variable ξ_R. According to relation (1) updated critical load can be obtained.

$$P_{red} = \xi_R . P \tag{1}$$

Variables	Unit	Distribution type	Mean	CoV
Load P	kN	LN (2 par.)	216,5	0,140
Modeling uncertainties ξ_R	-	LN (2 par.)	1,0	0,100
Reduced load P_{red}	kN	LN (2 par.)	216,7	0,173

Tab. 2. Shear capacity random variable

Results of partial simulation in form of LD diagram (load vs. deflection) and course of theoretical crack at the moment of achievement of critical load are shown in Fig. 2. Cracks pattern obtained by numerical simulation corresponds to cracks pattern obtained from real experiments.

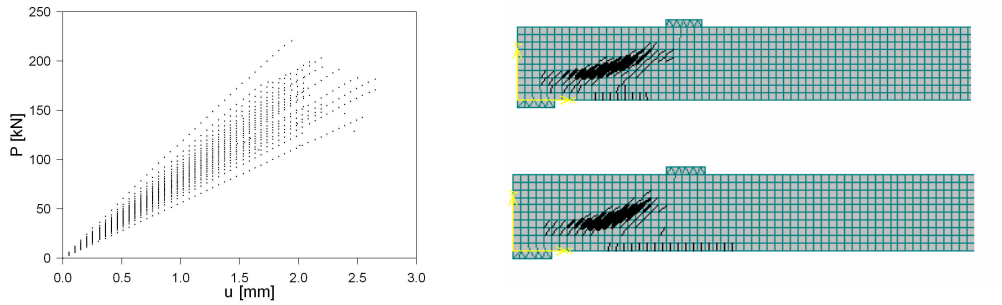

Fig. 4. Numerical simulations, LD diagram.

3. Experiment

Experiment was done in laboratory of Technical and Test Institute for Construction Prague, Branch Ostrava. The aim was inquest the value of concentrated load during shear capacity testing according to CSN EN 11 68. For experimental testing three units type ELEMATIC length 4.5 m with average age of 60 days were available.

Fig. 5. Test configuration, shear failure of unit.

At critical load value diagonal macro cracks directing from loading point to support with angle 45-60° occurred. In all experimental tests expected failure by depletion of shear capacity occurred. A value of concentrated load was measured as follows: 235.0, 218.0 and 172.0 kN. Results of test highlights the existence of problem of randomness of shear capacity of concrete units.

4. Conclusion

The result of virtual reliability simulation of shear capacity represents reality as shown in Fig. 7 together with 3 experimental tests (black dots) and individual deterministic design techniques by valid codes in Czech Republic. Also confidence intervals are depicted for probabilities 0.05 (0.95) and 0.001 (0.999). The picture gives us an overall view where we are when using design techniques and provide us “a virtual reliability control” to support decision on design value of shear capacity of particular concrete units in concrete prefabrication.

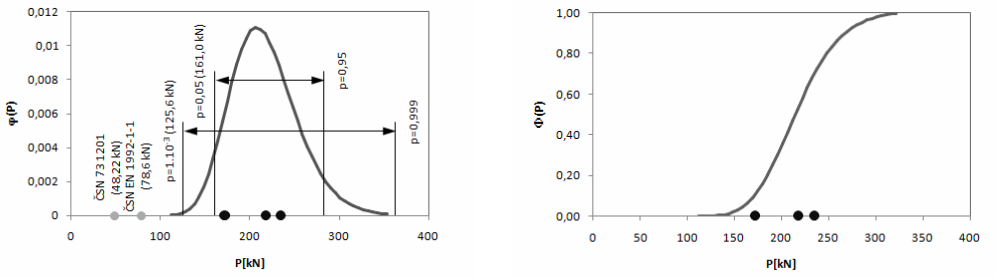

Fig. 6. Probability distribution functions of shear capacities.

Acknowledgement

The presented work is related to the research funded by the project the Ministry of Education of the Czech Republic, project No. MSM0021630519 and by the grant No.103/08/1527 from the Grant Agency of the Czech Republic. Authors gratefully acknowledge this support.

References

[1] ČERVENKA, V., JENDELE, L., ČERVENKA, J. (2007) *ATENA Program Documentation – Part1:Theory, Cervenka Consulting*. Prague, Czech Republic, 2007.

[2] ČERVENKA, V., JENDELE, L., ČERVENKA, J. (2007) *ATENA Program Documentation – Part2:User´s manual, Cervenka Consulting*. Prague, Czech Republic, 2007.

[3] KERŠNER, Z., LEHKÝ, D., NOVÁK, D., ŘOUTIL, L., SCHMID, P., ŽÍTT, P. *Hodnoty lomově-mechanických parametrů materiálu panelů ELEMATIC. Zpráva zakázky HS 12825007*. Ústav stavební mechaniky a Ústav materiálového zkušebnictví, FAST, VUT v Brně, Česká republika, 2008b.

[4] LEHKÝ, D., NOVÁK, D., KERŠNER, Z. *Identifikace parametrů materiálu panelů ELEMATIC. Zpráva zakázky HS 12825008*. Ústav stavební mechaniky, FAST, VUT v Brně, 2008b

[5] JCSS. *JCSS working materials*, dostupné z URL: http://www.jcss.ethz.ch

[6] NOVÁK, D., VOŘECHOVSKÝ, M., RUSINA, R. *FREET - Feasible Reliability Engineering Efficient Tool, User's and Theory guides.* Brno/Cervenka Consulting, Czech Republic, 2006

[7] NOVÁK, D., VOŘECHOVSKÝ, M., LEHKÝ, D., RUSINA, R., PUKL, R. & ČERVENKA, V. *Stochastic Nonlinear Fracture Mechanics Finite Element Analysis of Concrete Structures.* In: G. Augusti and G.I. Schuëller and M. Ciampoli (Eds.) Proc. of ICoSSaR '05 the 9th Int. Conf. on Structural Safety and Reliability, Italy, Millpress Rotterdam: 781-788, 2005

[8] PUKL, R., ČERVENKA, V., STRAUSS, A., BERGMEISTER, K. & NOVÁK, D. *An advanced engineering software for probabilistic-based assessment of concrete structures using nonlinear fracture mechanics.* Proc. of 9th Int. Conf. on Applications of Statistics and Probability in Civil Engineering – ICASP 9, San Francisco, USA, Rotterdam Millpress: 1165-1171, 2003a.

Transcom 2009, 22-24 June 2009
University of Žilina, Žilina, Slovak Republic

Efficiency of the Ballast Material Recycling

*Ing. Zuzana Gocálová, Ing. Janka Šestáková, PhD., Ing. Martin Mečár
*University of Žilina, Faculty of Civil Engineering, Department of railway building and track management, Komenského 52, 010 26 Žilina, Slovakia
zuzana.gocalova@fstav.uniza.sk , janka.sestakova@fstav.uniza.sk, martin.mecar@fstav.uniza.sk

Abstract Integration of ecological processes into the technologies of sub-ballast of railway infrastructure brings economical and ecological advantages. The maximum reapplication of the extracted ballast material as well as optimal utilization of the recycling formation may be reached only by effective and qualitative technological recycling process. Recycling efficiency is represented by quality of recycled products.

Key words: ecological process, recycling ballast material, recycling efficiency, formation protective layers.

1. Introduction

Ecological processes in technologies of sub-ballast of railway tracks should be in valid legislation a necessary part of modernization, reconstruction and repair works. The technologies with included ecological processes allow recycling the excavated ballast material, which may be repeatedly used in the construction layers of railway tracks as ballast material and/or material of formation protective layers (reinforced or unreinforced). In order to achieve a required quality of recycled product it is necessary to monitor efficiency of these ecological processes during recycling. In our grant project we are dealing with observation and evaluation of efficiency of the recycling processes realised on the ballast material samples taken after recycling chosen size fractions, needed for reapplication of this material in the reinforced or unreinforced formation protective layers during modernization works. The observation of recycling efficiency interlocks on the results from the previous research period 2005 – 2007.

2. Recycled material in sub-ballast of railway tracks

Need for the protection of environment, especially the natural mineral resources, the waste minimisation as well as need for reduction of the shopping and transport costs of new materials lead to use of the new material production possibilities in the railway subgrade. The ballast material recycling represents such a possibility, when the input material (ballast) is obtained during the railway subgrade repair and reconstruction works.

Recycling process returns to the excavated ballast material its technical and ecological quality in order to be repeatedly applied in the formation protective layers (reinforced or unreinforced).

Technology of the production of recycled aggregate from the recovered ballast material is based on primary separation, during which the recovered ballast material is purged from

clay and decontaminated. Then it is crushed to the required granularity. The production of recycled aggregate is performed in two ways:

- Continuously without break in one step,
- Divided in two steps – in the first step, the recovered material is separated and decontaminated, and in the second step, the recycled semi-product is separated to partial size fractions, which are then mixed.

Detailed descriptions of both the continuous and the divided technological recycling processes are presented in [1].

The production of recycled aggregate out of the track axis is realised in recycling stations, which are equipped by special machines and appliances for manipulation and treatment of the recovered ballast material. According to location of the treatment area, the recycling stations are differentiated as permanent and temporary.

The permanent recycling stations use stationary recycling lines and they recycle the ballast material out of the recovery site. They are fixed to the location of the recycling station and they are able to make a qualitative recycling product. Disadvantages of the permanent recycling stations are high establishment costs, a persistent ground occupation and a variable distance of the ballast recovery site (related to the transport costs).

The temporary recycling stations treat the recovered ballast material "in situ" and they use for recycling the mobile recycling lines. Their advantages are mobility, a small ground occupation, simplicity and unassuming attendance, lower establishment costs and a possibility to treat in place even relatively small amounts of the recovered ballast material.

Technologic lines of the recycling stations use for production of recycled aggregate with required size fraction the separators and crushers. The transport of material between partial components of the recycling line is performed by means of belt conveyers. Charging and conveyance of the recyclable and recycled aggregate is realised by means of loaders and lorries or railway carriages eventually. Technologic appliances of the recycling line are (Fig. 1):

- pre-separator (primary separation of the aggregate – purging from clay, decontamination),
- rebound crusher (crushing aggregate, renewal of angularity of grains),
- separator (separation of aggregate of required size fractions),
- loader,
- removal equipment (lorries, railway carriages).

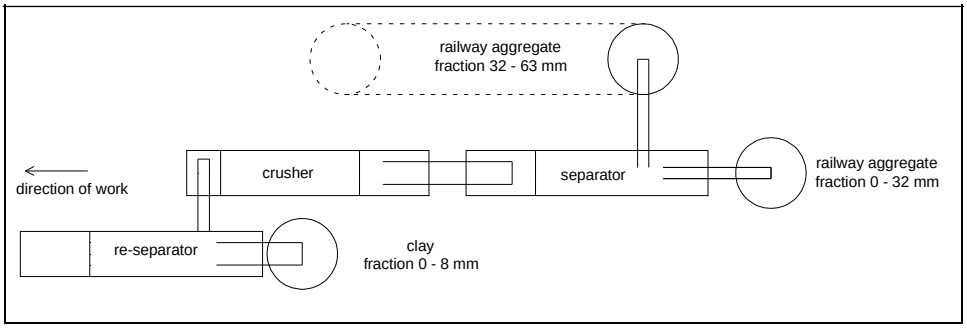

Fig. 1 Example of technologic arrangement of recycling line

During modernization of Slovak railways, the ballast material recycling is realised mostly in the temporary recycling stations equipped by mobile recycling line, because the cost

of transport of recycled aggregate is minimized in consequence of their appropriate location near the place of structure.

The recycled aggregate into construction layers of railway tracks should be supplied only by such a supplier or producer who was given the licence of Slovak Railways. The recycled material should satisfy the technical and ecological criterions according to corresponding legislation [4]. The possible suppliers of recycled aggregate for Slovak Railways are presented in Tab. 1.

Suppliers of recycled railway aggregate	Recycled railway aggregate			
	fraction	construction layer	kind of	realise place
ŽSD Slovakia s.r.o	0 - 32	formation protective	regenerated aggregate	mobile recycling line
	0 - 63			
	0 - 45			
	32 - 63	ballast		
KDS s.r.o, Košice	0 - 32	formation protective		
	0 - 63			
	32 - 63	ballast		
TSS a.s. Trnava	0 - 32	formation protective		
	0 - 63			
ENZO Žilina	0 - 32	formation protective		
	32 - 63	ballast		

Tab. 1 Possible suppliers of recycled railway aggregate for Slovak Railways

3. Efficiency of recycling and quality of recycled aggregate

The quality of recycled aggregate is directly proportional to recycling efficiency. Decontamination of the ballast material is prescribed on the basis of results of input diagnostic. The decontamination is realised by removal of elements of the size fraction 0 – 8 mm (contamination carrier), which becomes a production waste.

Realisation of output diagnostic of recycled material is integrated to the end of recycling process. The way of production of recycled product (continuous/divided) [2] is given by the recycling form (partial/full in the track axis, full out of the track axis). Also evaluation parameters of output diagnostics are given by the recycling form – by determination of the technical quality of recycled goods.

According to the final use of recycled products, the taken average samples of technological outputs from recycling line are farther laboratory treated and analysed for the following technical parameters:

production waste of the size fraction 0 – 8 mm: granularity and unit weight,

- recycled product of the size fraction 0 – 32 mm: unit weight, granularity, number of grain irregularity and washing-off elements,
- recycled product of the size fraction 0 – 63 mm: unit weight, granularity, number of grain irregularity, washing-off elements, oversize fraction grains, unknown and organic elements.

The material sampling has to guarantee the representative samples for analysis of technical parameters [4]. The average samples are prepared by gradual quartation of the gross sample, prepared from simple samples, until the minimal required weight of average sample (10 kg) is reached. The simple samples of minimal weight 10 kg were taken once an

hour during the minimum eight-hour working shift of the recycling line (i.e. at least 8 simple samples were taken and the minimum weight of the gross sample was 80 kg. Taking of simple samples was realised manually from last belt conveyers of the technical recycling line.

The material granularity was determined by means of laboratory screens and shake separator [5, 6]. The standard set of screens with size of holes 0.063, 0.125, 0.250, 0.500, 1, 2, 4, 8, 16, 31.5 and 63 mm was used for granularity analyses. The standard set was completed by screens 22 and 45 mm. Screens with square holes can be used only. The tested sample is dried at temperature 110 ± 5 °C until the steady weight achieved. The test process consists of material washing and dry screening. The washing is realised on screen size 0,063 mm until the water passing through the screen is clear. The washed and dried again sample is screened on shake separator. The weight of material rest on all screens is then related to the weight of original average dry sample.

4. Evaluation of recycling efficiency

Efficiency of the recycling process is evaluated for a consideration of the output diagnostics results, which compose a base of database [2]. The database data has been collected since 2005 (Tab. 2). Technological efficiency of the primary separation (product is production waste of the size fraction 0 – 8 mm) and technical efficiency of achieved quality of the final recycled product of the size fraction 0 – 32 mm and 0 – 63 mm with its application to reinforced/unreinforced formation protective layer of railway tracks

Years	Amount of average samples	Evaluated size fraction	Average efficient of recycling according to [%]			
			Size fraction	Recycling station *		
				ENZO	TSS	ŽSD
2005 - 2007	26	0 - 63 mm	76,92	62,50	85,71	75,00
	44	0 - 32 mm	81,57	57,14	87,50	89,63
	42	0 - 8 mm	77,95	77,76	79,81	60,70
* Efficient of ballast material recycling according to recycling station by fraction 0-8 mm was evaluated per 36 samples						

Tab. 2 Efficiency of the ballast material recycling according to size fractions and recycling stations

The technological efficiency of recycling process is determined on the basis of results of the grain size analysis of the production waste material. The efficiency is represented by the share (in %) of the separated size fraction 0 – 8 mm, which is the holder of contamination [3] (Fig. 2).

The technical efficiency of recycling process is determined on the basis of results of the analysis of technical quality of the recycled material of the size fraction 0 – 32 mm or, eventually, 0 – 63 mm as a final product of recycling. Comparing the results of analyses of the essential technical parameters with limit values, required for application of recycled material to reinforced/unreinforced formation protective layer, is a base for evaluation of technical efficiency. Technical efficiency of the ballast material recycling process is determined on the basis of results of the technical quality of recycled material [3] (Fig. 2).

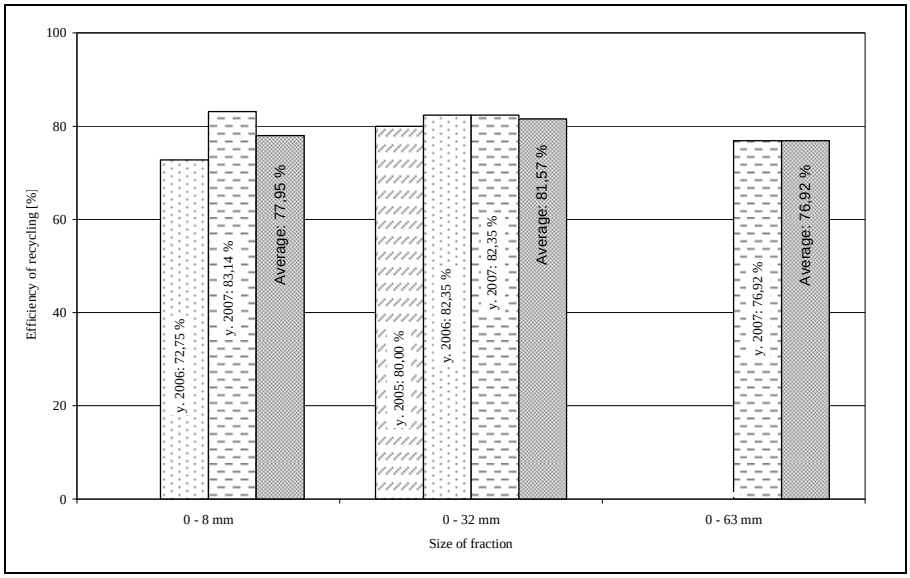

Fig. 2 Technical and technological efficiency of ballast bed material recycling

5. Conclusion

Integration of ecological processes into the technologies of sub-ballast of railway infrastructure brings economical and ecological advantages. Economical claims to buying new material are reduced by application of the recycled ballast bed material. Negative effects on environment are reduced by minimisation of extracted ballast bed material storage. The aim of monitoring and valuation of recycling efficiency is to ensure an effective application of extracted ballast material for production of recycled material and, consequently, to reduce the necessity of new material. Achievement of effective use of recycling technology should be in the interest of recycling stations operators – for production of recycled goods with required quality in one (continuous), no repeated, technological process.

Acknowledgement

The contribution is published with the support of project of Scientific Grant Agency of Ministry of Education of the Slovak Republic and Slovak Academy of Sciences VEGA 1/4172/07.

References

[1] MIKŠÍK, M. – ŠESTÁKOVÁ, J.: Účinnosť recyklácie materiálu koľajového lôžka na koridore, In: 12. seminár traťového hospodárstva STRAHOS 2007, Trenčín, Zborník prednášok, s. 45 – 54, ISBN 978-80-8070-708-8

[2] ŠESTÁKOVÁ, J. – GOCÁLOVÁ, Z. – MEČÁR, M. – ŠPÁNIK, J.: Ekologické procesy technológií pre spodnú stavbu železničnej infraštruktúry, In: XVII POLISH – RUSSIAN – SLOVAK SEMINAR, Theoretical Foundation of Civil Engineering, Warszawa, Proceedings, s. 398 – 407, ISBN 978-80-8070-855-9

[3] GOCÁLOVÁ, Z. – ŠESTÁKOVÁ, J. – MEČÁR, M. – ŠPÁNIK, J.: Využiteľnosť materiálu koľajového lôžka po recyklácii pre potreby modernizácie železničných tratí v SR, In: 13. seminár traťového hospodárstva STRAHOS 2008, Vyhne, Zborník prednášok, s. 163 – 170, ISBN 978-80-8070-920-4

[4] TNŽ 72 1514 Technické a ekologické podmienky na dodávanie materiálu do konštrukcie koľajového lôžka a podkladných vrstiev podvalového podložia, máj 2000

[5] STN EN 933-1 Skúšky na stanovenie geometrických charakteristík kameniva. Časť 1: Stanovenie zrnitosti - Sitový rozbor, apríl 2002

[6] STN EN 933-2 Skúšky na stanovenie geometrických charakteristík kameniva. Časť 2: Stanovenie zrnitosti – Skúšobné sitá, menovité veľkosti otvorov, november 1999

Transcom 2009, 22-24 June 2009
University of Žilina, Žilina, Slovak Republic

Light-Weight Fibre Reinforced Self Compacting Concrete

*Michala Hubertová
*Brno University of Technology, Faculty of Civil Engineering, Institute of Technology of Building Materials and Components, Veveří 331/95, 602 00 Brno, Czech Republic, hubertova.m@fce.vutbr.cz;
Lias Vintířov, LSM k.s., 357 44 Vintířov, Czech Republic, hubertova@liapor.cz

Abstract. The paper is concerned with the effect of synthetic and steel fibres on the properties of Lightweight Self Compacting Concrete (LWSCC) especially with the effect of fibres on LWSCC rheological properties, on the shrinkage in the initial stadium and on physico-mechanical properties of hardened LWSCC. The utilization of fibrous reinforcement is a new approach in the concrete technology and this paper describes the first results of research which is starting in this area. The experimental works which are described in the paper are based on the use of different fractions of the industrially manufactured Liapor lightweight aggregate in combination with natural aggregate. The results show that the impact of addition of different types of fibers is not the same with concretes using only light weight aggregate and concretes combining lightweight and natural aggregate. It can also be said that all used types of fibers can be used for technology of light weight vibrated concretes.

Keywords: light-weight self compacting concrete, expanded clay aggregate, synthetic fibres, steel fibres

1. Introduction

Light weight high-performance concretes, i.e. self-compacting concrete and light weight fibre reinforced concrete are new types of concrete that are not incorporated in any standard or directive. Therefore it is necessary to apply all existing knowledge about high performance, high strength and light weight concrete when developing light weight high performance concrete.

High water absorbing capacity, low volume weight and low strength of light weight aggregate (LWA) are the main problems of design, production and placing of light weight flowing concrete. Hence it is in particular the type and properties of light-weight aggregate that have the major effect on behaviour of this type of concrete. LWA Liapor produced in the Czech republic was the only light weight aggregate used for the experiments. The main task was to achieve high performance of the light weight concrete using LWA with strength less than 10 N/mm^2 and bulk density 900 kg/m^3.

2. Experimental method

Light-weight self compacting concrete has been developed at the Brno University of Technology since 2003. There are many size fractions of light weight aggregate Liapor and their bulk density differs. Therefore it was necessary to examine influence of different size fractions on workability of fresh concrete and on properties of hardened concrete (namely strength) in the first place. A set of mix-designs of light weight concrete with different combinations of size fractions of light weight aggregate and with natural aggregate was designed. Specimens of different mix designs were systematically compared and their physico-mechanical properties were examined. At the first stage, air entrainers were added to

test their effect on workability of fresh concrete and properties of hardened concrete. At the second stage, light weight pumpable concrete was designed. The most important issue was water absorbing capacity of light weight aggregate. Water absorbing capacity under higher pressure (i.e. in the course of pumping) has the highest influence on workability, yet it was not possible to find the right amount of water for soaking the light weight aggregate during transport and placing in normal laboratory conditions. Therefore an additional laboratory test of concrete pumpability was proposed. At the third stage, light weight self compacting concretes were designed using knowledge about water absorbing capacity influence on workability found at the second stage. Influence of batching by volume, batching by weight and using dry or soaked aggregate on properties of light weight self compacting concrete was tested. Different mixes were designed using light weight aggregate Liapor only or in combination with natural aggregate, ultra fine additives were added in order to achieve higher strengths (fly ash, micronized lime stone, silica dust, metakaolin). It was necessary to judge the appropriateness of applying methods of testing rheological properties used for standard self compacting concretes on light weight self compacting concretes. Knowledge in this field were published [1, 2, 3].

Light weight concrete is known for its brittle fractural behaviour. To improve ductility of concrete, dispersed fibre reinforcement is used. At the fourth stage, the possibility of adding fibre reinforcement (in particular synthetic, polypropylene and steel fibres) into the tested mix-designs of light weight concretes was examined. Homogeneity of this light weight fibre reinforced concrete was tested at the first place since homogeneity is the necessary condition for application of concrete in bearing structures. Basic physico-mechanical properties including basic volumetric changes were determined.

Two sets of mix-designs were made at this stage. Set I contained light weight aggregate Liapor combined with natural aggregate, set II contained light weight aggregate only. In each of the sets there was one reference mix-design, which was then modified using different types of fibres. Synthetic fibres 50 mm long were used in the amounts of 0,4 and 8 kg/m^3, which is the dosage recommended by manufacturer. Then 12 mm long polypropylene fibres were used in the amount of 0.91 kg/m^3 (0.1 per cent by volume) and two types of steel fibres - the type with circular cross-section of 0.4 mm was straight and 12 mm long, the type with circular cross-section 0.6mm was crimped lengthwise and 20 mm long. Dosage of both types of steel fibres was 25 kg/m^3. Each of the sets of mix-designs was created by seven different mix-design - one reference design and six designs with different fibres. Schemes of individual mix-designs are shown below (see Figure 1).

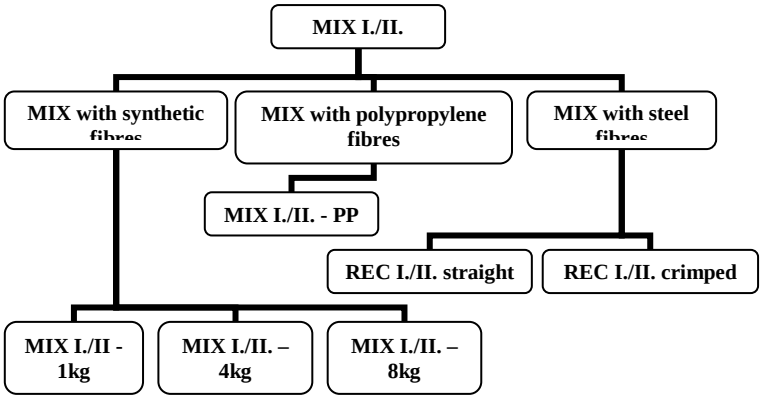

Fig 1. Schema and marking of set I and set II of mix-designs

The influence of addition of different fibres on rheological properties of individual mix-designs was observed. The properties were tested by conventional methods used for self-compacting concretes: slump flow, Orimet, J-Ring and L-box. Workability of mix-designs was tested immediately after mixing, after 60 and 90 minutes. Then volumetric changes were examined, immediately after mixing and during maturing of the hardened concrete. Finally, basic physico-mechanical properties including static elastic modulus were determined.

3. EXPERIMENTAL RESULTS AND DISCUSSION

3.1. Composition and evaluation of individual mix-designs

Composition of the reference mix-design of set I (i.e. using combination of light weight aggregate and natural aggregate) is stated in Table 1. Composition of the reference mix design of set II (i.e. using only the light weight aggregate Liapor) is stated in Table 2. Addition of individual fibres of modified mix-designs is stated in Table 3. Graphic presentation of some basic tested charakteristics of fresh and hard concrete is in Figure 2, 3, 4 and 5.

Components	Amount [kg/m^3]
CEM I 42,5R	370
Natural aggregate 0-4	580
Liapor 0-1D/650	99
Liapor 4-8/600	441
Water	190
Fly ash	111
Superplastisizer	5,55
Stabilizer	1..5
Micro silica	37
	1835

Tab. 1. Composition of the reference mix-design of set I of mix-designs (marking MIX II.)

Components	Amount [kg/m^3]
CEM I 42,5R	370
Liapor 1-4D/625	227
Liapor 0-1D/650	310
Liapor 4-8/650	269
Water	125
Fly ash	185
Superplastisizer	5,55
Stabilizer	1..5
	1493

Tab. 2. Composition of the reference mix-design of set II of mix-designs (marking MIX II.)

Marking of set I	Marking of set II	Type of fibres	Amount [kg/m^3]
MIX I. 1kg	MIX II. 1kg	synthetic fibres	1
MIX I. 4kg	MIX II. 4kg	synthetic fibres	4
MIX I. 8kg	MIX II. 8kg	synthetic fibres	8

MIX I. PP	MIX II. PP	PP fibres	0.91
MIX I. straight	MIX II. straight	steel fibres (straight)	25
MIX I. crimped	MIX II. crimped	steel fibres(crimped)	25

Tab. 3. Fibre additions of modified mix-designs

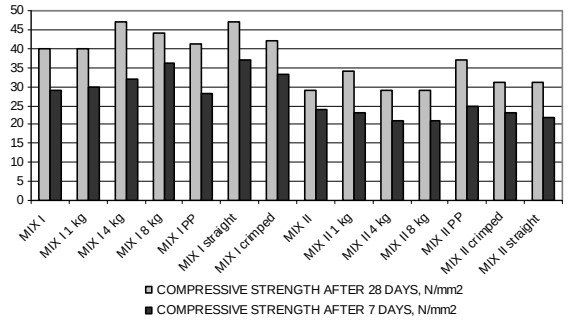

Fig. 2. Compressive strength after 7 and 28 days of both mix-design sets**.**

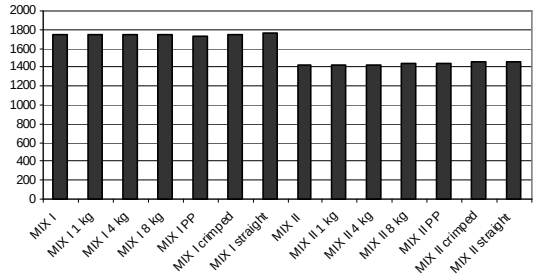

Fig. 3. Volume weight of both mix-design sets.

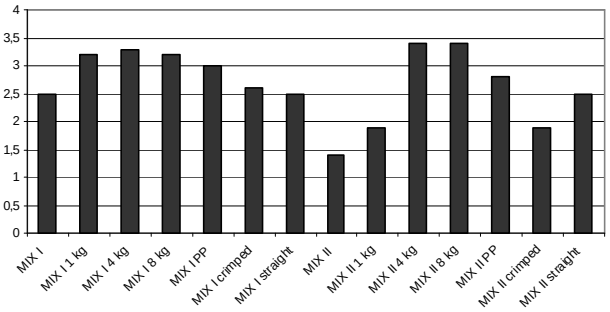

Fig. 4. Tensile bending strength of both mix-design sets.

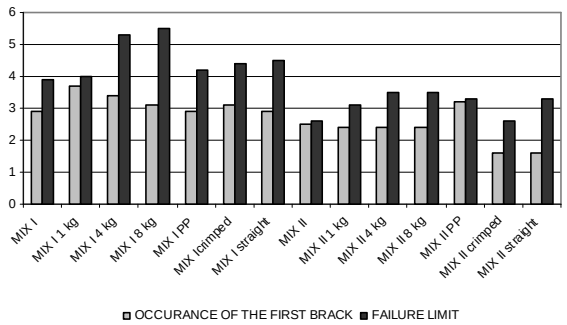

Fig. 5. Tensile splitting strength of both mix-design sets.

4. Discussion of experimental results

On the basis of existing knowledge of the influence of fibres on the concrete properties it was assumed that polypropylene fibres would affect volumetric changes of fresh and maturing concrete. Steel fibres were supposed to affect physico-mechanical properties, in particular tensile bending strength and tensile splitting strength.

Figure 7 shows volumetric changes of MIX I during maturing time up to 50 or 60 days after mixing. Specimens of individual mix-designs were tested for volumetric changes. Specimens were placed both in standardized water environment and in laboratory environment. The graphical representation of the results shows that all fibres decreased the value of shrinkage except for straight steel fibres and synthetic fibres in the amount of 8 kg/m^3 which showed slightly higher value of shrinkage. The cause of higher shrinkage of concrete with straight steel fibres is perhaps the straight shape and smooth surface of the fibres resulting in insufficient adhesion of cement paste. The mix-design with 8 kg/m^3 of synthetic fibres was probably non-homogeneous because such dosing is extremely high for 1 m^3 of concrete. This is apparent from the physical properties - strengths of mix-design with lower amount of synthetic fibres (4 kg/m^3) were higher. Concrete with addition of 4 kg of synthetic fibres in water environment showed rather non-standard behaviour, but this can be probably put down to error in measurement. In any case, it is apparent from the graphical representation that it is very important to cure these concretes properly, both with and without the addition of fibres. Concretes placed in laboratory environment (ca 22°C and low relative humidity) showed considerable shrinkage.

Set MIX II showed similar results in the course of maturation, however here the addition of fibres limited volumetric changes. The best results were achieved with synthetic fibres in the amount of 4 kg/m^3. It is apparent from the tendency of curves of reference mix-design that volumetric changes would be even greater, which was prevented by addition of all types of fibres.

As for rheological properties of individual mix designs, the recommended range of values of test methods was taken from the EFNARC Directive [4]. Criteria of individual test methods were met only by the reference mix-design and by both mix-designs with steel fibres. Synthetic an polypropylene fibres caused high degree of blocking and non-homogeneity of the concrete with lightweight aggregate only and when using synthetic fibres only. These results need to be further compared to results of physico-mechanical properties.

Reference mix-design MIX I reached the strength of 40 N/mm^2 with volume weight of 1740 kg/m^3. Polypropylene fibres, synthetic fibres in the amount of 1 kg/m^3 and straight steel

fibres did not affect compressive strength. Synthetic fibres (4 kg/m^3) and crimped steel fibres caused the highest increase of compressive strength (both mix-designs 47 N/mm^2). Tensile bending strength was most increased by synthetic fibres in amounts of 1 kg/m^3 and 8 kg kg/m^3 (by 28 %) and PP fibres (by 20 %). Tensile splitting strength was most influenced by synthetic fibres (4 kg/m^3), the limit of first crack was increased by 17 % and the failure limit was increased by 36 %, and by crimped steel fibres, where the limit of first crack was increased by 7 % and the failure limit by 13 %.

Reference mix-design MIX II reached the compressive strength of 29 N/mm^2 with dry volume weight 1430 kg/m^3. Compressive strength was increased only by addition of synthetic an polypropylene fibres (1 kg/m^3), which may seem surprising, but after thorough examination of cross-sections of tested specimens it was found that steel fibres tended to settle down due to their high weight (relatively to the weight of the light weight aggregate) and therefore the mixture was non-homogeneous. Mechanical bond or adhesion of synthetic fibres in greater amounts and cement paste was bad due to insufficient ravelling of ends of fibres caused by light weight aggregate. On the other hand, polypropylene fibres made the structure of concrete 'more compact' and prevented segregation and rising of light weight grains of Liapor to the surface. These fibres still increased tensile bending strength and tensile splitting strength of MIX II concrete. Tensile bending strength was considerably increased by synthetic fibres (4 kg/m^3 and 8 kg/m^3) - by 40 % and PP fibres - by 42 %. Tensile splitting strength was again most influenced by synthetic fibres (4 kg/m^3 and 8 kg/m^3); the limit of first crack did not change but failure limit increased by 35 %. PP fibres increased the limit of first crack by 28 % and failure limit by 27 %.

Static elastic modulus is another important parameter for design of concrete and reinforced concrete structures in addition to compressive strength. Static elastic modulus can be determined in two ways: by direct loading of testing specimen on testing machine and examining deformations, and by indirect, non-destructive dynamic methods (ultrasonic pulse and resonant method) followed by calculation of dynamic modulus to static modulus using reduction coefficient. On average, the value of dynamic elastic modulus of standard concretes is higher than the value of static elastic modulus and they depend on class of strength of the concrete. Static and dynamic elastic modules of all mix-designs were measured and compared. Dynamic elastic modulus of MIX I set was higher than static elastic modulus by 22 %, with the set MIX II the difference it was higher by 18 %. The results are stated in Figure 6. Static elastic modulus of MIX I set was increased by all types of fibres (with the exception of 1 kg/m^3 of synthetic fibres). Static elastic modules of MIX II (with light weight aggregate only) were increased only with higher amounts of synthetic fibres and polypropylene fibres. The relationship between dynamic elastic modulus and static elastic modulus or more precisely compressive strength is shown in Figure 8 and 9. The figures also state empirical formulas for these relationships and their respective coefficients of correlation. Based on the results, it can be said that:

- There is a relationship between dynamic elastic modulus found out by the ultrasonic pulse method and static elastic modulus or more precisely compressive cube strength. Especially the relationship between the modules has very close correlation ($r = 0.96$).
- Achieved results showed that ultrasonic pulse method can be used for stating elastic modules of light weight high performance concretes. However it is necessary to keep in prospect that these measurements have to be carried out under strictly defined conditions for the reason of influence of measurements results namely by water content in concrete.
- With respect to limited extent of observed set it is necessary to consider the conversion factors between elastic modules only informative. To determine them correctly it would be necessary not only to enlarge the observed set but also to widen the range of

observed classes of strength. The results presented are only a stimulus for further research in this field.

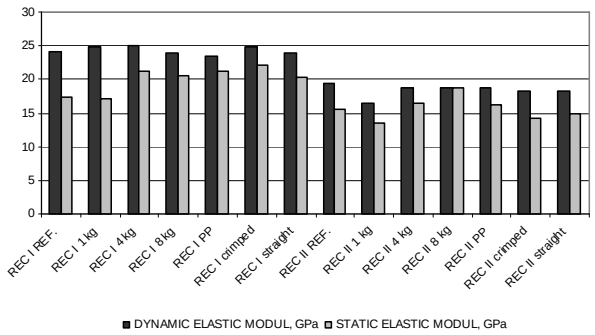

Fig. 6. Comparison of static and dynamic elastic modules of Stage IV mix-designs.

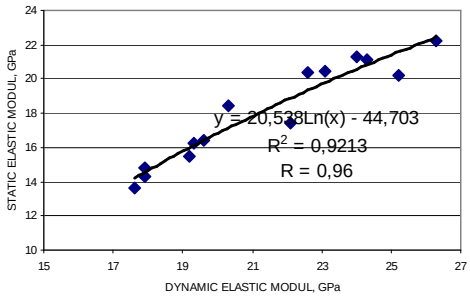

Fig. 8. Relationship between dynamic and static elasticity modules of LWSCC

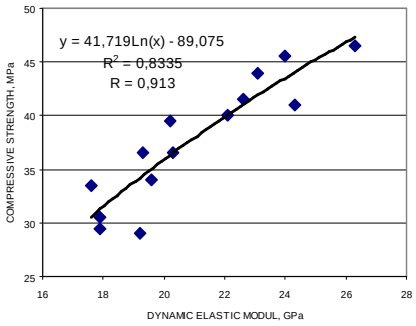

Fig. 9. Relationship between dynamic elastic modulus of light weight fibre reinforced concrete and compressive strength after 28 days

In the course of measurement of static elastic modules of all mix-designs all the values necessary for creating working diagram of concrete were read. Hence the working diagram has been created only up to 2/3 of compressive strength. The tendency of all curves implies that all types of fibre used enhanced deformation behaviour of light-weight concrete, the best results were achieved using synthetic fibres (8 kg/m^3) and both types of steel fibres (straight and crimped).

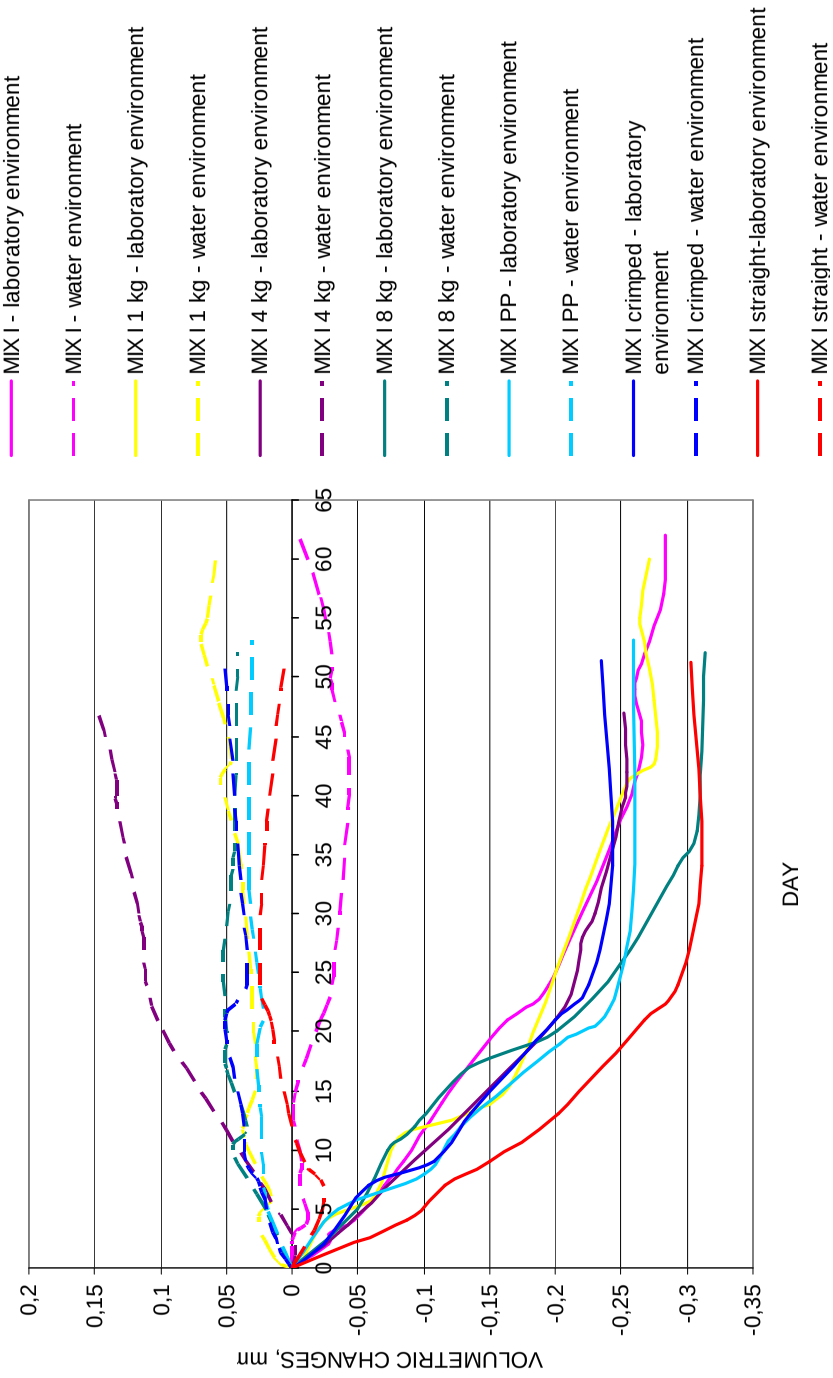

Fig. 7. Progress of volumetric changes during maturation (and after hardening) of REC I set of mix-designs

5. Conclusion

Using porous aggregate for high strength concretes might be surprising considering importance of strength of aggregate for strength of high strength concrete. Light weight aggregate is porous and not very strong. Nevertheless, drop of volume weight of concrete with strength of 50 - 60 N/mm^2 below 1800 kg/m^3 can represent certain cost saving due to reduction of total construction weight. LWSCC using LWA Liapor (maximal strength 10 N/mm2) with strength in compression of 50 - 60 N/mm2 can be at present ranked among light weight high performance concretes. Due to favorable physical properties, low volume weight and relatively high strength combined with good workability and reduction of consumed work in the course of placing, there is a wide range of application for LWSCC, in particular in the field of prefabricated elements and refurbishment of old buildings, where extra load would be undesirable. LWSCC was for the first time in the Czech republic applied in 2005. This enabled a comparison of properties of fresh and hardened concrete proportioned in laboratory and the same formula proportioned in place in the mixing plant. The comparison unambiguously proved that it is possible to produce and place LWSCC in practice, in spite of certain differences and high sensitivity of proportioning, batching and mixing. In conclusion we can say that it is possible to use fibers for technology of light weight self compacting concretes. With respect to rheological properties and positive effect of fibers to physico-mechanical properties, only steel fibers can be used, for technology of LWSCC using only light weight aggregate PP fibers can be recommended. Synthetic fibers are not desirable for the reason of inability to meet the rheological requirements. This type of fibers can be used for vibrated light weight concretes, because they have positive impact on physico-mechanical properties of hardened concrete. The same is true for PP fibers. The results show that the impact of addition of different types of fibers is not the same with concretes using only light weight aggregate and concretes combining lightweight and natural aggregate. It can also be said that all used types of fibers can be used for technology of light weight vibrated concretes.

Acknowledgement

This outcome has been achieved with the financial support of the Ministry of Industry and Trade of the Czech Reublic, MPO FI-IM5/016 „Development of light-weight high performance concrete for monolithic constructions and for precast elements" and with the financial support of project GA 103/07/076.

References

[1] HUBERTOVA, M. Self Compacting Light Concrete with Liapor Aggregates. In 6th International Congress Global Construction: Ultimate Concrete Opportunities. Dundee Skotsko UK. Thomas Telford Publishing London. 2005. p. 103 - 112. ISBN 0-7277-3410-5

[2] HELA, R. AND HUBERTOVA, M. Lightweight High Performance Concrete. In The Second fib Congress Naples 2006. 1. Neapol Italy. 2006. p. 316 – 317. ISBN 978-88-89972-06-9.

[3] HELA, R., HUBERTOVA, M. Lightweight Self Compacting Concrete in the Ready Mix. In The Sixth International Symposium on Cement & Concrete CANMET/ACI International Symposium on Concrete Technology for Suistainable Development. Xi´an China. 2006. p.1381-1390. ISBN 7-119-02249-0.

[4] EFNARC, Self-compacting concrete. Surrey United Kindom 2002. ISBN: 0-9539733-4-4. www.efnarc.org.

Transcom 2009, 22-24 June 2009
University of Žilina, Žilina, Slovak Republic

A Comparison of Portuguese and Polish Thermal Requirements and Varied Approach to Construction of External Wall

[*]Jacek Katzer, [**]Marcio Carvalho
[*]Technical University of Koszalin, Faculty of Structural Engineering, Department of Civil and Environmental Engineering, Śniadeckich 2, 75-453 Koszalin, Poland, {jacek.katzer}@tu.koszalin.pl
**Instituto Politécnico de Bragança, Escola Superior de Tecnologia e de Gestão, Campus Santa Apolónia - Apartado 1134 Bragança, Portugal, {marcio_ac_carvalho}@hotmail.com.

Abstract. This paper focuses on differences in thermal requirements connected with housing in Poland and Portugal. Climate differences create a different way of erecting external walls and a different approach to insulating buildings and dealing with thermal bridges.

Keywords: thermal properties, external walls, thermal transmittance

1. Introduction

The EU has developed a single market through a standardised system of laws which apply in all member states, guaranteeing the freedom of movement of people, goods, services and capital. Among all 27 member countries of the EU there are large climatic differences, and because of those differences there are various forms of building construction connected with thermal transmittance (U) of external walls. This area of civil engineering is very difficult to be uniformly standardized all over Europe. The need for conservation of energy resources makes it necessary to look more careful at the thermal properties of buildings in different EU countries.

2. Portugal

Portuguese climate can be classified as Mediterranean type *Csa* in the south and *Csb* in the north, according to the Köppen [1] climate classification. Portugal is one of the warmest European countries with the annual average temperature in mainland Portugal equal to 13°C in the north and equal to 18°C in the south. The warmest spots, like south coast of Madeira island are characterized by an annual average temperature equal to 20°C.

Portugal is divided into three winter climate zones (I1, I2, I3) and three summer climate zones (V1, V2, V3). Theses zones are presented in the Figure 1. Winter zones are characterized by different U_{MAX} values (a measure of the overall rate of heat transfer, by all mechanisms under standard conditions, through a particular section of construction) for walls and roofs. In case of external walls U_{MAX} value are equal to 1.8, 1.6 and 1.45 [W/m^{2}K] for I1, I2 and I3 zone respectively. Due to warm climate, concrete structure of a building is usually exposed (no thermal insulation) and forms a thermal bridge. This is the portion of a structure whose higher thermal conductivity lowers the overall thermal insulation of the structure. The bridge creates an area where heat loss is far greater in one area than it is for the general

building structure thus creating a number of problems like cold spots on the walls inside the building where condensation will form more rapidly resulting in damp patches and in the long term in the possible corrosion and deterioration of the building.

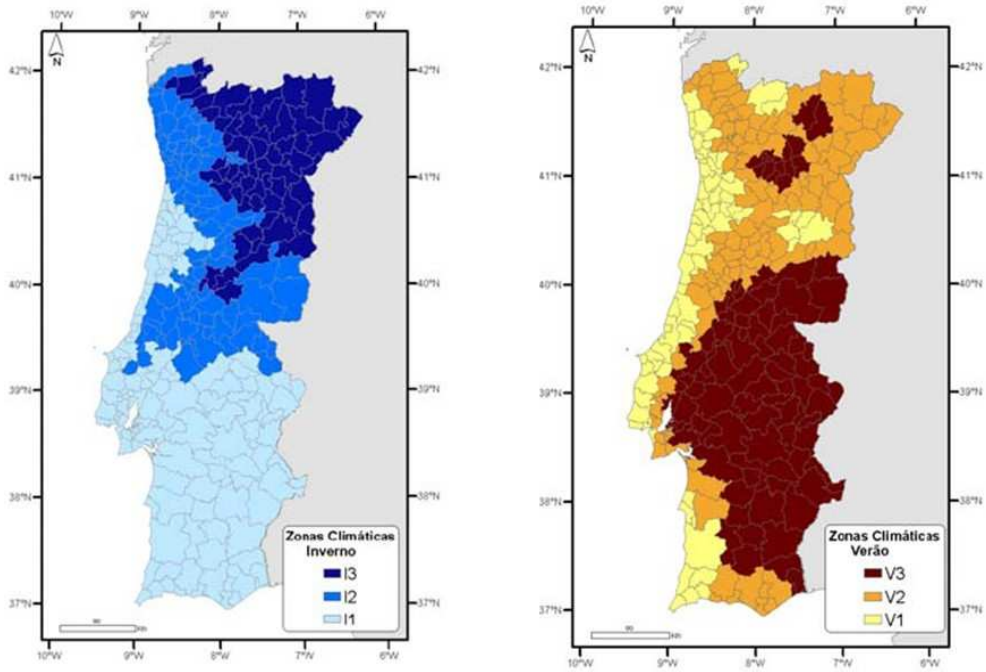

Fig. 1. Map of civil eng. climate zones of Portugal (winter and summer) [2]

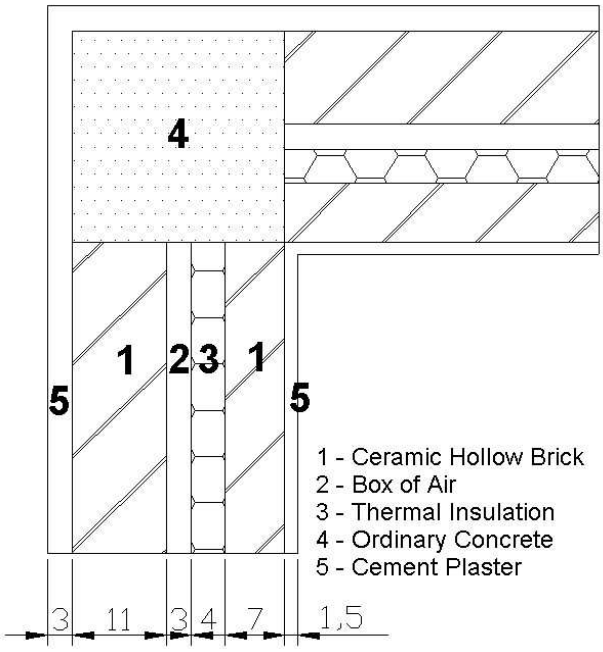

Fig. 2. An example of Portuguese external wall characterized by U_{WALL} = 0.52 [W/(m^{2}K)] < U_{MAX} =1.8 [W/(m^{2}K)]

According to Portuguese codes the thermal bridge must be characterized by the condition as follows $2 \cdot U_{BRIDGE} < U_{WALL}$. A typical Portuguese external wall is presented in Figure 2. Portuguese summer climate zones V1, V2 and V3 are characterized by low, average or high value of solar factor which describes the influence of solar activity on the temperature of an interior of a building. A value of a solar factor is mainly based on an area of windows in a building.

3. Poland

The climate is mostly temperate throughout the country. The climate is moderate in the north and west and becomes gradually warmer and continental as one moves south and east. Summers are generally warm, with average temperatures between 20°C and 27°C. Winters are cold, with average temperatures around 3°C in the northwest and −8°C in the northeast. The climate can be classified as *Dfb* according to the Köppen [1] climate classification.

Poland is divided into six climate zones I, II, III, IV ,V and VI which are characterized by winter temperatures (used for thermal calculations) -14, -16, -18, - 20, - 22, and -24ºC respectively. These climate zones are presented in the Figure 3. Polish external walls have to be characterized by $U_{WALL} < U_{MAX} = 0.55$ [W/(m^{2}K)]. Thermal bridges created by exposed elements of a concrete structure are not allowed to occur in any Polish wall. An example of a Polish external wall characterized by $U_{WALL} = 0.36$ [W/(m^{2}K)] [4] is presented in the Figure 4.

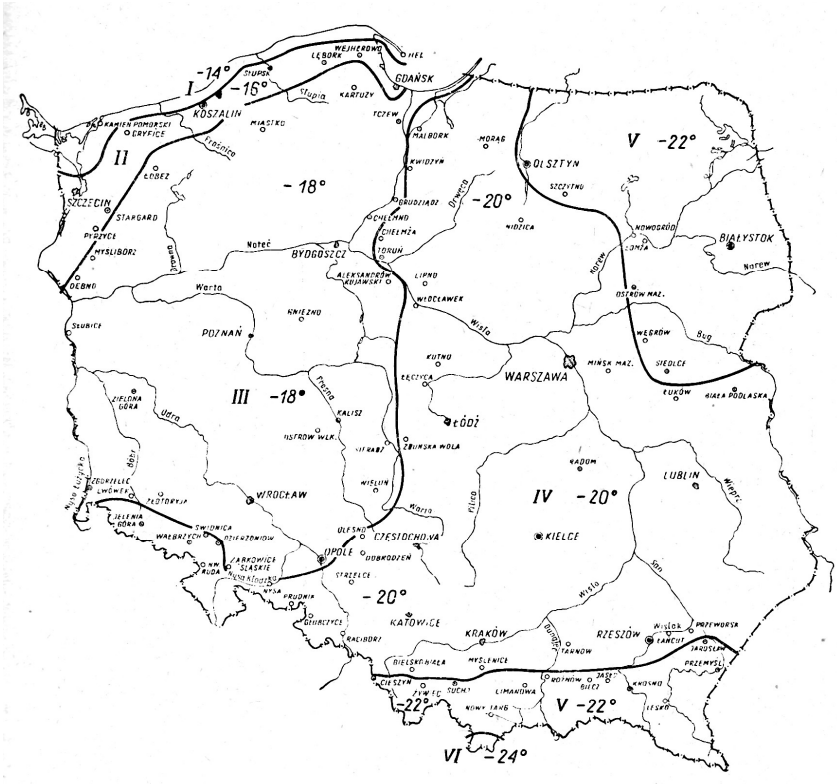

Fig. 3. Map of Polish climate zones used in civil engineering [3]

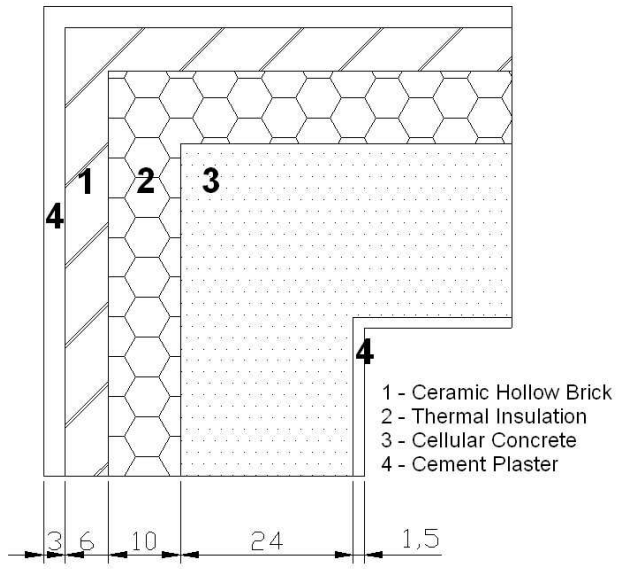

Fig. 4. An example of a Polish external wall characterized by U_{WALL} = 0.36 [W/(m^{2}K)] < U_{MAX} =0.55 [W/(m^{2}K)]

4. Conclusions

The differences between Portuguese and Polish approach to thermal properties of external wall illustrate the complexity of the future problems associated with preparing uniform European thermal legislation. In harsh climates, utilizing thermal insulation in the building can substantially reduce the building thermal load and consequently its energy consumption, which in some cases can be similar to energy consumption of a building erected in a warm part of the continent. A new procedure should be proposed for comparing the thermal performance differences between diverse types of wall systems erected in different EU countries. This procedure should ultimately include four elements: whole-wall U-value, thermal mass benefits, airtightness, and moisture tolerance.

Acknowledgement

The authors would like to acknowledge support of European Region Action Scheme for the Mobility of University Students (ERASMUS programme) which enabled a visit of Marcio Carvalho in Poland.

References

[1] McKNIGHT T., et al. *Climate Zones and Types: The Köppen System. Physical Geography: A Landscape Appreciation*. Upper Saddle River, NJ: Prentice Hall 2000.
[2] RCCTE (DL 80/2006) *Regulamento das Características de Comportamento Térmico dos Edifícios, Decreto-Lei n.º 80/2006 de 4 de Abril.*
[3] ŻENCZYKOWSKI W. *Budownictwo ogólne tom IV, Izolacje i roboty wykończeniowe*, Arkady 1962.
[4] EN ISO 6946:1996 *Building components and building elements -- Thermal resistance and thermal transmittance - Calculation method.*

Transcom 2009, 22-24 June 2009
University of Žilina, Žilina, Slovak Republic

Corridors of Transport Infrastructure (Heavy Lines Through the Europe)

* Marta Kanderková,
*University of Transport, Faculty of Civil engineering, KPSaU, Marta.Kanderkova@fstav.uniza.sk

Abstract. There is presented in this paper a model of transport infrastructure planning in Europe, if we are ready to accept really Europe without frontiers. The model is an issue of research of natural geographic limits and potential of regions (states), accepted in transport infrastructure planning jet in Neolithic Europe. It is an issue of my research, concerning creating the model of Environmental Impact Assessment of Transport Infrastructure Planning (Title of my dissertation thesis is "Environmental Indicators of transport infrastructure in process EIA", changed from "Environmental problems in spatial transport planning").

Keywords: Environmental Impact Assessment (EIA), Strategic Environmental Assessment (SEA), Transport Infrastructure Planning, Regional Development, European Union Regional Policy

1. Central Europe in the past and today

1.1. History of transport corridors in Europe and in Slovakia

Transport corridors crossing European continent from ages were created to connect centres of interest (centres of commerce, pilgrim's places, administrative and strategic points…). At the same times these routes produced administrative and commerce nodes along their corridor and contributed to economical and cultural development of the whole area.

Geographic position predestined area of Slovak republic to place of passing and crossing some important corridors of ancient Europe. (For example part of **Danube corridor**, utilized for ore and wood transporting. Some of European **Salt roads**, also **Magna Via** road (passing through Austria, Slovakia, Hungary, Romania and Ukraine), a branch of **Amber road** starting at Baltic sea in the north of Europe, passing through plains of Poland, Moravia, Vlárs´s gate, along the Váh river, Devín (near junction of rivers Moravia and Danube), Austria, Hungaria and Slovenia plains, ending in Aquileia (next to Veneto region) (Fig. 1). And a couple of years later **Post road** staring in Vienna via Bratislava, Trnava, Hlohovec, Topoľčany, Prievidza, Ružomberok, Lučivná, Levoča, Prešov, Michalovce, Sobrance, via Ukraine (Mukachevo), Hungaria (Debrecen), ending in Romania (Hermannstadt). There were some **Linen roads**, starting in the north of Slovakia passing to Krakow, Hungary, Balkan and Bohemia.

At the other hand some of the item important ones leave area of Slovakia, because of difficult terrain. For example **Silk road from China.** Also **European medieval pilgrim roads** (from Lithuania to **Santiago de Compostela** in west of Spain and to **Rome), Crusades** and so on, were all missed the area of our country.

Fig. 1
There is on the figure one of the most important corridors of ancient Europe "Amber Road", known from ***Eneolit****. Its main branch missed the area of Slovakia, because of difficult terrain and chose the corridors through plains of Poland, Moravia, Austria, Hungary, Slovenia to Aquileia (near Venezia). [2]*

Fig. 2
Medieval *Pilgim´s routes to Santiago de Compostela (Spain) and to Rome (Italy). They miss area of our country because of unknown and difficult terrain. [3]*

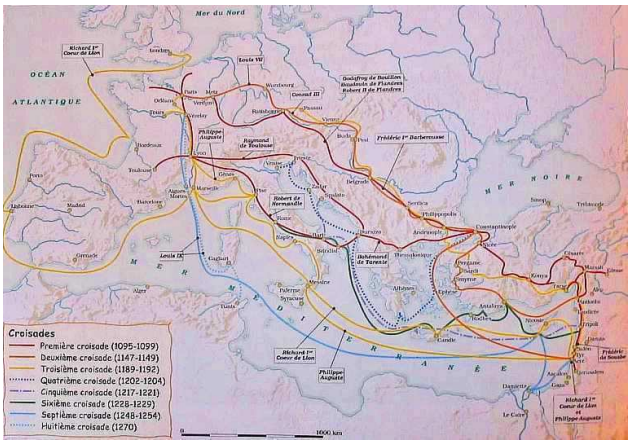

Fig. 3
Figure shows majority of the ways of ***Crusades*** *passing from Western Europe to Jerusalem. Most of them missed area of Austro-Hungarian Empire. [4]*

1.2. Transport infrastructure planning after Second World War

After the Second World War the development of transport infrastructure planning at European continent process from:

- creating connections between biggest European cities (transport connections within western and southern Europe),
- to connecting new member countries (after spreading of European Union),
- and finally to create local transport network within the regions.

I will stop for a while in the second and third step. In May 2004 Slovakia become a member of European Union and at the same time the state frontiers between western and new member states were officially cancelled. The act can contribute to better cooperation between the neighborhoods states and their transport infrastructure planning. Also the SEA process can be providing at international scale. Why (in spite of benefits we got by this frontiers canceling), the transport infrastructure planning is still providing primary at the state (regional) scale? Of course it is similar also with the Strategic Environmental Assessment. Why the SEA is not providing at international scale? European Union policy tries to support decentralization, transferring the competences from state to region and from region to town. The member states at the other hand still prefer model of organization directed and controlled from one centre. Regions are created within one state; cooperation between frontier regions is accepted (if it is in accord with the state policy). So are there any others limits except the (non-existing) frontiers between countries breaking transport infrastructure planning and its Strategic Environmental Assessment at the European (international) scale? What are the impacts of mentioned way of planning for regional development (in Slovakia), proclaiming by European Union regional policy?

1.3. Slovakia = European region

In European scale the area of our country can be consider as a region; the area of Slovak republic involve 49.035 km^2. Biggest region in France, Rhone-Alps, involve an area of 43 698 km^2. France is nearly 14 times larger than Slovakia. Poland, for example, more than 6 times larger.

At the other hand, distance from east and west () of the country is quite long to create connections at the same high level. The fact mentioned and spreading of the schengen´s area propose an opportunity to develop relationships between the nearest regions, it does not matter if there are situated at the area of neighborhood state. It seems reasonable, if we try to imagine how often the frontiers did change together with state organisation. Just for illustration, today Slovakia is a member of EU, since 1993 till May 2004 was an independent state, since the end of the second world war made a part of Czechoslovakia, between the wars "Slovak state" (1939–1945), before, part of Austro-Hungarian Empire, before, Great Moravia, before, Samo´s Empire. Some frontier parts of the country were alternately parts between neighbourhood countries. With the changes of political organisation the frontiers were changed consequently. (There is remarkable the similar process in the most of others frontiers regions in other European stares (Alsace-Lorainne (Germany-France), Prussia (Poland-Germany), Basque (Spain-France)… These regions everywhere were the places of mixing cultures; they were often the strategic points, interesting for both neighbourhood counties.)

2. Limits and opportunities

2.1. Morphology and geographic situation

Political frontiers between member states were cancelled, but till today geographic situation of the states did not change. Countries have similar opportunities as they had in the past. While the technical progress contributes to transport development, we should remember the geographical situation and the configuration of the terrain still remain too. Our human possibilities are also limited. This should be key factor in transport infrastructure planning also for today.

2.2. Slovak Spatial Development Perspective

In Slovak republic the key document for planning activities in the country is Slovak Spatial Development Perspective (SSDP) (Koncepcia územného rozvoja Slovenska), (in Slovak). SSDP takes into accounts potentials and limits of the area, but this planning is providing primary at the regional (national) scale, like I have already mentioned. It is similar with providing the Strategic Environmental Assessment (SEA).

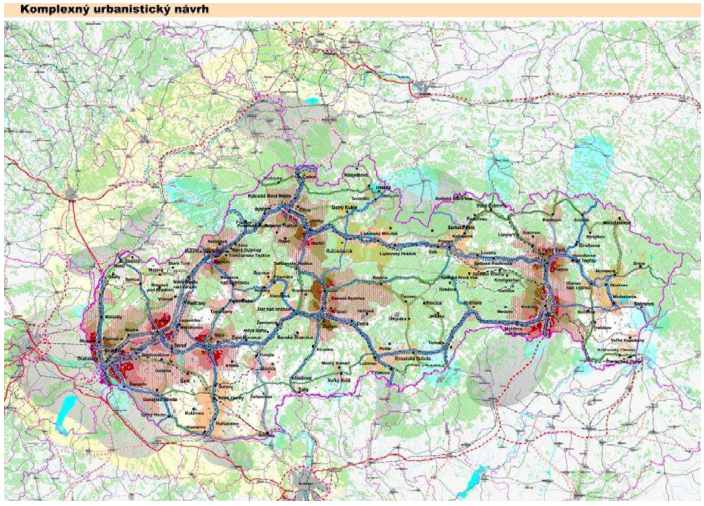

Fig. 4
Slovak Spatial Development Perspective (SSDP), Koncepcia územného rozvoja Slovenska (KURS), (in Slovak) *[4]*

3. Spatial planning

After the Second World War contracts between the neighbourhood states were essential to avoid new conflicts and keeping peace. That was the reason to create the alliance between the France and Germany that change to European Union by the integrating the other member states. Support of regional development is one of the key goals of European Union policy.

First (2004) and second (2007) extension of European Union, formed one big state, involving 41% of the whole European area and 69% inhabitants. One state, without political frontiers, enabling free moving and travelling in the whole European space was formed. By this change also development of transport infrastructure can be planned at a bigger (European scale). In

practice it means, we can try to find the simplest solutions – the simplest corridors, similar like it was in the past.

In spite of possibilities we have, we plan primary at a national scale; we try to connect regions geographically too far and culturally too different. Their cooperation even in the future still remain just the pray. Slovak example can be connection of Bratislava with Košice, at the other hand, good connection Bratislava – Wien is still in the project.

The affectivity of transport infrastructure is in their contribution to regional development. Regional development is possible in regions that are close enough to each other and their cultural background is similar. It can be maybe interesting to see how many people use daily the whole route from Bratislava to Košice. The most of them use just the sort segments. Energy, time, resources and money invested in complicated technical design can be used more usefully. **We can connect Bratislava and Košice via Hungary**. The terrain there is suitable for cheaper solutions.

(That was an example from one state. There are few similar megalomaniac projects in Europe; highway corridors passing across the continent as heavy lines from west to east and north to south. Than TGV project from Paris to Budapest… still the same question; how many people use the whole lane and how often? Most of them will use the segment Paris – Strasbourg or the connections within Germany. Are there a lot of Viennese travelling daily to Budapest or vice versa?)

4. Regional development and the possibilities we got

On one hand there is a possibility to connect very distant parts of continents. On the other hand we should wise up to our real opportunity. Not either the technical capacity but the human ones. We are not able to comprise as large space. Is there any reason to assume important cooperation between Sweden and Italy or between the Netherlands and Bulgaria? There is a great geographical distance and even not smaller cultural difference between them.

The greatest paradox is we did not remark opportunities we got here, at arm's length in our regions. The inspiration we can find in the past again. There are a lot of good examples of international cooperation between frontiers regions. In Slovakia the most well known is agglomeration Bratislava – Vienna (SK-A), Košice – Miškolc (SK-H), Zamagurie and Tatra´s region (SK-PL), Tokay region (SK-H), Slovácko (SK-Morava), Ostrava – Žilina (SK-CZ), Krakow – Zamagurie (SK-PL) and so on.

5. Conclusion

Slovakia is a young member of the European Union. Our road and railway network will be maybe soon connected to the Europeans´ one in a couple of years. Historical and geographical rich country as it is, assume profit from this connection. At the same time, the negative effects of the transport infrastructure (barrier effect, fragmentation of the country) can devaluate the potential of the country. Good assessment of the impact of the human action can contribute to regional development.

Cancelling the frontiers (together with European Union policy) offer possibility to renew the cooperation in frontiers regions; as it was in the past. Political organisation and system change quite often, what remains are the relations between the neighbourhood regions, similar cultural background and geographical proximity. That is the positive we can build on. The identity and originality of each region is essential to keep development of European space. Spatial Infrastructure planning and its Strategic Environmental Assessment (SEA) have an impact to regional development.

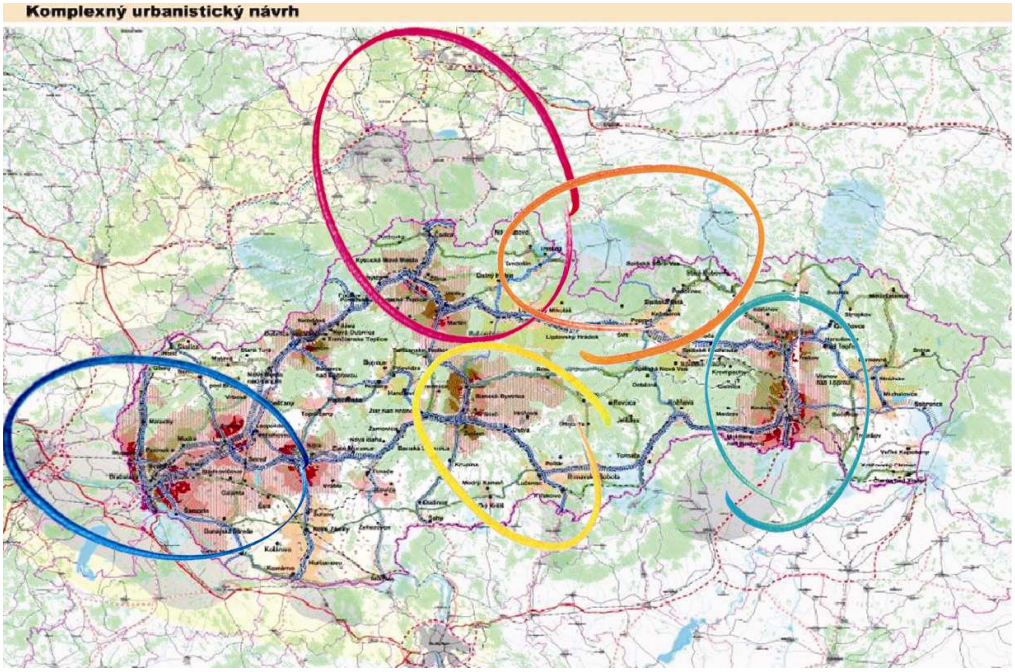

Fig. 5
Opening the frontiers can contribute to regional development within the frontier neighbourhood regions.
(blue: Bratislava - Vienna, red: Žilina – Katowice - Ostrava, orange: Zamagurie – High Tatra´s region, green: Prešov – Košice -Miškolc, yellow: Banská Bystrica – Zvolen - Novohrad (H). It is usable to invested more energy and resources to plan transport infrastructure within one region or neighbourhood regions like to spend so many resources and energy to connect geographically and culturally distant regions.

References

[1] Slovenská správa ciest, 2008. Diaľnice a tunely na Slovensku [online] SSC [2 of July 2008]. web : http://www.highways.sk/

[2] Wikipedia, 2009. Jantárová cesta [online] [19 of February 2009]. web : httpimages.google.skimgresimgurl=httpencyklopedie.divoch.infoimagescommonsthumb99bRota_do_%2525C3%2525A2mbar.jpg180px-Rota_do_%2525C3%2525A2mbar.jpg&imgrefurl=httpencyklopedie.divoch.infocsJantarov%25C3%25A1_stezka&usg=_

[3] Les chemins de st. Jacques de Compostelle [online] [13 of April 2009]. web : http://images.google.sk/imgres?imgurl=http://www.culture-routes.lu/uploaded_files/infos/pa/00000003/img/CheminsdeSaintJacques2.jpg&imgrefurl=http://www.culture-routes.lu/php/fo_index.php%3Flng%3Dfr%26dest%3Dbd_pa_det%26id%3D00000003&usg=__BrQNsrHQjIn6i

QZIsXTjWNSrjQg=&h=305&w=400&sz=23&hl=sk&start=41&um=1&tbnid=OH-O5DTocR3ybM:&tbnh=95&tbnw=124&prev=/images%3Fq%3Dles%2Bchemins%2Bde%2Bst.%2Bjacques%2Bde%2Bcompostelle%26ndsp%3D21%26hl%3Dsk%26sa%3DN%26start%3D21%26um%3D1

[4] Francúzka história, križiacke výpravy [online] [13 of April 2009]. http://francehistoire.free.fr/moyen/croisades/carte.jpg

[5] MVRR SR, 2009. Koncepcia územného rozvoja Slovenska (KURS), (in Slovak), Slovak Spatial Development Perspective [online] [18 of February 2009]. web : httpwww.vucke.skAPIRclankyDocumentskurs.jpg,

[6] KANDERKOVÁ M.: "Environmental problems in spatial transport planning", dissertation thesis, 2008.

[7] Act 24/2006 Coll. on environmental impact assessment and on amendments to certain acts

Transcom 2009, 22-24 June 2009
University of Žilina, Žilina, Slovak Republic

The Main Steps of Education Process for Numerical Simulation

[*]Ján Kortiš
[*]University of Žilina, Faculty of Civil Engineering, Department of Structural Mechanic, Komenského 52, 01026 Žilina, Slovakia, jan.kortis@fstav.uniza.sk

Keywords: Numerical simulation, education process, numerical model, CAD system

1. Introduction

The computer simulations become capable of predicting behavior of the system from a set of parameters and initial conditions. This assumption creates a new area to develop many kinds of simulation software. Customers may choose your favorite software product its possibilities prove satisfactory in all respects. But the latest generation of simulation software includes scientific knowledge which the users have to know if they want to use it. Therefore the right process of education is essential for using these tools. This article says about the main frame of education process.

2. The main steps of education process

A rational education process would have to include a few steps. The theory is the main piece of the frame for all types of computing. Engineers and students often don't know correct connection between theory assumption used by computer simulations and real conditions. So understanding the theory assumptions remains the first priority in the education process.

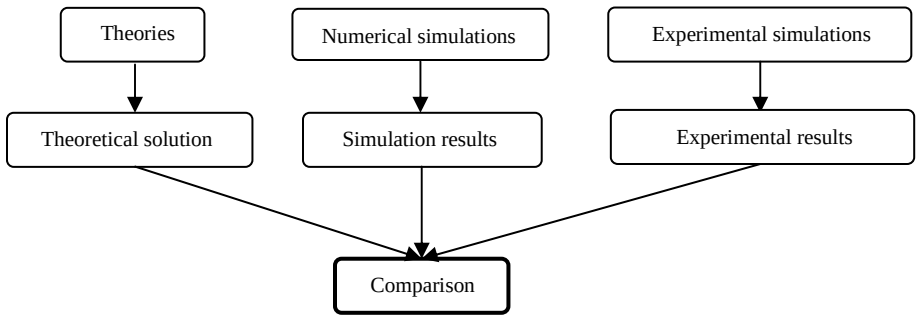

Fig. 1. Connection between the numerical simulations, theories and experiments

This helps them to eliminate major errors during a solution. It is very important to have good mathematical knowledge if you want to understand theory. So the theoretical fundament and mathematical knowledge should be learned at the beginning.

The next very important thing is ability to use CAD systems which enables to create virtual models. Many world-known companies offer their software products which abilities help users to create virtual models. You can create solid models at first, save that as a specific file format and import that model into your computing software. But if you can do it the right way you have to know the foundation of CAD systems. You can also use abilities of computing software to create yours virtual models. But these usually offer only fundamental tools.

Model is after importing geometry meshed and physics attributes are assigned to each region within the model. Sometimes the generated mesh is not appropriate and you need to change the mesh. You can easily improve it by using new element size specifications, refine the mesh locally or improve the mesh by other methods. You can choose the right methods to improve the mesh only if you have a lot of practical experiences. You don't have to create mesh with too many incorrect elements because the results could be wrong. The right boundary conditions are assigned to right places as well as possible to create the realistic physicals conditions.

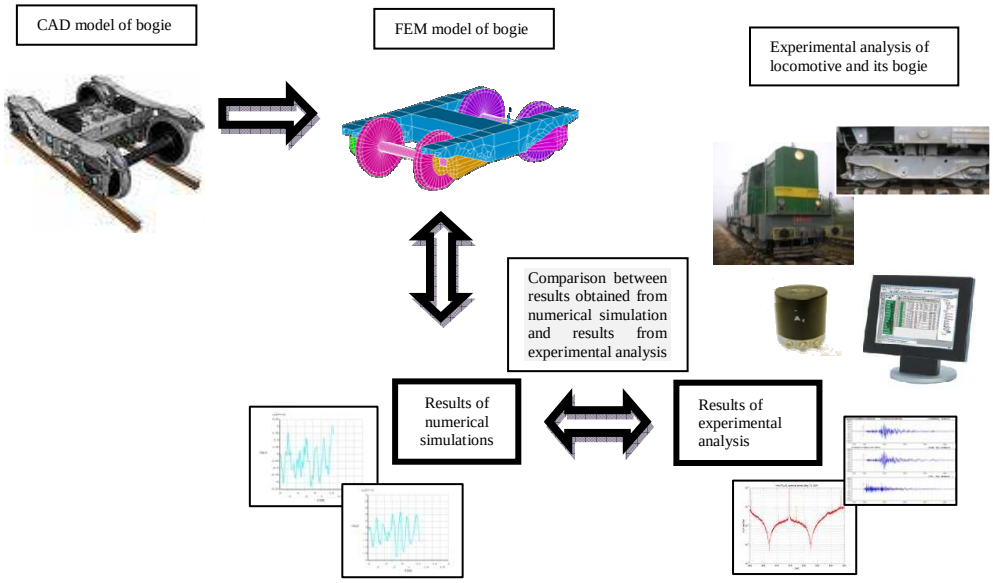

Fig. 2. Example of the main steps of numerical simulation and comparison with results of experimental analysis

After creating FEM model you have to choose some types of analysis. You can usually choose static, modal, transient and harmonic analysis. Next you have to choose if you like linear or nonlinear analysis. The right choice is depend on your requirement of the results and your experiences with numerical simulation. The last step is interpretation of solution results.

3. Interpretation of solution results

Interpretation of solution results is the last very important step. Computing software offer a lot of possibilities to publish results. You can choose band plot or vector plot of results. You can plot displacement, stress, forces and etc. You can plot graph data and you can select a different variable for the X-axis and Y-axis if you need it. Sometime you can even animate results. These possibilities allow creating clean readable and valuable output of results. You can often export output files to other software.

In this case experiences in this field are very rare. Without those you should be very careful during interpretation of results. Very often you can compare them with results which are from some similar previous numerical solutions. Prediction of the results using computer models should be compared with data recorded from experiment too. The experimental analysis provides valuable results if the correct methods are used. So at last the experimental methods should be understood by researcher.

4. Conclusion

You have to know the theory very well if you want to do computer simulations on the right way. So if you can do some numerical simulations on the right way you need theoretical and mathematical knowledge at first. Then you should use CAD systems to create geometry of model and you have to know principles which you use to create FEM models. Experimental analysis is very expensive and need a lot of time to prepare for it but the results are valuable to verification.

References

[1] Liu G.R., Liu M.B. *Smoothed particle hydrodynamics*. 1ed. ISBN 978-981-238-456-0,2003

[2] Manual – ANSYS, release 10.0.

Transcom 2009, 22-24 June 2009
University of Žilina, Žilina, Slovak Republic

The Numerical Aalysis of the Airflow Modeling in the Closed System

[*]Ondrej Kubovčík
[*]University of Žilina, Faculty of Civil Engineering, Department of Structural Mechanics, Komenského 52, 010 26 Žilina, Slovak republic, ondrej.kubovcik@fstav.uniza.sk

Keywords: numerical simulation, computational fluid dynamics, aerodynamic tunnel

1. Introduction

Wind engineering is a very important branch in the present. It serves the purpose of defining and identifying the wind load within the boundary layer of the atmosphere in which many buildings are situated. The issue is actual because of the fact that constructions are designed more precisely and therefore it is necessary to identify the load and its influences on a construction more precisely so that consequently constructions can be utilized more effectively. The simulations of real designed situations of wind load in a wind tunnel or similarly computer simulations are more often used by scientific teams all over the world. Computer simulations are far more accessible nowadays. In comparison with the simulations in wind tunnels they save time though they are quite modern and hiding/containing many unsolved problems.

This article deals with numerical simulation of the airflow in an aerodynamic tunnel of the Laboratory belonging to The Department of Structural Mechanics of the University of Žilina while using one of the most complex software: ANSYS.

2. The Description of Numerical Software

The program ANSYS (made by ANSYS Inc.) is used for a numerical simulation. This program consists of the following modules:

- ANSYS Multiphysics
- ANSYS Mechanical
- ANSYS Structural
- ANSYS Mechanical with the electromagnetics add-on
- ANSYS Mechanical with the FLOTRAN CFD add-on
- ANSYS Professional
- ANSYS Emag
- ANSYS FLOTRAN
- ANSYS PrepPost
- ANSYS ED

ANSYS FLOTRAN is determined for the numerical simulation of models describing *Computational fluid dynamics* – CFD. This module makes it possible to solve adiabatic or thermal action and it supports solving laminar and turbulent flow of fluctuant and nonfluctuant fluid. *ANSYS FLOTRAN* solves tasks using iterative method from which it follows that finite

number of iterations has to be set. In addition the preciseness of the solution that should be achieved during the defined number of iterations. Initiated calculation ends either after the completion of defined numbers of iterations or after the achievement of defined preciseness of searched physical quantities during the n iteration.[1]

3. The Description of the Calculation Model

From the point of view of circumfluence around constructions the air can be considered continuous flowing environment. Its specific mass is ρ=1,226kg*m^{-3} at a temperature 15°C and pressure of 0,098MPa, The mass falls at rising temperature and falling pressure according to this equation:

$$\rho = \frac{1{,}293}{1+0{,}0367t^{\circ}} + \frac{p}{760}\ \left[kg \cdot m^{-3}\right], \qquad (1)$$

where: ρ - density [kg/m^{-3}],

t° - temperature [°C],

p - pressure [MPa]. [2]

To gain the basis for a model it was needed to take the measures of a room, furnishings and their disposition, and also the measures of a aerodynamic tunnel. Velocities were measured two times in three different points of the flow source and at three velocity levels: v(5), v(9), v(14) (the aerodynamic tunnel serving as the basis for numerical simulation has 14 velocity levels in total), from which arithmetical averages were calculated by which the functions of polynomial of the second grade were overlayed *Greisinger TA35 Thermal Anemometer* was used as a measuring device.

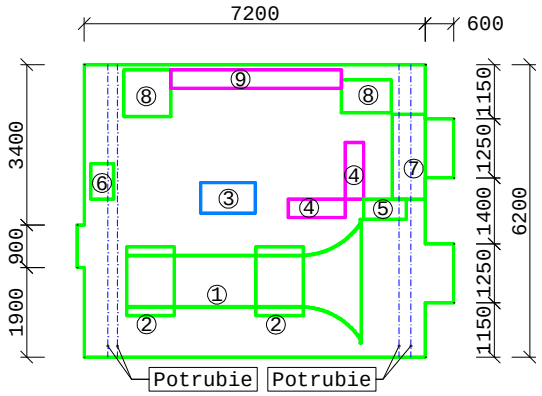

1- windtunel, 2- support od windtunel, 3- table, 4- cabinet, 5- engine, 6- stove, 7- bed, 8- drying stove, 9- wall of cabinet

Fig. 1. The plan of the laboratory belonging to the Department Structural Mechanics of the University of Žilina.

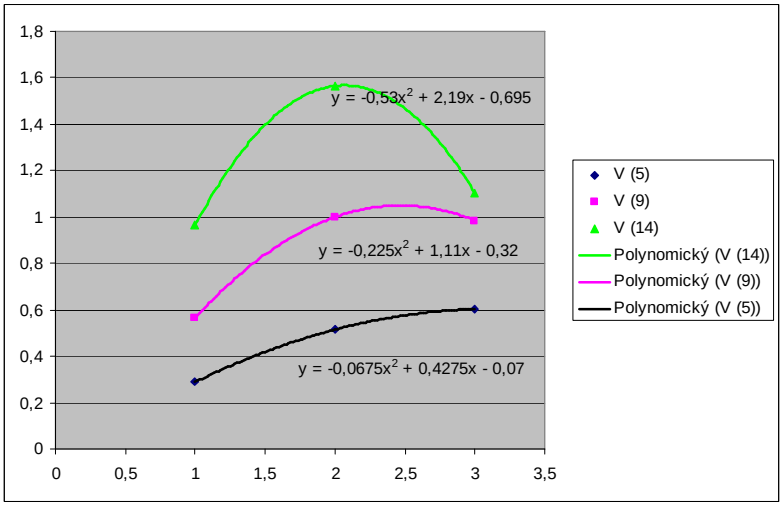

Fig. 2. Arithmetic averages calculated from measured velocities and corresponding functions of polynomial of the second grade.

Measurements were executed at a pressure p=100,4kPa and temperature t°=21°C. We calculated the specific mass by substitution into the following equation(1):

$$\rho = \frac{1{,}292}{1+0{,}00367\cdot 21} + \frac{0{,}1004}{760} = 1{,}2006\,\mathrm{kg}\cdot\mathrm{m}^{-3}\cdot$$

3D model of the room is usually imported into the program *ANSYS* as lines or eventually as surface in case when the object is hardly programmable such as e.g. the inlet of the tunnel – similarly in our case. The other objects were modelled by functions of the program ANSYS. The aim of modelling was to create one object that represents the volume of the medium in the room.

This was achieved when all objects in the room were substracted from its volume by means of a *ANSYS* function. Many issues were neglected while modelling such as the legs of the cupboards, the rounding of the edges and some other objects. Model contains just such objects that are hardly to be moved e.g. the glost oven, the cupboards, the accumulator stove, the tubes. It doesn't contain easily removable objects such as the chairs and people that also influence the airflow in the room.

When setting the model it was important to define marginal conditions correctly. These conditions (initiative) can be divided into three groups:

- setting the velocity vector of the fluid flow (in a closed system) or the flow entrance to the system with defined velocity vector (in an open system of the flow)
- exit of the airflow out of the system (only in open airflow system); only relative value of pressure is entered into the program. In most cases it is zero.
- all three components of the vector of the velocity on the walls overflowed by air has to be zero.

For initiative conditions punctual load was used in particular bonds between the surfaces of the flow source (the velocity vector was calculated for each bond by means of the function of polynomial of the second grade Fig 2). The element used for netting is *FLUID 142*. Predefined *Tetrahedra mesher* was used to create the net of finite elements.

After generating the net of finite elements the model has 756 890 elements and 139 162 bonds.The chosen algorithm is intended only for adiabatic action, laminar flow, and

nonfluctuant flow. The preciseness V_x, V_y, V_z were magnified to 10m/s. The calculation lasted 40 minutes and 508 out of 1000 iterations were realized.

4. The Results of the Numerical Simulation

In order to keep the range of the article the results of the numerical simulation of the airflow are shown just in a characteristic horizontal sectional view of the Laboratory belonging to The Department of Structural Mechanics of the University of Žilina situated at a height of 1,7 m and coming through the measured space of the aerodynamic tunnel.

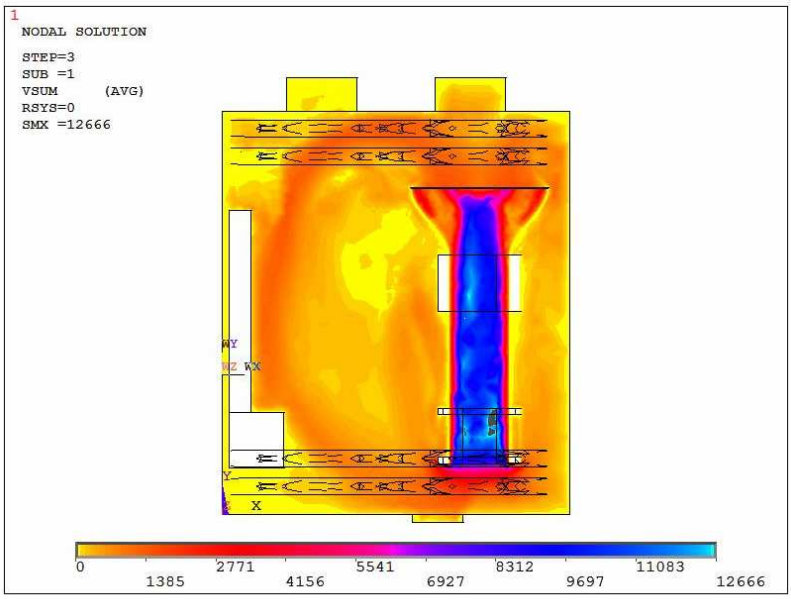

Fig. 3. Areas between isolines of velocity [mm/s] in charakteristic profile.

5. Conclusion

The gained average maximal velocity of the airflow is 11,8 m/s which follows from the measuring in the wind tunnel. It can be seen that the differences in the airflow from the numerical simulation and measuring in the aerodynamic tunnel are irrelevant. Regarding the chosen algorithm for adiabatic laminar flow, the lack of experience in the creation of the net of finite elements, and in choice of the algorithm for netting and of the solver in the program *ANSYS*, it is not possible to find definite elements of the possibility of numerical simulation. The algorithm for turbulent flow, the suitability of choice of algorithm for netting and the solver are the subject of further research.

References

[1] Theory Reference for ANSYS
[2] O. Fischer, V. Koloušek, M. Pirner: Aeroelasticita stavebných konštrukcií

Transcom 2009, 22-24 June 2009
University of Žilina, Žilina, Slovak Republic

The Behaviour of Structural Members Made from Lightweight and Ordinary Reinforced Concrete – Experiment, Analysis

[*]Barbara Kucharczyková, [*]Petr Žítt, [*]Petr Daněk
[*]Brno University of Technology, Faculty of Civil Engineering, Institute of Building Testing, Veveří 92, 602 00 Brno, Czech Republic, {kucharczykova.b, zitt.p, danek.p}@fce.vutbr.cz

Abstract. The article deals with the experimental laboratory tests of ribbed ceiling segments made from lightweight and ordinary concrete reinforced with current steel reinforcement. The laboratory loading tests were aimed at monitoring of the load forces and deformations in concrete and reinforcement, and the rise and development of cracks during the loading. The obtained values of deformations and load forces were compared with the FEM model made in software Atena3D which can describe the behaviour of cement composite very well. In this paper there are presented results of the comparison between deflection values obtained by loading tests and numerical analysis.

Keywords: Lightweight and ordinary concrete, reinforcement, deformation, FEM model, cement composite

1. Introduction

The range of experimental works resulted from a specific application of the lightweight concrete in the reconstruction of a hospital building. The shape of the testing segment corresponded to the real ceiling structure - steel-ribbed floor with the rectangular plan form. The span of the real structure was 6.0 m, distance between the ribs was 750 mm. The dimensions of the testing segments were modified in order to perform the manufacturing and load test according to the range of testing laboratory.

2. Details of Experiments

Two concrete mixtures were prepared. The first mixture was used for manufacturing of lightweight concrete (LWC) members. The fresh concrete was prepared from porous aggregates Liapor 4-8/600, heavy-weight aggregates Bratčice of 0-4 mm, cement CEM I-42.5 R, fluid fly-ash Třinec, super-plasticizer Sika Viscocrete 1035 and water. The second mixture was used for preparation of ordinary concrete (OC) members. This mixture was derived from the fresh mixture of lightweight concrete. All of the components were the same as in the first mixture, only the amount of porous aggregate was changed for the heavy-weight aggregates Tovačov of 4-8 mm and the water amount was reduced to achieve the same workability of the both fresh mixtures. The grade of concrete was determined in compliance with the Czech standard ČSN EN 206 [1]. It means that lightweight concrete LC 35/38-D1.8 and C 35/45 with a volume density of 2230 kg/m^3 was made. The modulus of elasticity of the LWC was 19 GPa and of the OC was 25 GPa. The technological process of the manufacturing and curing of ceiling segments is presented in details in [2], [3].

The loading of reinforced concrete slabs was proceeding continuously up to reach the ultimate state. All tests and mixtures were carried out in laboratory of experimental method at the Institute of Building Testing of the Faculty of Civil Engineering in Brno.

2.1. Geometry and Loading Test

The cross dimension and distance between ribs was held the same as the real structure only the span of the ceiling was one half of the real span. The total form dimensions were 1.5 x 3.0 m. The member cross-section including the reinforcement is given in Fig. 1.

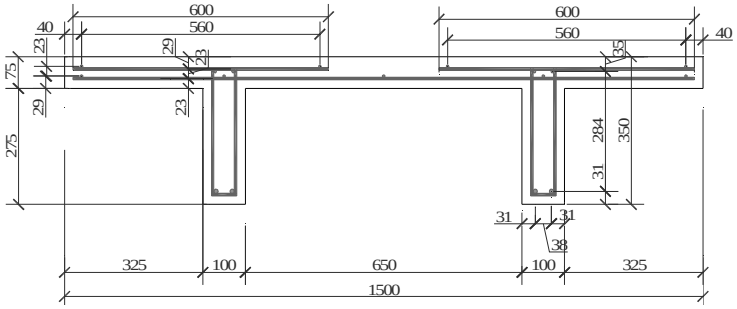

Fig. 1. Member cross-section including the reinforcement

The simply supported segments were loaded by the four-point bending test (Fig. 2). The loading was carried out continuously according to the designed regime up to reaching the failure. Details of the loading regime can be found in [2]. The segments were loaded with a hydraulic two stage pressing pump with load capacity of 250 tons and the force was recorded by a strain gauge dynamometer (S1). The deflections were recorded by the track sensors – potentiometers (P1 – P10) – and inductivity sensors (W1 – W5) placed at the supports, burdens and in the middle of the span (as shown in Fig. 3). The relative deformations of the concrete and reinforcement surface were measured by resistive strain gauges with the base length of 100 mm (TB1 – TB9). All of the used sensors were connected to the central monitoring station Spider8 HBM with the 5 Hz data logging frequency. Location of used sensors is shown in Fig. 3.

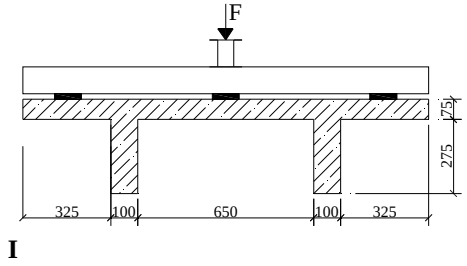

Fig. 2. Configuration of the four point bend test

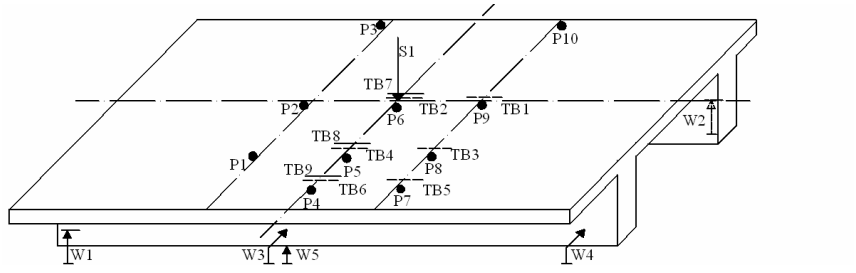

Fig. 3. Location of the used sensors

2.2. Numerical model

The 3D model of testing members was made in software Atena3D [4] which enabled to define the mathematical model of the concrete and reinforcement sufficiently. The nonlinear model CC3DNonLinCementious2 with the experimentally determined physical and mechanical parameters (e.g. compressive strength, tensile strength, volume density, modulus of elasticity, fracture energy [2]) was used for description of the real behaviour of the concrete.

The reinforcement was determined by CCReinforcement material model with the multi-linear stress-strain diagram which was obtained by the experimental tensile test.

The 3D numerical model was loaded by the increment of deformation. The reaction and the corresponding deformation in monitoring points were recorded. These points were in compliance with the real testing members.

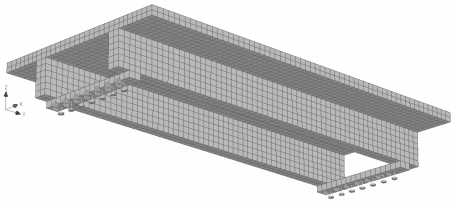

Fig. 4. Geometry of model, net of finite element

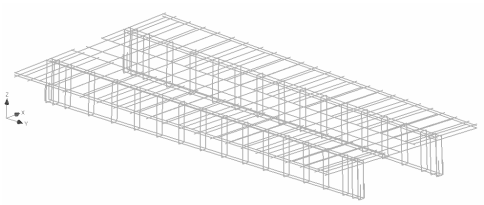

Fig. 5. Scheme of 3D model of reinforcement

3. Results of Experiments

The continual graphical outputs were achieved from the loading tests and numerical analysis. In this paper there are compared only deflections of segments and tension in tensile reinforcement of ribs that were measured in the middle of the span. The load deflection diagrams are shown in Fig. 6. The development of tension in tensile reinforcement of ribs is given in Fig. 7. The summary of the physical and mechanical parameters of both types of concrete are given in Tab. 1. The value of volume density in dried state is not stated.

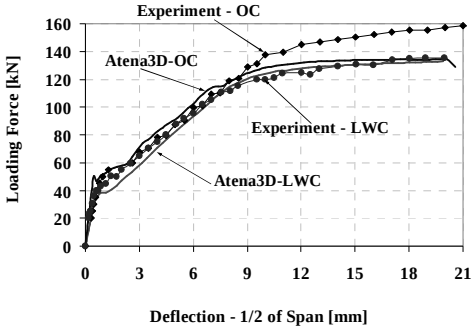

Fig. 6. Load deflection diagrams of loading tests and numerical analysis

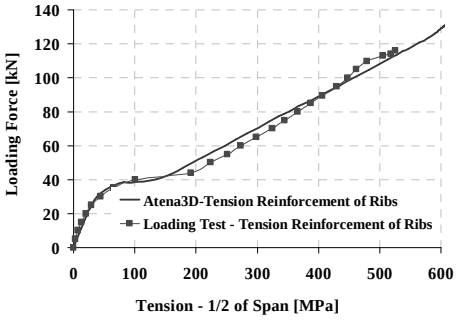

Fig. 7. Development of tension of tensile reinforcement of ribs

Kind of Concrete	The mean values of LWC and OC characteristic *(coefficient of variation in %)*			
	Volume density [kg/m^3]	Compressive strength [MPa]	Tensile strength (Simple tension test) [MPa]	Modulus of elasticity [GPa]
Lightweight concrete (LWC)	1740 *(1.2%)*	45.5 *(4.0%)*	1.64 *(5.7%)*	19 *(1.2%)*
Ordinary concrete (OC)	2230 *(0.8%)*	49.3 *(1.9%)*	*3.91* *(2.4%)*	*25* *(0.9%)*
Parameter (1.....OC)	The relative mean values of LWC and OC characteristics			
Lightweight concrete (LWC)	0,78	0,92	0,42	0,76

Tab. 1. The summary of the physical and mechanical parameters of the LWC and OC

4. Conclusions

The main aim of experiments was the comparison between the behaviour of lightweight and ordinary concrete members. Segments of lightweight concrete LC 35/38 and ordinary concrete C 35/45 were made. According to the performed loading test it can be conclude:

- The differences between the concretes were registered at the moment of the origin of cracks. While the cracks of the ordinary concrete (OC) segments were registered on the load level about 50 – 55 kN, the cracks of the lightweight concrete (LWC) appeared between 35 – 40 kN. The main factor that influences the moment of the formation of cracks is the difference in the tensile strength of both types of concrete. The tensile strength of the lightweight concrete determined by the simple tension test was about 40% lower then the tensile strength of the ordinary concrete.
- The values of deformations in the first linear part of the load diagram were influenced by differences in values of modulus of elasticity of both types of concrete as shown in Tab. 1.
- The total failure of the OC segments occurred at about 190 kN and 160 kN when the LWC segments were measured. Differences were also registered in the failure of the LC an OC segments. It was noticed that the bond between the reinforcement and concrete of the ordinary concrete was better. The failure of the OC segments was caused by the simultaneous collapse of the bearing reinforcement in ribs and slab which caused the total breaking of the OC members in the middle of the span. The failure of the LC segments was caused by the collapse of bearing reinforcement only in the ribs. Total breaking of segments didn't occur.
- Generally it can be said that the performed experiments provided relatively broad and exact outputs which enabled to describe the real behavior of the LC and the OC ribbed reinforced members. The experiments provided a good database for the creation of a numerical model which can be further used for mathematical simulation of similar structures.

Acknowledgement

This outcome has been achieved with the financial support of the Czech Grant agency project No. 103/09/P057 and project MŠMT No. 0021630511.

References

[1] The Czech Standard ČSN EN 206 Concrete – *Specification, properties, manufacturing and conformity*, ČNI, 1993 (2003) (in Czech)

[2] KUCHARCZYKOVÁ, B. *Analysis of influence of characteristics of lightweight structural concrete from porous aggregates on its utilisation in load-carrying structures*. PhD thesis, Brno University of Technology, Brno, 2008

[3] KONVIČNÝ, L. *The experimental and numerical analysis of lightweight and ordinary concrete TT ceiling segments*. Diploma thesis, Brno University of Technology, Brno, 2008

Transcom 2009, 22-24 June 2009
University of Žilina, Žilina, Slovak Republic

Mutual Comparison of Plane Computing Models of Vehicles

*Ivana Martinická
*University of Žilina, Faculty of Civil Engineering, Department of Structural Mechanics,
Komenského 52, 01026 Žilina, Slovakia, ivana.martinicka@fstav.uniza.sk

Abstract. There is possible to use the computing models of vehicles on various level of complicity for the purpose of solution of vehicle roadway interaction problems. Individual computing model can follow the effects only on the certain level. In suggest paper the plane computing models of vehicles are mutually compared. The goal is to clarify the influence of pitch effect on the magnitude of kinematical quantities of computing model and on the magnitude of interacting forces.

Keywords: Vehicle, computing model, dynamics, numerical simulation, contact forces, pitch effect.

1. Introduction

Vehicle – road interaction is actual engineering problem. It can be solved from the point of view of many practical aspects [1], [2], [3], [4]. The methods of numerical simulation are commonly used in praxis. They assume the creation of computing models of vehicles. The computing models of vehicle can be created on various qualitative levels, on principle as three dimensional - 3D, two dimensional - 2D or one dimensional -1D. Equations of motion can be derived in the form of differential equations. The main difference between various computing models is the possibility to model various effects as heave effect, pitch effect or roll effect. The submitted paper is dedicated to comparison of plane 1D and 2D computing models of vehicle and to the specification of the pitch effect on the kinematical and force values of individual computing models of vehicle.

2. Computing models of vehicles

The possible quarter computing model of vehicle is shown on the Fig. 1. Disadvantage of this computing model is that it can model only heave effect on the values of kinematical and force quantities of vehicle computing model. The possible plane computing model of vehicle is shown on the Fig. 2. It can model the heave effect and pitch effect on the values of kinematical and force quantities of vehicle computing model.

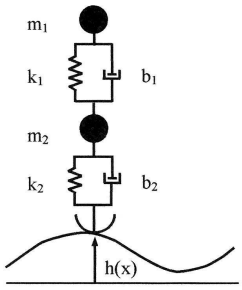

Fig. 1. Quarter computing model.

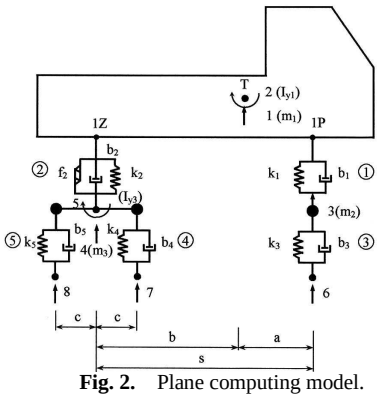

Fig. 2. Plane computing model.

3. Mutual comparison of individual computing models

Essential difference between computing models shown in the chapter 2 is the possibility respectively impossibility to model the heave pitch and roll effects. The best way how to follow the pitch effect is to compare the results for quarter and plane model during numerical simulation its motion along the runway. For the following of pitch effect the comparative study was carried out. During this study the mutual comparison of the results for quarter and plane models are carried out during the modeling of vehicle passing with the speed V = 40 km/h along road unevenness in the shape of 10 cosine waves with amplitude $2.h_0$ = - 2 cm and with length $2.l_0$ = 120 cm. The total length of road unevenness is 12 m. The unevenness is mathematically described by the equation (1)

$$h(x) = \frac{1}{2} \cdot 2 \cdot h_0 \cdot (1 - \cos(\frac{2 \cdot \pi \cdot x}{2 \cdot l_0})) \text{ resp. } h(t) = h_0 \cdot (1 - \cos(\omega \cdot t)). \quad (1)$$

The following designation is used in the upper equation

$$x = c \cdot t, \qquad \omega = \pi \cdot c / l_0, \quad (2)$$

where c is the speed of vehicle motion in m/s.
The topic of mutual comparison are:

1. time courses of vertical displacements $r_{1P}(t)$ of the point 1P situated on the sprung mass m_1 at point of connecting of the front axle of plane computing model with time courses of vertical displacements $r_1(t)$ of the sprung mass m_1 of quarter computing model, Fig. 3,
2. time courses of vertical displacements $r_{3P}(t)$ of the point 3 situated on the unsprung mass m_2 of the front axle of plane computing model with time courses of vertical displacements $r_2(t)$ of the unsprung mass m_2 of quarter computing model, Fig. 4,
3. time courses of contact force $F_3(t)$ in the point of contact of the front axle of plane computing model with runway and time courses of contact force $F_2(t)$ in the point of contact of quarter model with runway, Fig. 5.

Some numeral quantities are presented in Table 1 and 2.

Monitored values		2D	1D	DIF = |2D|–|1D|	DIF v %2D
Vertical displacement of sprung mass m_1 over front axle	*t*	0.5496	0.3308	0.2188	39.8108
	y	-19.2437	-17.3529	1.8908	9.8255
Vertical displacement of unsprung mass m_2 over front axle	*t*	1.1199	1.1159	0.0040	0.3572
	y	8.0672	8.2408	-0.1736	-2.1519
Contact force F_3 under wheel of front axle	*t*	0.9015	0.6848	0.2167	24.0377
	y	-5.3991	-5.2497	0.1494	2.7671

Tab. 1. Pitch effect, comparison of extreme (maxima).

Monitored values		2D	1D	DIF = |2D|–|1D|	DIF v %2D
Vertical displacement of sprung mass m_1 over front axle	*t*	1.6763	1.4231	0.2532	15.1047
	y	7.8733	6.7699	1.1034	14.0144
Vertical displacement of unsprung mass m_2 over front axle	*t*	0.5167	0.2997	0.2170	41.9973
	y	-26.0374	-26.3320	-0.2946	-1.1314
Contact force F_3 under wheel of front axle	*t*	0.5237	0.3063	0.2174	41.5123
	y	-53.6316	-53.2160	0.4156	0.7749

Tab. 2. Pitch effect, comparison of extreme (minima).

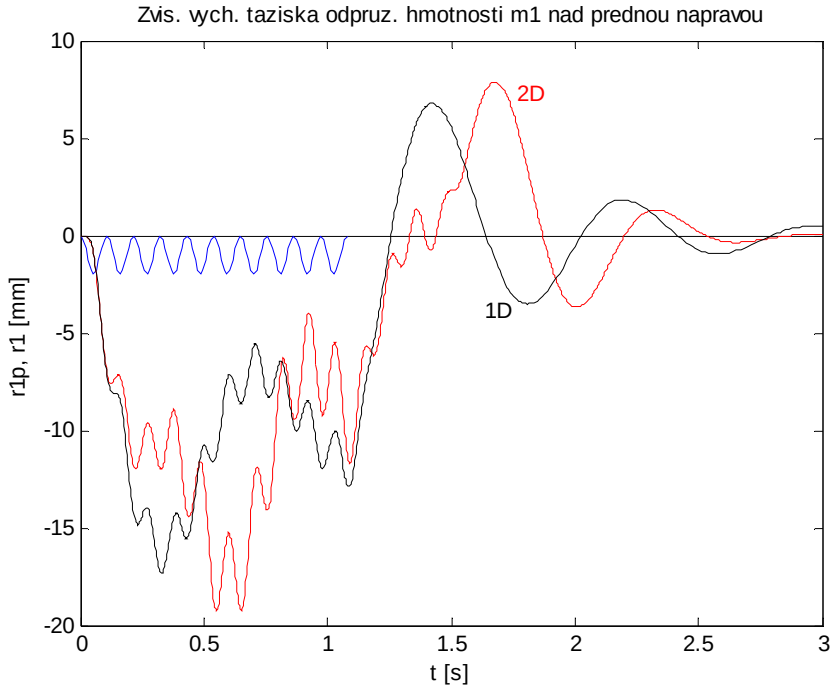

Fig. 3. Pitch effect, sprung mass vertical vibration.

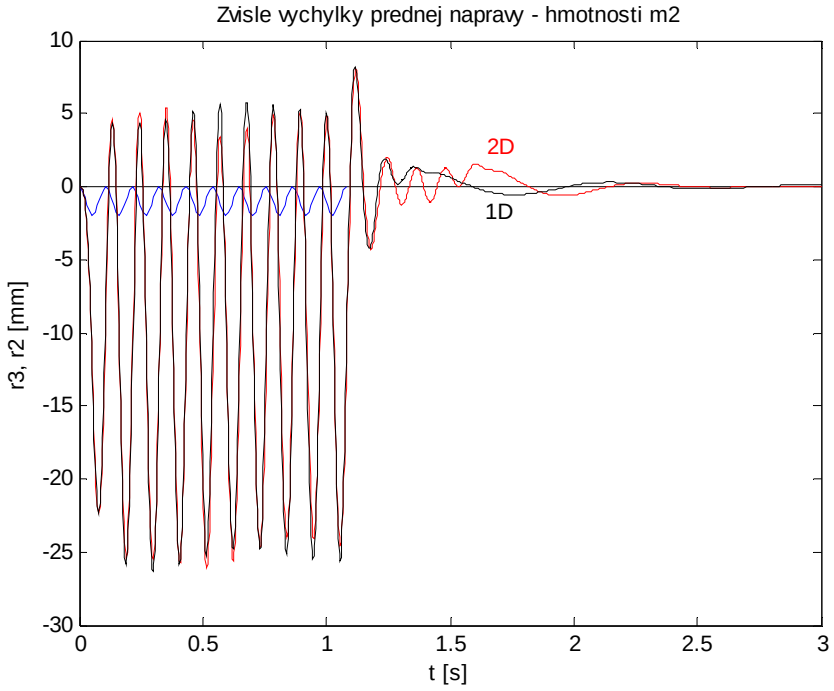

Fig. 4. Pitch effect, unsprung mass vertical vibration, front axle.

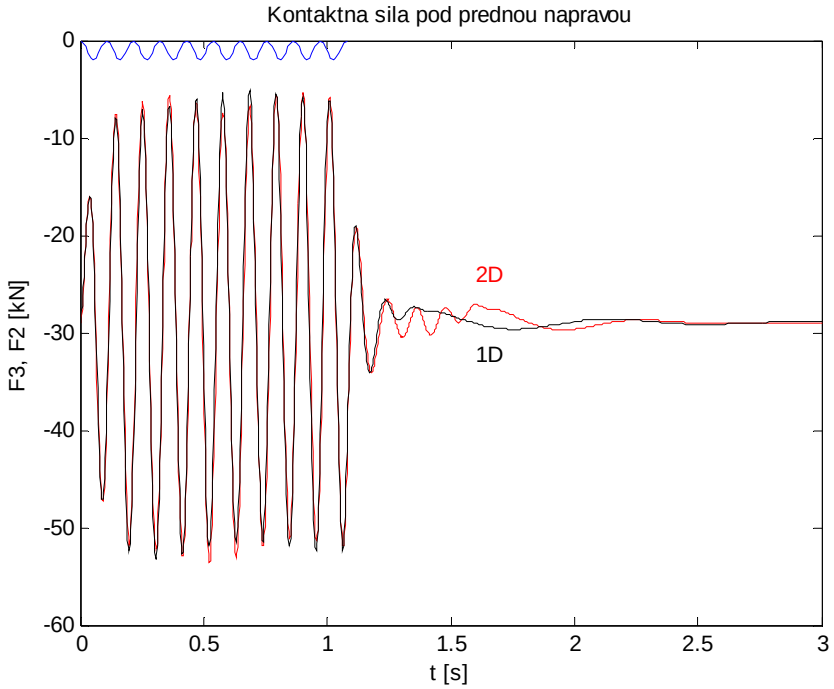

Fig. 5. Pitch effect, contact forces, front axle.

4. Conclusion

The differences of extremes of vertical displacements of sprung mass are 10-15 %. The differences of extremes of vertical displacements of unsprung mass are 1,0-2,2 %. The differences of extremes of contact forces are to 3 %.

Acknowledgement

The paper was supported by the Slovak Grant National Agency VEGA.

References

[1] ZÁHOREC, O. *Contribution to the Analysis of Linear Dynamics Systems with Stationary Random Excitation.* Proceedings of the 1st Conference on Mechanics, Tom 2, p.204-207, Praha, 1987.

[2] POLACH, P. *Polach, P.: Multibody modely nízkopodlažního trolejbusu ŠKODA 21 Tr – modifikace s nápravami RÁBA a kompozitovou přední stěnou.* Výzkumná správa Škoda výzkum, s.r.o, VYZ 0577/2002, Plzeň, 2002.

[3] KRÁLIK, J. – IVÁNKOVÁ, O. – ŠIMONOVIČ, M. *Riešenie problému odolnosti konštrukcie podzemných kanálov za uváženia interakcie s podložím a seizmického zaťaženia.* 8. Ansys – User Meeting 2000, Lednice na Morave, ČR, 2000, s.1-6.

[4] MELCER, J. *Dynamické výpočty mostov na pozemných komunikáciách.* EDIS, Edičné stredisko ŽU, Žilina, 1997.

Transcom 2009, 22-24 June 2009
University of Žilina, Žilina, Slovak Republic

The Impact of the Low – Viscosity Modifier on the Properties of Asphalt Concrete

[*] Grzegorz Mazure, [*]Marek Iwański,
[*]Kielce University of Technology, Faculty of Civil and Environmental Engineering, Al. 1000-lecia P.P. 7, 25314 Kielce, Poland, {gmazurek.Author,iwanski }@tu.kielce.pl

Abstract. The use of an additive that lowers bitumen viscosity results in a significant reduction in temperature of the production of asphalt concrete, which is particularly important if asphalt pavements are laid in autumn. In the experimental tests of the basic bitumen properties (such as penetration and softening point) syntetic wax was used as an additive (low – viscosity modifier) which had a favourable impact on the mechanical properties. The low – viscosity modifier applied in the optimal quantities led to a considerable improvement in the physical and mechanical properties of asphalt concrete (such as structural density, stability, void fraction content) in comparison to the use of traditional bitumen to the production of asphalt concrete and contributed to the reduction in its compaction temperature.

1. Introduction

Various defects occur in asphalt pavements as a result of the combined impact of traffic and climatic factors, which cause constant changes in the values of stress, deformations, temperature and humidity [1]. Bitumen and bitumen – mineral mixes are thermoplastic materials. The proper compaction process of bitumen concrete is undoubtedly significantly influenced by the optimal range of temperatures, under which it is conducted [2]. It has an impact on the bitumen viscosity range, in which the proper efficiency of coating of aggregate grains and the required amount of energy for asphalt concrete compaction are ensured [3].

During the production of asphalt pavements it should be kept in mind that asphalt concrete which has been designed under laboratory conditions and possesses the required properties might not be durable under field operational conditions. It may happen if during compaction the required void fraction content and density, which ensure proper fitting of aggregate grains in the mix, are not reached.

One of the methods of solving these technological and ecological problems of the asphalt concrete technology as well as other kinds of mineral and bitumen mixes produced with the „hot" technology is the application of low – viscosity modifiers in their production. To the framework composition other components (paraphines produced in the Fischer-Tropsch synthesis) have been added, which lower viscosity in higher temperatures. These components are aliphatic and polymer hydrocarbons of long chains. Moreover, bitumen of this kind have much higher softening point and lower penetratrion at 25^{o}C in comparison to traditional bitumen [4].

2. Investigation of the impact of the low – viscosity modifier on the bitumen properties

The tests of the impact of the low – viscosity modifier on changes of the bitumen properties were preliminarily conducted for the traditional 35/50 bitumen from Petrochemia Płock (Poland) which served as a binder. The changes of penetration and the softening point for different modifier contents have been presented in figure 1.

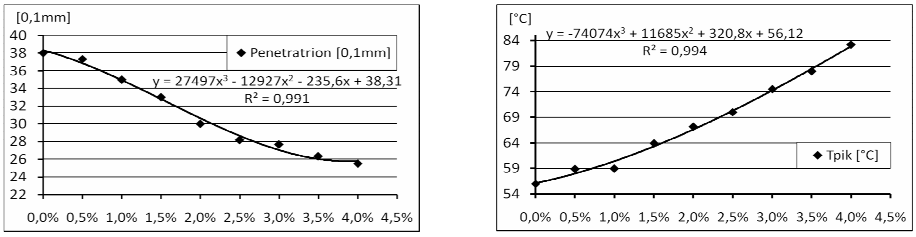

Fig.1. The impact of the low – viscosity modifier content on penetration and the softening point of the traditional 35/50 bitumen.

The analysis of the test results reveals that the low – viscosity modifier influences the selected rheological properties of bitumen as its content increases. At the modifier content of up to 1 % changes are insignificant. At higher concentrations of the modifier it is possible to observe a considerable change in penetration and the softening point. The impact of the modifier becomes weaker as its concetration reaches about 3,5 % with regard to penetration, as opposed to the softening point, which still constantly rises. A favourable impact of the 2 – 2,5 % modifier content ensures an advantageous hardening of asphalt. It also enables to obtain the softening point which is higher than the operational value of about 60 °C. The modified bitumen with such modifier content can be used in the production of asphalt concrete whose physical and mechanical properties are at the required level.

3. Design of the asphalt concrete composition

In order to determine the impact of the low – viscosity modifier content on the properties of asphalt concrete the tests were conducted on asphalt concrete whose grading was 0/12,8 mm which is used to produce the wearing coarse of transit roads pavements. Asphalt concrete with the main diabase aggregate (BA-D) and gabbro aggregate (BA-G) was designed. A dolomite mix 0/4 and granite fractured sand were used to increase fraction contents.

The framework composition of the mineral mixes of the tested asphalt concrete has been presented in table 1.

BA-D	diabase 6,3/12,8	diabase 2/6,3	mix 0/4	granite sand	limestone powder	-
	24 %	23%	23%	24%	6%	-
BA-G	gabbro 8/11	gabbro 5/8	gabbro 2/5	mix 0/4	granite sand	limestone powder
	26%	13%	11%	23%	24%	6%

Tab. 1. The framework composition of the asphalt concrete mineral mixes.

In order to ensure the required adhesion between bitumen and aggregate grains of the mineral mix the adhesive agent Teramin 14 was used in the amount of 0,2 % in relation to bitumen for the tested asphalt concrete with gabbro and diabase aggregate. The required

bitumen content in the designed asphalt concrete was determined basing on the strength measurements according to Marshall methodology.

4. Methodology and test results analysis

In order to determine the impact of the low – viscosity additive content on the properties of asphalt concrete for the selected bitumen, it was decided that the content of the additive Sasobit will very in the range of 1,5% to 4,0% with changes every 0,5%. All the samples were compacted at a reduced temperature in relation to the standards, namely 125 °C, determined during the assessment of an impact of the compaction temperature on the properties of asphalt concrete [5].

During the tests the basic physical and mechanical properties of asphalt concrete were determined. An assessment of the uniformity of the conducted tests was an important element of the project. The measurements were taken only for samples whose void fraction content ranged between (V - 2s ; V + 2s), where: V – is a mean void fraction content value in asphalt concrete in the given group, while s – standard deviation.

The dependences between the low – viscosity additive content and the void fraction content as well as stability of asphalt concrete have been presented in figures 2 and 3. The dashed line describes the void fraction content when the low – viscosity agent was not added.

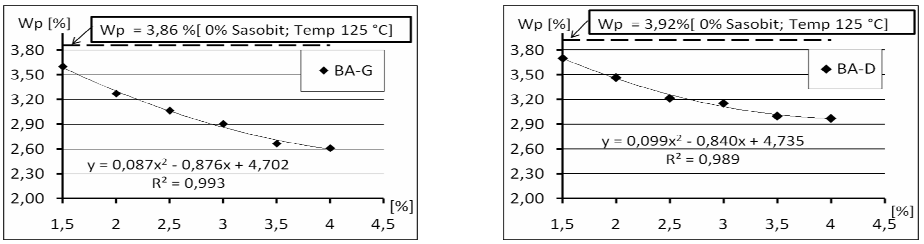

Fig. 2. The impact of the low – viscosity additive content on the void fraction content [Wp] at the compaction temperature of 125°C.

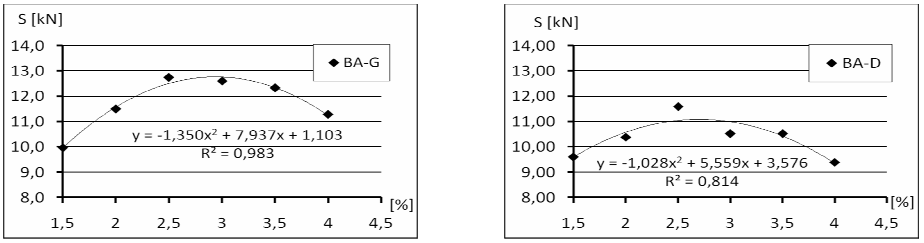

Fig. 3. The impact of the low – viscosity additive content on stability S at the compaction temperature of 125°C.

The statistical analysis of the impact of the low – viscosity additive focused on the one parameter variance analysis. The results have been presented in tabel 2 and tabel 3.

Source	degree of freedom	Square total	Square mean	F value	Pr > F
Model	5	4.19079725	0.83815945	8.46	<.0001
Error	48	4.75619428	0.09908738		
Total corrected	53	8.94699153			

Tab. 2. The variance analysis of the void fraction content in the mixes with diabase aggregate.

Source	degree of freedom	Square total	Square mean	F value	Pr > F
Model	5	6.50481072	1.30096214	8.07	<.0001
Error	48	7.73915970	0.16123249		
Total corrected	53	14.24397042			

Tab.3. The variance analysis of the void fraction content in the mixes with gabbro aggregate.

It needs to be noted that, due to the statistic value of Pr-value <0,05, the content of the viscosity reducing modifier significantly influences the void fraction content. Consequently, the mechanical properties such as stability are also changed. The analysis of the figures in which stability changes are plotted reveals that the maximal value occurs within a certain range of the void fraction content in asphalt concrete of 3÷3,4 %. Thus, it should be concluded that the additive content needs to be precisely applied and that it depends on the physical and mechanical parameters of asphalt concrete with unmodified bitumen. In the present study, due to the stability criterion, the optimal modifier content ranged between 2,5 and 3,0 %. With regard to the void fraction content, an increase in void compression in asphalt concrete of about 0,9 % in comparison to asphalt concrete with the unmodified binder was observed at temperature 20 °C lower than the recommended value of 145 °C.

Analysing the dynamics of the changes of the investigated physical and mechanical parameters of asphalt concrete it should be noted that their enhancement is particularly important in stiff mixes of low binder contents. The kind of aggregate has no impact on the observed relation.

Consequently, the use of an agent which lowers viscosity will considerably reduce compaction resistance in mixes of high chippings fraction contents and significantly reduce the risk of insufficient compaction of thin layers of mineral and bitumen mixes.

5. Conclusions

Basing on the analysis of the test results of asphalt concrete the following conclusions can be drawn:

- the 35/50 bitumen with the low – viscosity modifier has higher softening point and lower penetration in comparison to the traditional bitumen,
- the content of the low – viscosity modifier should be determined in relation to the parameters of concrete with the unmodified binder,
- a modification of the 35/50 bitumen with low – viscosity modifier of the optimal content lowers the void fraction content in asphalt concrete of about 0,9 % at the compaction temperature reduced of 20 ^{0}C.

References

[1] Judycki, J., Jaskuła, P., *Badania oddziaływania wody i mrozu na betony asfaltowe o zwiększonej odporności na deformacje trwałe.* Drogownictwo 12, 1999.

[2] Iwański, M., Dobrowolski, A., *Impact of long-term termal action on the properties of asphalt concrete.* Drogownictwo 8, 1994.

[3] Gaweł, I., Kalabińska, M., Piłat, J., *Road bitumen.* WKŁ, Warszawa, 2001.

[4] Opracowanie Danowskiego, M., *Application of hot mix asphalt of low-term consolidation – german experiences.* Nowości Zagranicznej Techniki Drogowej 196 Warszawa, 2007.

[5] Iwanski, M., Mazurek, G., *Wpływ temperatury zagęszczania na właściwości betonu asfaltowego.*, Krynica: 54 Konferencja Naukowa, Wrzesień 2008, Poland

Transcom 2009, 22-24 June 2009
University of Žilina, Žilina, Slovak Republic

The Diagnostics of Suspended Construction of the Footbridge

[*]Andrej Villim, [**]Lucia Figuli, [*] Peter Polónyi, [***]Marek Bajtala
[**]University of Žilina, Faculty of Civil Engineering, Department of geodesy, Komenského 52, 010 26 Žilina, Slovak Republic, {andrej.villim}@fstav.uniza.sk, {peter.polonyi}@fstav.uniza.sk,
[**]University of Žilina, Faculty of Civil Engineering, Department of Structures and Bridges, Univerzitná 8215/1, 01026 Žilina, Slovak Republic, {lucia.figuli}@fstav.uniza.sk
[***]Slovak niversity of technology in Bratislava, Faculty of Civil Engineering, Department of Surveying, Radlinského 11, 813 68 Bratislava, Slovak Republic, {marek.bajtala}@svf.stuba.sk

Abstract.

Permanent diagnostics and maintenance is necessary for provision of reliability and projected lifetime of bridge constructions. In the report we inform about interdisciplinary co-operation at monitoring of suspended construction for pedestrians in Piešťany.

Keywords: diagnostic, steel bridges, 3D measurement, local geodetic network,

1. Introduction

For improvement of technical condition of bridge constructions it is necessary to pay increased attention to maintenance and reconstruction. They guarantee a reliable function of the bridge construction throughout the entire life expectancy. The statistics indicate that one of five bridges in the area of the Slovak Republic includes defects that are to be removed by reconstruction of maintenance.
The introduced report deals witch the diagnostics of footbridge over Biskupský channel in Piešťany. There is described the diagnostics and the defects of bearing surfaces and the subsequent geodetic surveying of the entire bridge construction.

2. Diagnostic of Bridges

The diagnostics of bridges is essential at determination of operation and for their eventual reconstruction. Its purpose is to provide basic data that enable to examine the state of construction in operation or to determinate ultimate limit state of the bridge [1]. There is generally number of degradation factors that affect the bridge construction and change its reliability. The most often fault source is the corrosive action of metal parts of the bridge. The increased spreading of corrosion effects is caused by the aggression of environment which is induced by intensive industrial environment pollution. Another influence is the mechanical material break – up of the construction caused by load irregularity. The introduced carcase, the footbridge, has been in operation for more than 30 years.

There is neither available original drawing documentation nor static footbridge analysis. There was made detailed diagnostic search of an upper structure and approachable parts of a lower structure. At surveys there were taken basic measures and there were measured

dimensions of load carriers of the constructions. There was found out that the beam hangers are irregularly stressed and the profile of a bridge floor is irregular. The frame pylons have a renovated coating system, their maintenance condition is relatively good. The radius of cable bending at the tops of the pylons is relatively small.
It comes to a complicated tensioning of the cable during the bending at current side thrust. The beam hangers are on many places locally defected and pass through incompetently broken openings in runners. The framework of the bridge floor that serves at the same time as horizontal fixing against wind, it consists of runners, traverse and diagonal members. (Fig. 1)

The parts of the bridge floor are slightly corroded. The coating system has not been restored here. The maintenance condition of a gravity reinforced concrete component is good without bigger failure cracks [2]. Documents from the diagnostics serve for the static recalculation and the footbridge reconstruction design.

Fig.1 Bridge floor corrosion

2.1 Geodetic surveying

Another part of the detailed diagnostics is 3D geodetic measurement which creates a progressive platform for the subsequent design creation for calculation of inner forces, deformations and defects of carcases. For spatial measuring can be used the technology of digital ground photogrammetry [3], 3D scanning or as in our case 3D measurement by means of electrooptical tacheometer with a passive reflexion. Before the detailed footbridge construction measurement itself we build up local geodetic network. It is created by four pinpoints which take into account configuration of the surrounding terrain, vegetation cover and

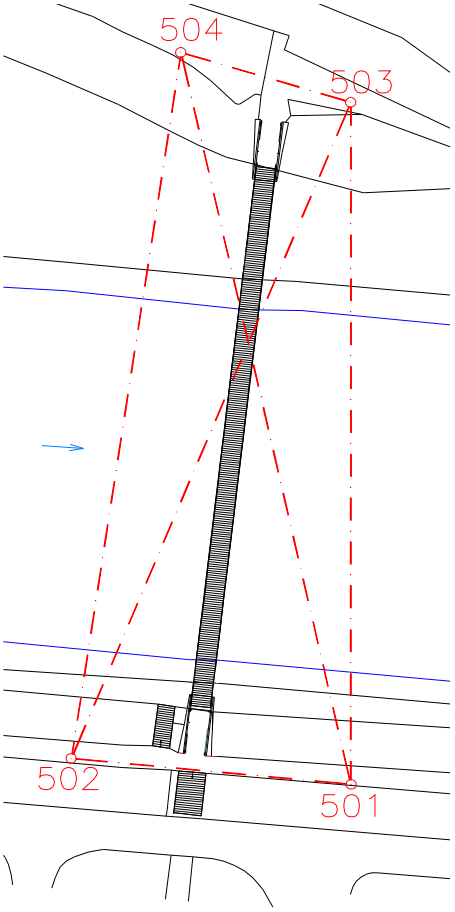

Fig.2 Geodetic network configuration

they are optimally chosen in consideration of the range and shape of the construction work. (Fig. 2). The parameters of the local geodetic network were measured with the instrument Leica TCR 705, (the accuracy of the angle measurement is 2 mgon and the accuracy of the length measurement is 2 mm + 2ppm) and with digital levelling instrument Leica NA 3003. The network was subsequently levelled out as free with

2. linear model – an indirect measurement [4]. The levelled out coordinates and average errors of the network pinpoints are introduced in Tab. 1.

The detailed footbridge pinpoints were measured from the built up local geodetic network with the electrooptical tacheometer Leica TCR 705. We registered directly the coordinates X, Y from the separate detailed footbridge pinpoints.

Point	Coordinates			Average errors coordinates		
	Y [m]	X [m]	Z [m]	mY [mm]	mX [mm]	mZ [mm]
501	500,000	593,285	101,256	1,3	1,9	0,7
502	536,167	589,729	101,436	1,7	1,8	0,6
503	500,000	500,000	101,209	1,8	2,1	0,8
504	521,990	493,182	101,403	1,5	1,6	0,6

Tab. 1. Coordinates and characteristics of the accuracy of the pinpoints of the local geodetic network.

The detailed footbridge pinpoints were measured from the built up local geodetic network with the electrooptical tacheometer Leica TCR 705. We registered directly the coordinates X, Y, from the separate detailed footbridge pinpoints.

2.2 Architectural presentation

For the 3D presentation itself the software CIVIL 3D, AutoCAD 2008 were used. There were imported the coordinates of all pinpoints into the programme. The pinpoints were joined by means of the field sketches made in terrain and by means of photo documentation. The separate parts of the object were divided into various levels in the drawing. It enables wide variability of choice and combination of separate construction parts into the spatial model (Fig. 3). It is possible to export the 3D model created this way into the programmes enabling static, dynamic and stress analysis of building construction.

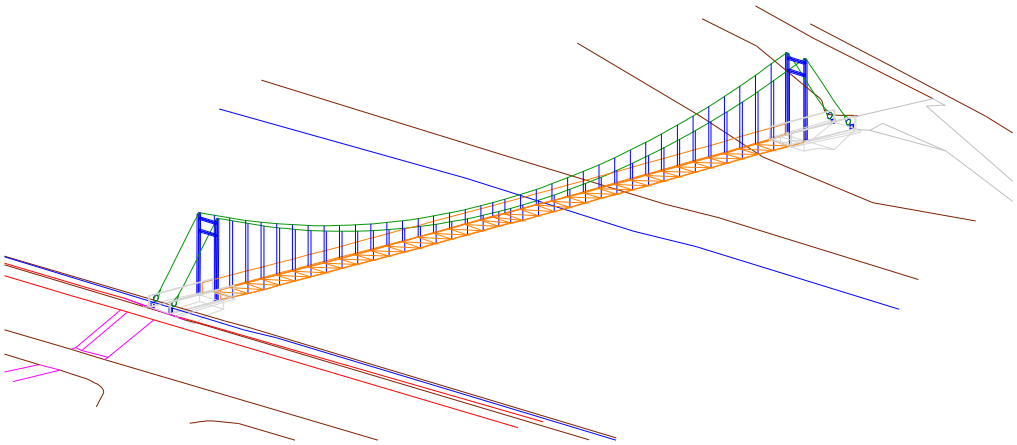

Fig.3 3D object of footbridge

3. Conclusion

At bridge diagnostics the co-operation of statistician and land surveyor enables a progressive creation of 3D models concluding from the real production of the construction work.
The geodetic methods enable us on the one hand to acquire disposition plan of the construction, if there is no available original project documentation and on the other hand to note down the actual imperfections from the original design.
We create this way modelling space for static, dynamic and stress analyses of construction works as well as for expertise judging and designs of necessary reconstructions. Reference of the object in geodetic systems also enables to implement the construction work into information system [5] and [6] and subsequent multivariant and time analyses [7].

This work was supported under the research project VEGA no. 1/0781/09.

References

[1] Bujňák, J. *Kovové mosty. Spravovanie, údržba a rekonštrukcia*. Žilinská univerzita, Žilina 2005

[2] Expertízne posúdenie a návrh úprav visutej konštrukcie lávky pre peších nad biskupickým kanálom v Piešťanoch, SvF Bratislava, 2005

[3] Krušinský P. – Pisca, P – Babjaková, Z.: Nedeštruktívne monitorovanie trhlín na stavebných konštrukciách s využitím digitálnej fotogrametrie. Zborník referátov medzinárodná konferencia Železničné pozemné stavby 2008, Slovensko, Vysoké Tatry – Tatranské Zruby, 09-10.10. 2008, ISBN 978-80-968847-8-0, p.147-154.

[4] Bitterer, L.: Vyrovnávací počet, Žilina, SvF ŽU v Žiline 2004, http://svf.utc.sk/kgd/vp, s.164

[5] Hodas, S.: Turnout layout in ZHIS – increasing the quality and accuracy of the geodetic measurements of the spatial objects position processing. In: Civil and Environmental Engineering - Scientific-Technical Journal: 3, 2007, No.1, University of Žilina, Faculty of Civil engineering, svf.uniza.sk/cee, SK, 2007. - ISSN 1336-5835, p. 67-78

[6] Koťka, V.: GIS na riadenie miest a obcí. Kandidátska dizertačná práca. Žilina 2007.

[7] Ižvoltová, J.: Control of the Building Construction Parameters. Civil and Environmental Engineering Vol. 4th/4, Issue 1/2008 , ŽU Žilina 2008, p. 12-16

Transcom 2009, 22-24 June 2009
University of Žilina, Žilina, Slovak Republic

RSV Program and its Use as a Tool in the Process of Risk Assessment and Management

* Ľuboš Remek, * Milan Valuch
*University of Žilina, Faculty of Civil Engineering, Department of Construction Management, Komenskeho 52, 01026 Žilina, Slovakia, {Milan.Valuch, Lubos.Remek}@fstav.uniza.sk

Abstract. The article focuses on introduction of RSV program as a system tool for management of production of constructions and explains its function from a viewpoint of a constructor of structures who introduced this system and software into his company. It explains risk assessment and management issues and shows the benefits of using the RSV system as an efficient tool in the process of risk assessment and management.

Keywords: RSV, civil engineering management, risk assesment, risk management,

1. RSV program tool

The RSV program made by FIRST information system company is a system tool which combines software environment for creation of a database, maintaining, evaluation and monitoring of production processes with complete structural ordering of a civil engineering company.

Program RSV – Building Management Program is designed for the companies – suppliers of construction works, practically of any size. It is able to satisfy companies with thousands of employees and multilevel management system due to its general conception. On the other hand it is also a suitable tool for small building companies as it can be bought at a reasonable price. Criterion of its efficiency is not size of a company but primarily awareness of necessity of an information system and effort to use the information in management of the company.

1.1. Aims of the RSV system

Although this system has multipurpose features which enable a company benefit from its capabilities, its principal aims are as follows:

- To create an information system providing comprehensive information by supplementation and integration of routines used in the building company until now.
- To record and/or generate information necessary for management of particular structures, centres, plants and company as a whole. To make the information accessible to the authorized persons on all levels.
- To make information existing in a scattered form in routines used until now accessible and display it in a uniform environment and in corresponding relations; again respecting competency.
- To become a useful tool in the management process of a building company.

Crucial fact is that all these aims lead to profit formation by increasing efficiency and minimalizing scope of works that would be otherwise needed to fulfil these operations. [1]

1.2. Benefits in RSV implementation

Financial effect achieved by proper use of the RSV program is finds expression mainly in savings. They increase the economical effectiveness by providing:

- Comprehensive and timely information about building.
- Project management of specific orders.
- Complex management of construction production.
- Efficient monitoring of subdeliveries.
- Support of implementation of ISO 9000 in practice.
- Time saving.
- Reduction of risks connected with realization of buildings.

1.3. Model of RSV program

A building order undergoes a certain life cycle in practice. This cycle is simulated by a tree of phases and states in an information system. Passage of an order through a company defined this way becomes a basic skeleton on which individual processes carried out in various states or phases of the order are „hung".

Every state is subordinated to a phase in which it occurs. Every phase can include more states in dependence on the requirements.

Every phase and every state as well as transitions between them are freely definable. It means in practice that whenever in the course of application of the program a requirement for a change comes out, it is possible to carry out this change immediately by a mere configuration.

The following figure shows a scheme of phases and states proposed for standard building orders [1]:

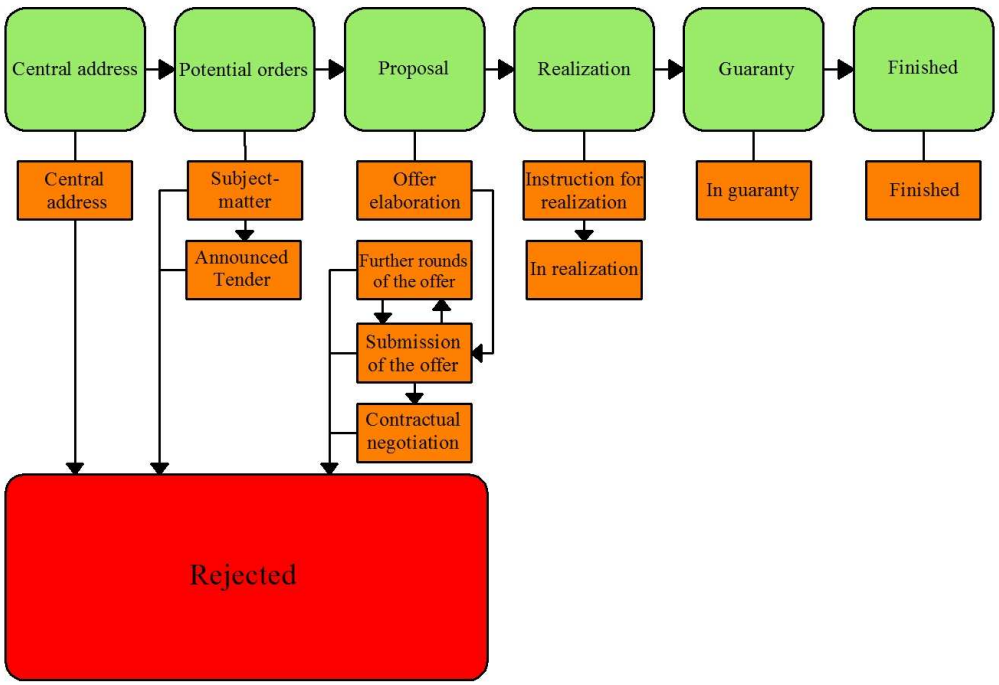

Fig. 1. Phases and states proposed for standard building order.

2. Risk assesment and management

Risk management is increasingly being viewed as a core business driver that influences all decision making, rather than an activity undertaken as an isolated process. A corporate risk management framework needs to be consistently applied across the organization.

2.1. Risks in construction production

Risks appearing in management of construction production differ in their character and environment in which they can occur. The risks can be divided accordingly as follows:

- Risks at a corporate level
- Financial and investment risks

Risks at a corporate level – problems of safety and health protection at work, issues of personal management, organizational operation of a company, assets used by the company etc. are involved

Financial and investment risks – risk connected with an order and phase in which it is occurs, for instance competitive environment on the market or risks connected with legal liability for a building project.

2.2. Risk assessment

The first condition of correct risk assessment is determination of a risk frame. A correctly determined frame is the main assumption for execution of a risk analysis.

Following issues should be determined:

- Environment in which the risk occurs
- Stakeholders
- Criteria influencing risk occurrence

Subsequent risk assessment will provide a guidance for selection of a correct strategy how to deal with the risk. Risk assessment is based on risk analysis. The risk analysis includes:

The risk analysis includes:

- Risk classification.
- Probability that a risk occurs.
- Consequences in a case of possible failure.
- Inspections carried out to follow changes of risk probability and its consequences.

2.3. Risk treatment

In a case of a failure or the danger of imminent failure, strategies can be developed to avoid or react to such circumstances. If the presented danger is critical to the organization, then the avoidance of it is likely to be more effective than reactive activities.

At a corporate level an organization should understand its total risk exposure from all sources, so that it can adopt cost-effective corporate approaches to risk management.

For example, the strategy in some organizations is to self-insure for all types of risk to a specified value, then use insurance to cover higher cost risk. Unless the organization is aware of the level of its total exposure it cannot set an effective self-insurance level or know what risk level has been retained. [2]

Organizations need to weight the cost of avoidance against the cost incurred by accepting risk. This involves cost-benefit analysis.

Several strategies to manage the total business risk are available:

- Reduce the risk by capital or maintenance expenditure.
- Reduce the impact of a failure by actions such as preparing emergency plans.
- Accept some risk and carry consequential costs.
- Insure against the consequential costs.
- A combination of the above.

3. RSV program as a tool in risk assessment

As it is apparent from the chapters 1.and 2. the RSV program can be used also as a tool of risk assessment and management. Capability of the program to register information for building management makes from it a database file whose data can be used in this process. Thus application of the RSV system helps this way also to reduce costs and/or increase efficiency of the construction production.

3.1. Risk assessment on corporate level

Capability of the program to provide a detailed review of operation of the company and its employees proves useful mainly in a case of risk evaluation at a corporate level. Operational and economical routines which can provide basic data for risk analysis at a corporate level are involved above all.

3.2. Financial and investment risk assessment

The RSV program includes tools for detailed monitoring of the market, customers, competitors and subcontractors. These databases are an excellent source of information necessary for investment risk assessment.

Checking of an order in all its stages includes examination of economical plans, interim and final economical assessments of the orders, cost-benefit plans, lists of executed works, invoicing, schedules etc. Besides, the program has also an interface for quality supervision. These tools used to increase efficiency of the building production centralize simultaneously basic data used on elaboration of financial risk analysis.

4. Conclusion

Information used in risk assessment, which is decentralized in the frame of a company organization under common circumstances, and gathering of which can waste time and resources, is collected in one centralized unit when using the RSV program. As a fair amount of consistency is presupposed in the RSV system on its operation, all basic data obtained from it can be considered exact and actual. Thus, application of this system as an information source is a factor reducing among others probability of faults in data collection for the needs of their assessment.

References

[1] First information systems s.r.o. *Popis stasndardní funkcionality RSV* v1.0 20.1.2008.

[2] Association of Local Goevernment Engineering New Zealand (INGENIUM), National Asset Management Steering (NAMS) Group, *International infrastructure management manual version 3.0 2006*.

Transcom 2009, 22-24 June 2009
University of Žilina, Žilina, Slovak Republic

Design of Compression Members for Durability

[*]Marián Sýkora,[*]Josef Vičan,
*University of Žilina, Faculty of Civil Engineering, Department of Structures and Bridges, Univerzitná 8251/1, 01026 Žilina, Slovakia, vican@fstav.uniza.sk marian.sykora@fstav.uniza.sk

Abstract. General principles of structural elements design for durability and their application in the case of compression members are presented in this paper. The degradation effects of material deterioration due to corrosion cause the loss of member resistance, but the limit states method does not directly reflects design and verification for failures caused by material deterioration. The time – variant loss of compression member resistance was computed for specific corrosion models to express the time – dependent approximation function taking into account effects of corrosion degradation. The design member resistance can be obtained using buckling member resistance multiplied by a time - dependent function considering corrosion degradation effects within the member lifetime.

Keywords: durability, prediction of ultimate strength, time – dependent corrosion effects.

1. Introduction

Present standard methods of the reliability theory are based on verification of the structural reliability from the viewpoint of limit states caused by the permanent, variable and accidental actions. Structural failures and damages caused by environmental actions in the form of various material degradations due to aggressive environment and its changes within bridge lifetime are taking into account indirectly or neither in member design. Therefore, durability of steel structures is ensured by choice of an appropriate material resistant against the aggressive environment, using appropriate and verified structural details ensuring to minimize environment influences and enabling inspections and maintenance, by structural redundancy and by the choice of an appropriate corrosion protection system.

The general concept of the structural member design for durability is given in standard [1], but the form is useless for practical applications. The reason is, on one hand, the shortage of information about transfer mechanism by which the environmental influences are transferred into agents acting on the structure to cause damages like corrosion. On the other hand, the processes have stochastic character depending on many random variable parameters, so that the mathematic interpretation for structural design is very complicated.

Generally, two concepts of structural verification for durability should be used. The first approach is based on the concept of the bridge design structural service life t_s, where the probability shall be verified according to formulae

$$P_f = P\left(t_S \le t_D\right) \le P_{fd} \,. \tag{1}$$

where t_D is the bridge design lifetime, P_f is the probability of failure and P_{fd} is the target probability of failure. The second approach is based on the limit state concept design considering effects of environmental actions in the form

$$P_f\left(t\right) = P\left\{R\left(t\right) - E\left(t\right) \le 0\right\} \le P_{fd} \,. \tag{2}$$

where *E(t)* represents the random variable time dependent action effects and a *R(t)* is the random variable time dependent structural member resistance. *E(t)* and *R(t)* are functions of random variables X_i , which are also time dependent functions in relation with the models of material degradations.

Because of random variable character of many parameters entering corrosion process, the probability theory and mathematic statistics should be the most appropriate approaches to describe it. At present, several corrosion models are known, which could be generally used for analysis of the corrosion influence on the structural member reliability. Review of the most frequent corrosion models describing loss of material in time is presented in Table 1.

Author	Mean [mm]	Standard deviation [mm]	Distribution
Southwell-Melchers [2]	$0.084t^{0.823}$	$0.056t^{0.823}$	Normal
Frangopol [3]	$0.03207t^{0.5}$	$0.00289t^{0.045}$	Normal
Qin-Cui [4]	$1.67\left[1-\exp\left(-t/9.15\right)^{1.97}\right]$	$0.0674\left[1-\exp\left(-t/0.181\right)^{0.0294}\right]$	Normal
Guedes Soares [5]	$d_{corr}(t)=1.5\left(1-e^{(-t/10)}\right)$ where t is time in years		—

Tab. 1. Probabilistic corrosion models.

2. Time – dependent buckling member resistance

Taking into account the buckling effects and the effects of variable randomness which are influencing the resistance of compression member, the buckling member resistance can be expressed in the form (3), that is a function of many material and geometric random variables

$$R = \chi . f_y . \varphi_A . \prod_{i=b}^{n} \varphi_i \, . \tag{3}$$

where χ is the actual value of reduction factor covering buckling effects and so on,
f_y is the actual value of yield strength f_y,
φ_A is the ratio of actual value to nominal value of a member cross-sectional area,
$\varphi_i = F_i/F_{ni}$ is ratio of actual value to nominal value of i - partial effect on member resistance or material.

Following the Ayrton – Perry approach, the ultimate strength of an initially curved member respecting the random variables effects can be rewritten the equation to following formula

$$R_c = \left\{ \frac{1}{2}\Psi - \left[\frac{1}{4}\Psi^2 - \frac{\varphi_{fy}\,\varphi_E\,\varphi_I}{\varphi_A \cdot \overline{\lambda}_n^2} \right]^{0,5} \right\} \cdot \varphi_A \cdot A_n \cdot f_{yn} \, , \tag{4}$$

where

$$\Psi = \varphi_{fy} + \left(1 + e_{0k} \cdot \frac{A_n}{W_n} \cdot \varphi_{e0} \cdot \frac{\varphi_A}{\varphi_W} \right) \frac{\varphi_E \cdot \varphi_I}{\varphi_A \cdot \overline{\lambda}_n^2} \, , \tag{5}$$

$$\overline{\lambda}_n = \sqrt{\frac{f_{yn} L_{crn}^2 A_n}{\pi^2 E_n I_n}} \, , \tag{6}$$

and the basic random variables are for the Ayrton – Perry approach introduced in the non dimensional forms as a ratio φ_i.

$$\varphi_{fy} = \frac{f_y}{f_{yn}}; \quad \varphi_{e0} = \frac{e_0}{e_{0n}}; \quad \varphi_E = \frac{E}{E_n}; \quad \varphi_A = \frac{A}{A_n}; \quad \varphi_W = \frac{W}{W_n}; \quad \varphi_I = \frac{I}{I_n} \, , \tag{7}$$

3. Parametric study of the time – dependent buckling member resistance considering corrosion degradation

To determine effects of the corrosion losses on the buckling member resistance, the parametric study of I-cross-section member was realized (the results of previous parametric studies for 6 beams realized for bending moment resistance are presented in [6]). All cross-sectional dimensions b_f, t_f, h_w, t_w as well as the yield strength f_y were considered as random variables. Standard deviations of the considered cross-sections were determined using the standard for tolerances of web heights and flange widths and according to standard for tolerances of web and flange thicknesses (class A). They were obtained based on the assumption of the normally distributed random variable standard tolerance *a* and that 95% of random variable realization are in interval $(m_x - a\ ;\ m_x + a)$, so called 2σ rule.

To determine the buckling resistance of an initially curved member respecting the time – dependent degradation effects, which were arose due to corrosion of its flanges, the above mentioned approach was used. Numerical analysis of the determining time - variant moment resistance taking into account the randomness of the cross-sectional dimensions and yield strength was realized using software MATLAB. This parametric study was calculated for the non dimensional slenderness $\lambda_y=\lambda_z=0{,}25$; 0,50 ; 0,75 ; 1,00 ; 1,25 a 1,50. The values of random variables were generated by means of Latin Hypercube Sampling (LHS) for 10 000 samples considering normal distribution. For all the prediction models of corrosion losses, the time - dependent development of moment resistance within the design working life of 100 years was computed. The corrosion losses d_{corr} described by the previously mentioned probabilistic models were considered as reduction of flange thickness given by formula $t_{f,\,red} = t_f - d_{corr}$, where t_f is the flange thickness without corrosion effects.

Degradation function *F(t)* was derived as the ratio of time variant resistance *R(t)* of degraded member and resistance R_0 at the beginning of bridge member exploitation. For further general use, the degradation function *F(t)* has been approximated by means of regression techniques based on the function given by formulae (**Chyba! Nenašiel sa žiaden zdroj odkazov.**) using MATLAB software environment.

$$F(t) = R(t)/R_0 = a.e^{-b.t} + c\,. \tag{8}$$

From this study follows, that value *b* remains for relevant corrosion model unified and constants *a*, *c* are only changing. This fact leads to an idea that for practical application, the relevant corrosion model could be used in dependence on environmental condition in the form of (8) knowing "degradation constant *b*" and the "shape constants *a*, *c*" should be computed in dependence on cross-sectional characteristics. For practical use, the degradation constant *b* is supposed to represent time - variant corrosion progress depending on the relevant corrosion prediction model and constants *a*, *c*, are defining the cross - sectional characteristics.

For better understanding of this problem, the second parametric study for 2000 I- beams with random cross – sectional characteristics was realized allowing for higher bound 3,0 for non dimensional slenderness. Finally, the time – dependent buckling resistance of the deteriorated structural imperfect member at time *t* could be obtained using the following formulae

$$N_{Rd}(t)_{\lambda \le 0,2} = N_{Rd,\,t=0}.F(t) = A.f_y.\left[1 + a\left(e^{-bt} - 1\right)\right]. \tag{9}$$

$$N_{Rd}(t) = N_{Rd,\,t=0}.F(t) = A.\chi.f_y / \Delta(\lambda).\left[1 + a\left(e^{-bt} - 1\right)\right]. \tag{10}$$

$$a = 2.b_f / A\,.\,\alpha_{\text{corr. model}}\,. \tag{9}$$

where the value of the constant a is calculated according to (9) while for constants b, $\alpha_{corr.\ model}$ the values in accordance with table 2 are valid.

Corrosion model	Constant	
	"b"	"α"
Frangopol	0.0194	3.278E-04
Melchers	0.0055	8.460E-03
Qin - Cui	0.2158	1.655E-03
Guedes Soares	0.1003	1.490E-03

Tab. 2. Values of corrosion constants.

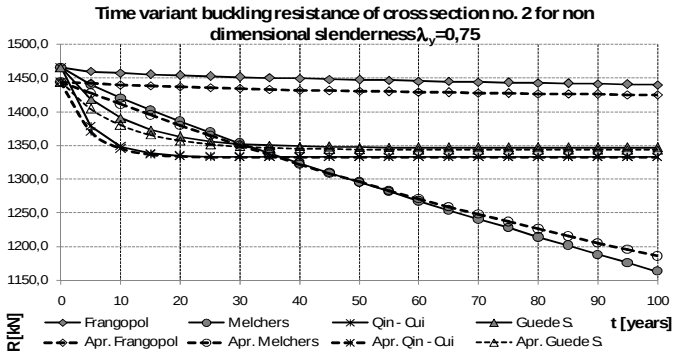

Fig. 1. Comparison of the numerically and according to (10) determined time - dependent buckling resistance

4. Conclusion

The member resistance is significantly influenced due to degradation effects in the form of corrosion and therefore the corrosion effects should be taken into account for structural design. This paper presents simplified approach to the determination of the time - variant member resistance. Nevertheless, the above described approach for design of compression members for durability is not worked up for standard using up to now. The more complex stochastic analysis comparing obtained results with experimental ones should realized.

Acknowledgement

This work was supported by the Scientific Grant Agency of the Slovak Republic under the project 1/0311/09.

References

[1] ISO DIS 13823: *General principles on the design of structures for durability*. ISO/TC 98/SC 2.

[2] MELCHERS, R.E. *Corrosion uncertainty modelling for steel structures.* Journal of Constructional Steel Research, Elsevier, 1999.

[3] AKGÜL, F. – FRANGOPOL, D.M. Lifetime *performance analysis of existing steel girder bridge superstructures*. Journal of Structural Engineering v. 130, No. 12, pp. 1875-1888.

[4] QIN S. – CUI W. *Effect of corrosion models on the time-dependent reliability of steel plated elements*. Marine Structures, Elsevier, 2003.

[5] GUEDES SOARES, C. – GARBATOV, Y. *Reliability of maintained, corrosion protected plates subjected to non-linear corrosion and compressive loads*. Marine Structures, Elsevier, 1999.

[6] VIČAN, J. – SÝKORA, M. *Navrhovanie mostných konštrukčných prvkov s ohľadom na trvanlivosť*. Civil and environmental engineering, vol. 4, 2008, No. 2.

Transcom 2009, 22-24 June 2009
University of Žilina, Žilina, Slovak Republic

Bridge Computational Model for Vehicle – Bridge Interaction

[*]Renáta Sýkorová
[*]University of Zilina, Faculty of Civil Engineering, Department of Structural Mechanics, Univerzitná 8251/1, 01026 Zilina, Slovakia, renata.sykorova@fstav.uniza.sk

Abstract. Vehicle – bridge interaction forces can reach significant values which can influence the race comfort and also have negative effects on a bridge structure response. As well as a vehicle also a bridge is a mechanical system which is in the frame of solution substituted with computational models. There are presented two spatial finite computational models of bridge structure for further vehicle – bridge interaction analysis in this contribution. The basic dynamic calculations were carried out in the form of natural frequencies and natural shapes. Both models were modelled using ANSYS software environment and composed from solid and shell elements.

Keywords: Vehicle – bridge interaction, natural frequencies, natural shapes, bridge structure computational model, ANSYS.

1. Introduction

Vehicle – bridge interaction is still actual engineering problem solved on various special levels and from various viewing angles [1], [2]. Traffic load represented by a vehicle forms a significant dynamic factor. The magnitude between the system of vehicle – bridge interaction is changing in time according to various initial conditions of a moving vehicle. As well as a vehicle also a bridge is a mechanical system which is in the frame of solution substituted with computational models. Computing models of the vehicles are usually chosen as discrete computing models with *n* degrees of freedom. They are described with the system of ordinary differential equations. The bridge computing model can be chosen as the continual system (system with continuously distributed mass) described by the system of partial differential equations or as the discreet system (system with lumped masses) described by the system of ordinary differential equations. The author of the article considers to solve this problem particularly by using classic methods.

However it is intended to verify these calculations with the finite element analysis through the ANSYS software environment. The author gradually planes to solve the vehicle – bridge system interaction using simpler models of vehicles at the beginning and then more complicated ones and the most exact spatial models within the finite analyses.

This article deals with finite element analysis model of a bridge and its fundamental dynamic computations.

2. Dynamic model of a bridge

2.1. General

The dynamic behaviour of bridges is the key problem, which has been widely investigated by lots of researchers for many years and it is not still finished on sufficient level. In earlier studies, the bridge has been modelled as a beam structure and the vehicle as a system

of moving loads. This consideration allowed to solve the problem analytically in many cases, for example [1]. Simple models can describe the main aspects of this phenomenon. However, later on the effort was given for improvement in the dynamic interaction between the passing vehicles and bridges in the two – dimensional range to obtain the vertical and also the longitudinal vibrations. By taking in consideration realistic modelling it is necessary to use spatial three – dimensional models, which are considering other dynamic effects as lateral, rotational or torsion vibrations. Fundamental dynamic characteristics are represented by natural frequencies and mode shapes, which have to be known also by investigating the vehicle – bridge interaction, because the dynamic effects can significantly influence the race comfort and they can have negative effects on the bridge structure response. According to the natural frequencies and mode shapes it is possible to predict what would the bridge structure respond by like when those modes would be excited.

2.2. Bridge structure description

The bridge structure used in this study is modelled according to the actual bridge structure, which is situated on the track Varín – Mojš in the district of Zilina. The bridge carries the traffic over the railway track with three single span bridge structures. In every span the structure has 8 prestressed and precasted concrete beams of type I – 73 with the span of 29m. The beams are 1.4 m high and they are built from concrete of quality B500 with elasticity modulus E_b=38.5 GPa. In the cross direction the beams are connected together with seating of joints from concrete of quality B330 with elasticity modulus E_b=33 GPa. There is also concrete haunched layer from 2 to 11 centimetres thick on the top of the cross section. The cross section of described bridge structure is possible to see on Fig. 1.

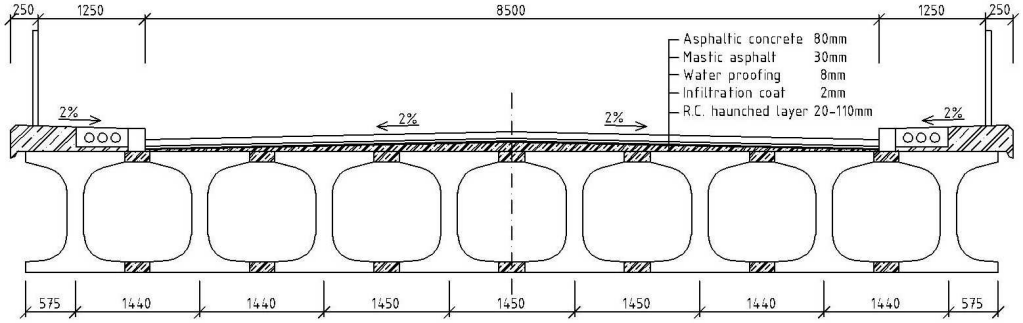

Fig. 1. Bridge cross section.

Fixed bearings are realized with the help of elastomeric bearings and multidirectional ones are realized with the help of pot bearings.

2.3. Bridge computational model description

For determination of structure dynamic response there was created a spatial finite computing model in ANSYS software environment using solid 3D elements. For the following investigation of vehicle – bridge interaction problem it is necessary to simplify the bridge finite model, however the required accuracy has to remain unchanged. Therefore there arose an effort to reduce complicated solid finite model to a spatial model using shell elements according to Fig. 2.

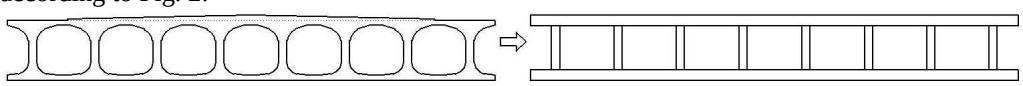

Fig. 2. Effort to change the solid finite model to the shell one.

Detail volumetric finite computational model consisted of solid elements SOLID 45 and the simplified model comprised of shell elements SHELL 181. Bearing system was simulated by spring - damper elements COMBIN 14, to which the spring constant was dedicated. There were globally used 464122 elements and they had 798276 nodes for volumetric model and 27000 elements and they had 26664 nodes for shell model. The finite computing model from solid elements is presented by Fig. 3 and shell model is on Fig. 4.

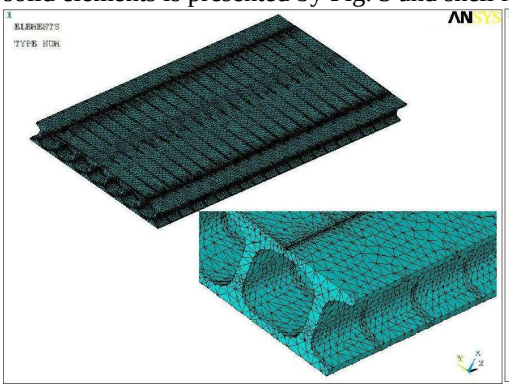

Fig. 3. General view of volumetric finite solid model

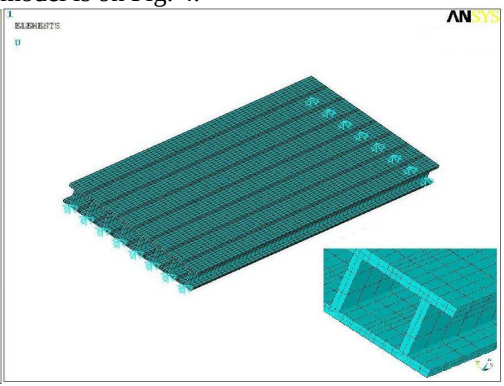

Fig. 4. General view of finite shell model

3. Modal analysis of bridge

The determination of natural frequencies and natural shapes in the sense of FEM solves the basic equation of motion (1)

$$[K].\{r(t)\}+[M].\frac{\partial^2\{r(t)\}}{\partial t^2}=\{0\}, \tag{1}$$

where $[K]$ is the stiffness matrix, $[M]$ is the structural mass matrix and $\{r\}$ is nodal displacement vector. For most cases the Block Lanczos is used as a mode extraction method or it can be used the subspace method or other ones.

There were computed the first 20 natural frequencies and vibration shapes, which are presented in Tab. 1 for both finite models.

Mode no.	Solid model	Shell model		Mode no.	Solid model	Shell model
	Frequency (Hz)	Frequency (Hz)			Frequency (Hz)	Frequency (Hz)
1	4,0324	4,0355		11	39,8365	35,5395
2	9,5207	8,4236		12	48,0121	37,6682
3	14,7184	14,9014		13	52,6069	46,6942
4	16,9490	17,2741		14	52,6810	47,5195
5	21,5501	20,0797		15	56,2834	51,5661
6	22,0233	24,7479		16	56,9874	53,3326
7	31,2618	25,0567		17	58,2455	54,6023
8	33,4386	33,2280		18	68,5692	54,7077
9	36,4803	33,8214		19	69,6935	60,3689
10	37,7887	35,2380		20	69,9636	62,4498

Tab. 1. Eigen frequencies for both volumetric and shell finite model.

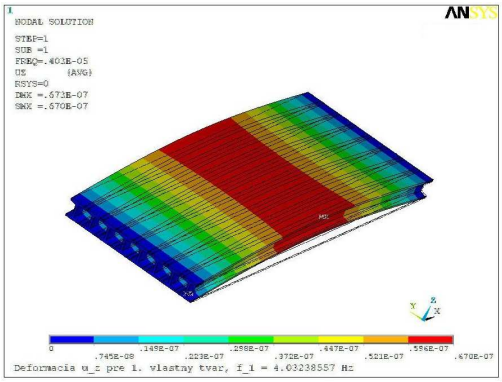

Fig. 5. 1st natural shape for volumetric model

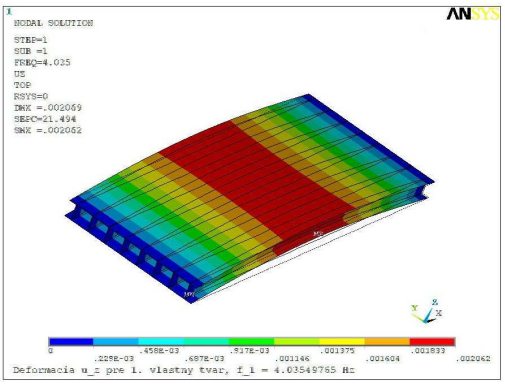

Fig. 6. 1st natural shape for shell model

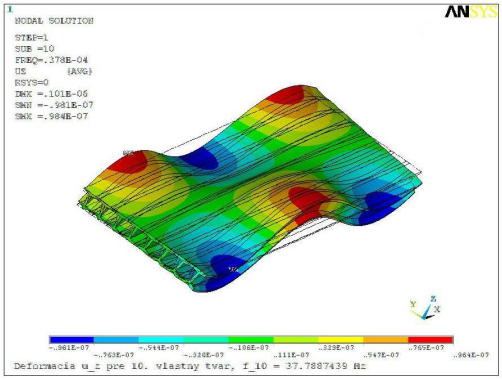

Fig. 7. 10th natural shape for volumetric model

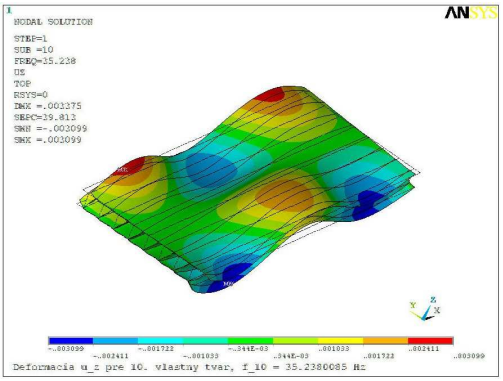

Fig. 8. 10th natural shape for shell model

4. Conclusion

Performed computations proved that for further working on simulation of vehicle – bridge interaction it is possible to change finite solid model to a simpler one which consists of shell elements. Thereby the saving of computing time can be achieved, because it will be necessary to simulate vehicle model using solid and contact elements. After comparing determined 1st natural frequency with frequency according to realized experiment is possible to see good accordance, which proves sententiousness of computing model. Further works are concentrated on vehicle model simulation and simulation of its effects on bridge structure vibration.

Acknowledgement

This work was supported by the Slovak Grant Agency, grant No. 1/0031/09.

References

[1] FRÝBA, L. *Title Vibration of Solids and Structures under Moving Loads*. ACADEMIA, Praha, Noordhoff International Publishing, Groningen, 1972.

[2] MELCER, J. *Dynamic computation of Highway bridges (In Slovak)*. EDIS ŽU, Žilina, 1997.

[3] ANSYS Release 10.0 Documentation

Transcom 2009, 22-24 June 2009
University of Žilina, Žilina, Slovak Republic

Estimation of Variance Components of 2D Geodetic Network

[*]Andrej Villim
[*]University of Žilina, Faculty of Civil Engineering, Department of geodesy, Komenského 52, 010 26 Žilina, Slovakia, {andrej.villim}@fstav.uniza.sk

Abstract. By estimation of variance components in concrete experiment represents application of LMVQUIE (Locally Minimum Variance Quadratic Unbiased Invariant Estimator) the latest theoretical information from mathematical statistic by parameter estimation of 2D geodetic networks.
In this paper there is introduced application of model by properly ordered experiment, which consists of the wide spectrum of measured parameters.

Keywords: LMVQUIE, variance component, rangefinder, trilateration.

1. Introduction

There are many measuring instruments, precision of which can't be described solely by standard deviation [1]. For instance, some electro-optical range finders has it's standard deviation given

$$\sigma_s = a + bs\,. \tag{1}$$

where s is an observed distance, a and b are precision characteristics. Parameter a is also called additive and b multiplicative constant and can be determined in two following ways:

- we have the opportunity to carry out auxiliary experiment, point of which is to estimate the parameters (on observation base)
- we've got a data file from practical experiment and the parameters come out as by-products from estimation

In our paper we deal with the later alternative using some experimental data obtained at Waterwork Gabčíkovo (WwG).

2. Experiment description

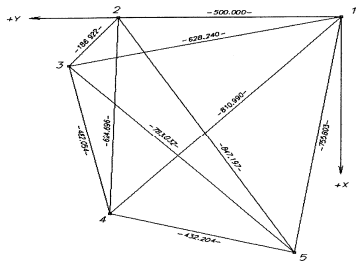

Fig. 1. Local geodetic network used for experiment.

Measurements was performed within the local geodetic net by WwG, which serves for deformation monitoring and contains 236 deeply stabilised pillars equipped for dependent centering of instruments [3]. We picked out 5 verticaly diverse points distanced at most 847m (see Figure 1). Observations lasted no longer than 30 minutes per station, horizontal distances were observed six times with Zeiss Elta Trimble 3602 DR rangefinder. Precision quoted by manufacturer is 2 + 2ppm, observed values are summarized in Table 1.

between points		observation number						mean
		1	2	3	4	5	6	
		[m]						
1	2	500.0010	500.0021	500.0012	500.0023	500.0015	500.0020	**500.0017**
1	3	628.2402	628.2413	628.2400	628.2412	628.2413	628.2409	**628.2408**
1	4	810.9908	810.9919	810.9905	810.9916	810.9917	810.9914	**810.9913**
1	5	755.8057	755.8048	755.8059	755.8056	755.8051	755.8043	**755.8052**
2	3	186.9229	186.9218	186.9226	186.9228	186.9215	186.9222	**186.9223**
2	4	624.6967	624.6968	624.6965	624.6954	624.6962	624.6958	**624.6962**
2	5	847.1985	847.1996	847.1993	847.1999	847.1988	847.1993	**847.1992**
3	4	482.0555	482.0567	482.0565	482.0553	482.0560	482.0565	**482.0561**
3	5	783.0330	783.0345	783.0337	783.0343	783.0335	783.0337	**783.0338**
4	5	432.2040	432.2050	432.2044	432.2042	432.2043	432.2054	**432.2046**

Tab. 1. Observed distances.

3. Matematical model

The purpose of our model for 2D geodetic network is to estimate all the unknown coordinates of network points and to determine instrument's variance components by the Locally Minimum Variance Quadratic Unbiased Invariant Estimator (LMVQUIE) method [5]and [7] .

Deterministic model, briefly denoted

$$\mathbf{X} = \mathbf{f}(\boldsymbol{\Theta}) . \tag{2}$$

where function **f** for measured distance is not linear

$$\mathbf{s}_{kl} = \sqrt{(Y_l - Y_k)^2 + (X_l - X_k)^2} . \tag{3}$$

is to be linearized

$$\mathbf{X} = \mathbf{f}(\boldsymbol{\Theta}_0) + \mathbf{A}\,\Delta\boldsymbol{\Theta} . \tag{4}$$

and rearranged

$$\mathbf{Y} = \mathbf{A}\,\Delta\boldsymbol{\Theta} . \tag{5}$$

s is a vector of distances included in vector of observations **X**, *Y* and *X* are coordinates, $\boldsymbol{\Theta} = \boldsymbol{\Theta}_o + \Delta\boldsymbol{\Theta}$ is a vector of unknown parameters, **A** design matrix, $\mathbf{Y} = \mathbf{f}(\boldsymbol{\Theta}_0) - \mathbf{X}$ denotes a known constant vector and *k*, *l* indices of the five involved points.

As for dispersion of realized distance $\mathrm{E}(\varepsilon_s^2) = \mathrm{Var}(\varepsilon_s) = \sigma_s^2$, where ε_s is random error, it may be rewriten with respect to (1)

$$\sigma_s^2 = (a_0 + b_0 s)^2 + 2(a_0 + b_0 s)\delta_a + 2s(a_0 + b_0 s)\delta_b . \qquad (6)$$

where a_0 = 2mm and b_0 = 2ppm. Let's denote $\upsilon_1 = \delta_a$, $\upsilon_2 = \delta_b$ and because of trilateration network the Var(ε_s) is configured

$$\boldsymbol{\Sigma}_{(\upsilon)} = \mathbf{V_0} + \upsilon_1 \mathbf{V_1} + \upsilon_2 \mathbf{V_2} . \qquad (7)$$

where υ_1, υ_2 are precision characteristics of instrument (variance components),
$\mathbf{V_0}$, $\mathbf{V_1}$, $\mathbf{V_2}$ diagonal matrices 10×10

$$\begin{array}{lll} \{\mathbf{V_0}\}_{i,i} = (a_0 + b_0 s)^2 & \{\mathbf{V_1}\}_{i,i} = 2(a_0 + b_0 s) & \{\mathbf{V_2}\}_{i,i} = 2s(a_0 + b_0 s) \\ \{\mathbf{V_0}\}_{i,j} = 0 & \{\mathbf{V_1}\}_{i,j} = 0 & \{\mathbf{V_2}\}_{i,j} = 0 \end{array} . \qquad (8)$$

i, j = 1,…10 are indices of observables. (9)

Stochastic model has the form

$$\mathrm{E}(\mathbf{X}) = \mathbf{f}(\boldsymbol{\Theta_0}) + \mathbf{A}\,\Delta\boldsymbol{\Theta} + \boldsymbol{\varepsilon} . \qquad (10)$$

and variances

$$\mathrm{Var}(\mathbf{X}) = \sum_{i=1}^{p} \upsilon_1 \mathbf{V_i} + \mathbf{V_0} . \qquad (11)$$

where p is the number of variance components, in our case p = 2. Because of first three coordinates having locked ($Y_1 = X_1 = X_2 = 0$ m, see Figure 1) dim($\boldsymbol{\Theta}$) = 5×2 –3 = 7.
Variance components estimation follows [6])

$$\hat{\boldsymbol{\upsilon}} = \mathbf{S}^{-1}_{(\mathbf{M}_X \boldsymbol{\Sigma}_0 \mathbf{M}_X)^+} (\mathbf{a} - \mathbf{b}) . \qquad (12)$$

a, **b** are p-dimensional vectors

$$\mathbf{a} = \begin{pmatrix} \mathbf{Y}^{\mathrm{T}} (\mathbf{M}_X \boldsymbol{\Sigma}_0 \mathbf{M}_X)^+ \mathbf{V_1} (\mathbf{M}_X \boldsymbol{\Sigma}_0 \mathbf{M}_X)^+ \mathbf{Y} \\ \vdots \\ \mathbf{Y}^{\mathrm{T}} (\mathbf{M}_X \boldsymbol{\Sigma}_0 \mathbf{M}_X)^+ \mathbf{V_p} (\mathbf{M}_X \boldsymbol{\Sigma}_0 \mathbf{M}_X)^+ \mathbf{Y} \end{pmatrix} .$$

$$\mathbf{b} = \begin{pmatrix} \mathrm{Tr}\left[(\mathbf{M}_X \boldsymbol{\Sigma}_0 \mathbf{M}_X)^+ \mathbf{V_1} (\mathbf{M}_X \boldsymbol{\Sigma}_0 \mathbf{M}_X)^+ \mathbf{V_0}\right] \\ \vdots \\ \mathrm{Tr}\left[(\mathbf{M}_X \boldsymbol{\Sigma}_0 \mathbf{M}_X)^+ \mathbf{V_p} (\mathbf{M}_X \boldsymbol{\Sigma}_0 \mathbf{M}_X)^+ \mathbf{V_0}\right] \end{pmatrix} . \qquad (13)$$

$\mathbf{S}^{-1}_{(\mathbf{M}_X \boldsymbol{\Sigma}_0 \mathbf{M}_X)^+}$ is p×p matrix

$$\left\{\mathbf{S}^{-1}_{(\mathbf{M}_X \boldsymbol{\Sigma}_0 \mathbf{M}_X)^+}\right\}_{i,j=1\ldots p} = \mathrm{Tr}\left[(\mathbf{M}_X \boldsymbol{\Sigma}_0 \mathbf{M}_X)^+ \boldsymbol{\upsilon}_i (\mathbf{M}_X \boldsymbol{\Sigma}_0 \mathbf{M}_X)^+ \boldsymbol{\upsilon}_j\right] . \qquad (14)$$

$(\mathbf{M}_X \boldsymbol{\Sigma}_0 \mathbf{M}_X)^+$ represents Moore-Penrose inversion

$$(\mathbf{M}_X \boldsymbol{\Sigma}_0 \mathbf{M}_X)^+ = \boldsymbol{\Sigma}_\mathbf{0}^{-1} - \boldsymbol{\Sigma}_\mathbf{0}^{-1}\mathbf{A}(\mathbf{A}^\mathrm{T}\boldsymbol{\Sigma}_\mathbf{0}^{-1}\mathbf{A})\mathbf{A}^\mathrm{T}\boldsymbol{\Sigma}_\mathbf{0}^{-1}. \quad (15)$$

where $\boldsymbol{\Sigma}_\mathbf{0} = \sum_{i=1}^{p} \upsilon_{0i}\mathbf{V}_\mathbf{i} + \mathbf{V}_\mathbf{0}$,

$\boldsymbol{\upsilon}_0$ are approximate values taken from instrument's certificate (2mm and 2ppm).
The model is being iterated

$$\hat{\boldsymbol{\upsilon}} = \boldsymbol{\upsilon}_0 + \mathbf{S}^{-1}_{(\mathbf{M}_X \boldsymbol{\Sigma}_{0(\boldsymbol{\upsilon}_0)} \mathbf{M}_X)^+}(\mathbf{a}-\mathbf{b})_{(\boldsymbol{\upsilon}_0)} .$$

$$\hat{\hat{\boldsymbol{\upsilon}}} = \hat{\boldsymbol{\upsilon}} + \mathbf{S}^{-1}_{(\mathbf{M}_X \boldsymbol{\Sigma}_{0(\hat{\boldsymbol{\upsilon}})} \mathbf{M}_X)^+}(\mathbf{a}-\mathbf{b})_{(\hat{\boldsymbol{\upsilon}})} . \quad (16)$$

until the $(\hat{\hat{\boldsymbol{\upsilon}}} - \hat{\boldsymbol{\upsilon}}) = 0$ stop criterion.
Then unknown parameter estimation can be expressed

$$\Delta\hat{\boldsymbol{\Theta}} = (\mathbf{A}^\mathrm{T}\boldsymbol{\Sigma}^{-1}_{0(\hat{\boldsymbol{\upsilon}})}\mathbf{A})^{-1}\mathbf{A}^\mathrm{T}\boldsymbol{\Sigma}^{-1}_{0(\hat{\boldsymbol{\upsilon}})}\mathbf{Y} . \quad (17)$$

as well as covariance matrix of unknown parameters estimate

$$\mathrm{Var}(\hat{\boldsymbol{\Theta}}) = \sigma_0^2(\mathbf{A}^\mathrm{T}\boldsymbol{\Sigma}^{-1}_{0(\hat{\boldsymbol{\upsilon}})}\mathbf{A})^{-1}. \quad (18)$$

where σ_0 is a mean unit error, and covariance matrix of variance components estimates related to the point $\boldsymbol{\upsilon}_0$

$$\mathrm{var}(\hat{\boldsymbol{\upsilon}} \mid \boldsymbol{\upsilon}_0) = 2\mathbf{S}^{-1}_{(\mathbf{M}_X \boldsymbol{\Sigma}_0 \mathbf{M}_X)^+} . \quad (19)$$

4. Results

Here we provide estimation outcome involved in LMVQUIE procedure and comparison to a model of bondless network, which doesn't take the variance components estimation into account.
Firstly, the results of iteration (16) are values of variance components and their standard deviations

***a* = 1.75 mm**	**σ_a = 0.06 mm**
***b* = 1.92 ppm**	**σ_b = 0.10 ppm**

comparing with factory values for the laboratory temperature +20°C

a = 2.00 mm	σ_a = 0.20 mm
b = 2.00 ppm	σ_b = 0.10 ppm .

Table 2 shows estimate of coordinates and their precision characteristics by the LMVQUIE method, while Table 5 deals with distances instead. Comparizon to the alternative method with bondless network and alternative coordinates estimates are brought in Table 4 and Table 3, respectively.

point number	approximate coordinates		estimated coordinates		standard deviations	
	X_0	Y_0	X	Y	σ_X	σ_Y
	[m]				[mm]	
1	0	0	-	-	0	0
2	0	500.0000	-	500.0019	0	0.62
3	151.3135	609.7452	151.3136	609.7463	0.51	0.46
4	624.4515	517.4600	624.4525	517.4610	0.41	0.54
5	748.6833	103.4952	748.6855	103.4965	0.24	0.62

Tab. 2. Coordinates estimates by LMVQUIE.

point number	approximate coordinates		estimated coordinates		standard deviations	
	X_0	Y_0	X	Y	σ_X	σ_Y
	[m]				[mm]	
1	0	0	-	-	0	0
2	0	500.0000	-	500.0014	0	0.62
3	151.3135	609.7452	151.3135	609.7467	0.67	0.69
4	624.4515	517.4600	624.4528	517.4610	0.60	1.14
5	748.6833	103.4952	748.6854	103.4961	0.66	1.28

Tab. 3. Coordinates estimates by alternative method (bondless network).

As seen, the maximum difference is 0.4 mm in coordiantes, and -0.66mm in mean errors. Variances of estimated parameters clearly speak for including the variance components into estimation procedure. The same unequality in favour of LMVQUIE holds if considering Table 5.

point number	LMVQUIE		bondless network		differences	
	σ_X	σ_Y	σ_X	σ_Y	$\Delta\sigma_X$	$\Delta\sigma_Y$
	[mm]		[mm]		[mm]	
1	0	0	0	0	0	0
2	0	0.62	0	0.62	0	0
3	0.51	0.46	0.67	0.69	-0.16	-0.23
4	0.41	0.54	0.60	1.14	-0.19	-0.60
5	0.24	0.62	0.66	1.28	-0.42	-0.66

Tab. 4. Standard deviations comparison.

obs. number	distance	observed	estimate		standard deviation of estimates	
			LMVQUIE	bondless net	LMVQUIE	bondless net
		[m]			[mm]	
1	1 – 2	500.0017	500.0019	500.0014	0.62	0.62
2	1 – 3	628.2408	628.2407	628.2411	0.49	0.62
3	1 – 4	810.9913	810.9913	810.9915	0.18	0.68
4	1 – 5	755.8052	755.8052	755.8050	0.28	0.75

5	2 – 3	186.9223	186.9215	186.9219	0.72	0.48
6	2 – 4	624.6962	624.6966	624.6968	0.41	0.58
7	2 – 5	847.1992	847.1992	847.1991	0.11	0.66
8	3 – 4	482.0561	482.0550	482.0554	0.51	0.56
9	3 – 5	783.0338	783.0339	783.0343	0.23	0.65
10	4 – 5	432.2046	432.2042	432.2044	0.61	0.62

Tab. 5. Distances estimates.

5. Conclusion

All the results achieved by method LMVQUIE indicate we chose an appropriate mathematical model, which has a plus in estimating the variance components from direct observations (no auxiliary procedures are needed), and furthermore valid for particular outer conditions (factory parameters are limited in this way). As the matrix **S** from (14) is conditioned by a spectrum wideness of observed distances, we implemented this precondition into the experiment in order to utilize this modelling method effectively.
The estimated variance parameters of our rangefinder differs from those quoted in its certificate in values 0.25 mm for *a* and 0.08 ppm for *b*, however this is still in '$t\sigma$ criterion' boundaries ($t_{\alpha=0.05} = 2$).

This work was supported under the research project VEGA no. 1/0781/09.

References

[1] Abelovič, J. et al., 1990, '*Meranie v geodetických sieťach*', Bratislava, Alfa.

[2] Dobeš, J. et al.,1990, '*Presné lokálne geodetické siete*', Bratislava, VUGK.

[3] Kožár, J. and Lukáč, Š., 2000, 'Posudzovanie stability vzťažných bodov prívodného kanála VD Gabčíkovo', *Zborník zo seminára*, p. 63-64, Gabčíkovo.

[4] Kubáčková, L.,1990, '*Spracovanie experimentálnych meraní*', Bratislava, VEDA.

[5] Kubáček, L. and Kubáčková, L., 2000, '*Statistika a metrologie*', Olomouc, Přírodovědecká fakulta Univerzity Palackého v Olomouci.

[6] Rao, C. R. and Kleffe, J., 1988, 'Estimation of Variance Components and Applications', Amsterdam.

[7] Bajtala, M.: Vplyv horizontálnej refrakcie na geodetické merania. Kandidátska dizertačná práca. Bratislava 2006.

[8] Hodas, S.: Spatial position model control of turnout layout objects after geodetic measurements [Modelová kontrola priestorovej polohy objektov zhlaví po geodetických meraniach]. In: EURNEX-Žel 2008 Towards more competitive European rail, 16th International Symposium, CETRA - Centre for Transportation Research ŽU-Žilina, EURNEX - European Rail Research Network of Excellence FAV Berlin, D, SVSD Bratislava, University of Žilina, Žilina, SK, EU, 2008. - ISBN 978-80-8070-853-5, s. 299-308